Fusion: a tale of recombination in an asexual fungus: The role of nuclear dynamics and hyphal fusion in horizontal chromosome transfer in Fusarium oxysporum

Shahi, S.

Publication date
2016
Document Version
Final published version

Fusion: A tale of recombination in an asexual fungus

THE ROLE OF NUCLEAR DYNAMICS AND HYPHAL FUSION IN HORIZONTAL CHROMOSOME TRANSFER IN FUSARIUM OXYSPORUM

SHERMINEH SHAHI

FUSION: A TALE OF RECOMBINATION IN AN ASEXUAL FUNGUS.

THE ROLE OF NUCLEAR DYNAMICS AND HYPHAL FUSION IN HORIZONTAL CHROMOSOME TRANSFER IN *FUSARIUM OXYSPORUM*.

ACADEMISCH PROEFSCHRIFT

ter verkrijging van de graad van doctor aan de Universiteit van Amsterdam op gezag van de Rector Magnificus prof. dr. ir. K.I.J. Maex ten overstaan van een door het College voor Promoties ingestelde commissie, in het openbaar te verdedigen in de Agnietenkapel op vrijdag 9 september 2016, te 14:00 uur

door
Shermineh Shahi
geboren te Teheran, Iran

PROMOTIECOMMISSIE

Promotor: Prof. dr. B.J.C. Cornelissen (Universiteit van Amsterdam)
Copromotor: Dr. M. Rep (Universiteit van Amsterdam)

Overige leden: Prof. dr. M.A. Haring (Universiteit van Amsterdam)
Prof. dr. S. Brul (Universiteit van Amsterdam)
Prof. dr. H.A.B. Wösten (Universiteit Utrecht)
Dr. E.M.M. Manders (Universiteit van Amsterdam)
Dr. J.A.L. van Kan (Wageninen UR)

Faculteit der Natuurwetenschappen, Wiskunde en Informatica

The research presented in this thesis was carried out at the University of Amsterdam. This work was made possible by a NWO Vici Grant (865.10.002) awarded to M. Rep.

“If my mind can conceive it
and my heart can believe it
then I can achieve it.”

Muhammad Ali

Cover design by Maximilian Pecher.

TABLE OF CONTENTS

Chapter 1	General introduction and thesis outline	7
Chapter 2	Dynamics of establishment of multinucleate compartments in Fusarium oxysporum	15
Chapter 3	Nuclear dynamics and genetic rearrangement in heterokaryotic colonies of *Fusarium oxysporum*	35
Chapter 4	Suppressor of fusion, a *Fusarium oxysporum* homolog of *NDT80*, is required for nutrient-dependent regulation of anastomosis	65
Chapter 5	General discussion	93
Summary, Samenvatting & Zusammenfassung		107
Acknowledgements		117
Publications		121

GENERAL INTRODUCTION

The kingdom of fungi represents a group of ecologically and economically important organisms. Saprophytic fungi, for example, play an important role in decomposition of dead material and recycling nutrients into the cycle of life. Some fungi produce important drugs like penicillin and other antibiotics. Yeast might represent the oldest economically important fungus as a leavening agent for bread and as fermentation agent to produce beer and wine. Then there are fungi that adapted to a more sinister life form, having evolved into pathogens that infect plants or animals.

Fusarium oxysporum (*Fo*) is an apparently asexual, soil-borne filamentous fungus of the phylum ascomycota. *Fo* forms a species complex containing pathogenic strains that together have a broad host range, including economically important crops like tomato, melon and banana, causing root rot or wilting diseases. Single isolates are usually pathogenic towards a single plant species, allowing the grouping of isolates into *formae speciales* (*f. sp.*) based on host specificity (1). Comparative genome studies of *Fusarium* species has revealed that closely related species share a core genome harboring essential housekeeping genes. In addition, *Fo* also has lineage-specific chromosomes (Fig 1a). In the tomato pathogen *F. oxysporum f. sp. lycopersici* strain 4287 (*Fol*4287) four lineage-specific chromosomes accounting for more than 25% of the genome have been identified (2, 3). The two smallest lineage-specific chromosomes of the strain *Fol*007, one of which harbors virulence genes necessary for tomato infection, can be transferred to the non-pathogenic strain *Fo*47 resulting in acquired pathogenicity in the recipient (Fig 1b, 2). Non-sexual or horizontal transfer of entire chromosomes in eukaryotes is a recently discovered phenomenon and may accelerate evolution of pathogenicity. Increased understanding of the mechanisms of horizontal chromosome transfer in *Fo* is the driving force behind the studies presented in this thesis.

Horizontal transfer of genetic material has been well studied in bacteria and plays an important role in the emergence of new bacterial diseases of plants and animals (4). Until recently, it was believed that mutation and sexual recombination are the main mechanisms for genomic variation in eukaryotes. Studies in the past decade, however, have demonstrated that also in fungi horizontal transfer of genetic material has contributed to the emergence of new pathogenic traits. For example, horizontal transfer of a host-specific toxin has likely led to the acquirement of a new pathogenic trait in a *Pyrenophora tritici-repentis* strain (tan spot on wheat, Friesen et al., 2006). Furthermore, horizontal transfer of entire chromosomes has been demonstrated in two other fungal pathogens, *Colletotrichum gloeosporioides* and *Alternaria alternata* (6, 7). The high degree of genetic variability in asexual fungal pathogens suggests that horizontal transfer of genetic material might be more common than initially expected, but the underlying mechanisms are not well understood (8, 9).

Fungi lack the DNA transfer mechanisms of bacteria and it is believed that horizontal transfer occurs through hyphal fusion (11, 12). However, fungi have an elaborate non-self recognition system, termed heterokaryon incompatibility, which prevents mixing of genetic material by inducing programmed cell death. Read and coworkers demonstrated that during conidial anastomosis tube (CAT)

fusion heterokaryon incompatibility is, at least partially, suppressed, providing a possible solution for this obstacle (13). The question that then arises is what the nuclear dynamics in a heterokaryon are and how the actual transfer of chromosomes takes place. This is the main question taken up in this thesis.

THESIS OUTLINE

Nuclear dynamics at different stages of colony development is the focus of **Chapter two**. We used fluorescently labeled nuclei and live-cell imaging to observe nuclear behavior not only during colony initiation, but also during colony maturation. This chapter describes the complexity of nuclear behavior in *Fo* by changing between uni- and multinuclear modes. We propose that *Fo* is basically multinucleate, a state which is suppressed during sporulation and reactivated after colony initiation. **Chapter three** addresses the conditions allowing formation of viable heterokaryons between the tomato pathogenic strain *Fol*4287 and the non-pathogenic strain *Fo*47 and the nuclear dynamics in heterokaryons and in hybrid colonies. We show that after heterokaryon formation nuclei likely fuse. During the following development of a hybrid colony, genome rearrangement and uniparental elimination of chromosomes of the pathogenic strain takes place, a mechanism that likely leads to horizontal chromosome transfer. In **Chapter four** we present a novel role for a *Fo* homolog of the transcriptional repressor Non-Dityrosine 80 (*NDT*80), suppressor of fusion (*SUF*), as a nutrient-dependent regulator of fusion. *SUF*, a putative transcription factor, is involved in the regulation of heterokaryon formation and thus might indirectly influence horizontal chromosome transfer. Finally, **Chapter five** provides a general discussion and offers a hypothesis for how nearly identical chromosomes of both fusion partners could be distinguished as well as a possible explanation as to how transferable chromosomes escape chromosome elimination.

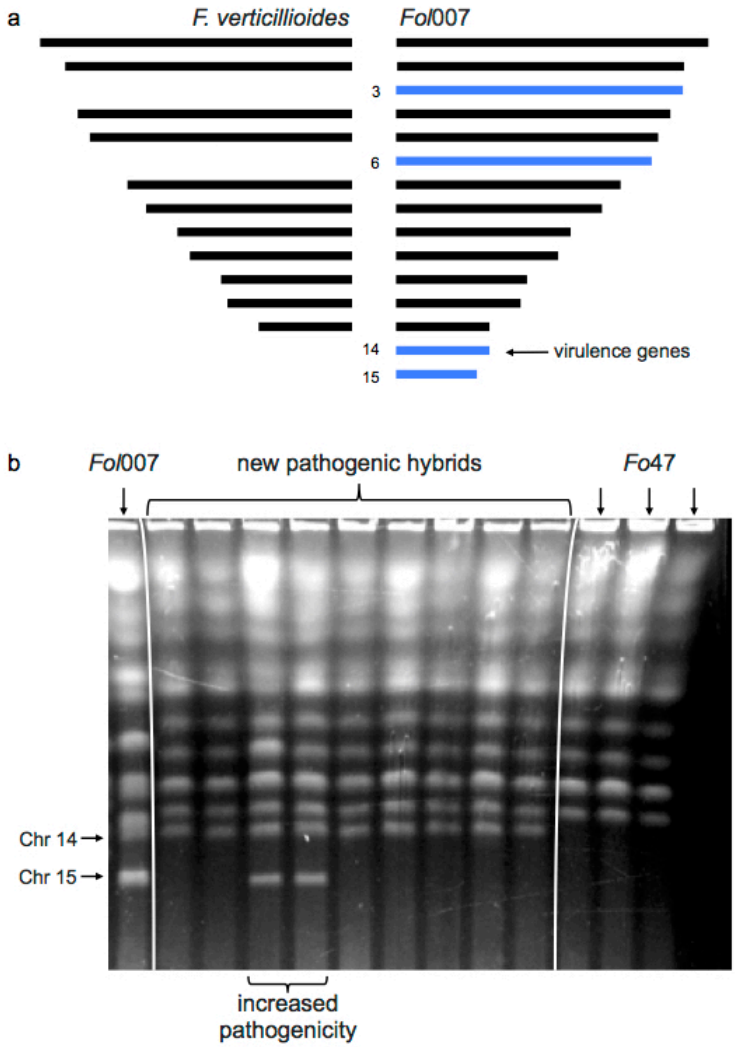

Fig 1: Horizontal transfer of lineage-specific chromosomes in *Fo*. a) The genome of a tomato pathogenic strain of *Fo* (*Fol*4287, right) is composed of a core of 11 chromosomes (black lines), which are conserved in closely related *F. verticilloides* (left). In addition, *Fol*4287 also harbors four lineage-specific chromosomes (blue lines). Interestingly, the identified virulence genes, Avr1, Avr2, and Avr3, are on one of the lineage-specific chromosomes, chromosome 14 or the "pathogenicity" chromosome (2, 10). b) Clamped homogeneous electric field (CHEF) gel depicting chromosomal composition of the tomato-pathogenic strain *Fol*007 and the nonpathogenic strain *Fo*47 and hybrid strains. Hybrid strains show a pattern similar to the non-pathogenic strain *Fo*47 with the addition of the pathogenicity chromosome and sometimes a second lineage-specific chromosome from the tomato-pathogenic strain *Fol*007. The hybrid strains have been shown to have acquired pathogenicity towards tomato and strains with both chromosomes show higher pathogenicity (from Ma et al., 2010).

REFERENCES

1. Gordon TR, Martyn RD. 1997. The evolutionary biology of Fusarium oxysporum. Annu Rev Phytopathol 35:111–128.
2. Ma LJ, van der Does HC, Borkovich KA, Coleman JJ, Daboussi MJ, Di Pietro A, Dufresne M, Freitag M, Grabherr M, Henrissat B, Houterman PM, Kang S, Shim WB, Woloshuk C, Xie X, Xu JR, Antoniw J, Baker SE, Bluhm BH, Breakspear A, Brown DW, Butchko RA, Chapman S, Coulson R, Coutinho PM, Danchin EG, Diener A, Gale LR, Gardiner DM, Goff S, Hammond-Kosack KE, Hilburn K, Hua-Van A, Jonkers W, Kazan K, Kodira CD, Koehrsen M, Kumar L, Lee YH, Li L, Manners JM, Miranda-Saavedra D, Mukherjee M, Park G, Park J, Park SY, Proctor RH, Regev A, Ruiz-Roldan MC, Sain D, Sakthikumar S, Sykes S, Schwartz DC, Turgeon BG, Wapinski I, Yoder O, Young S, Zeng Q, Zhou S, Galagan J, Cuomo CA, Kistler HC, Rep M. 2010. Comparative genomics reveals mobile pathogenicity chromosomes in Fusarium. Nature 464:367–373.
3. Coleman JJ, Rounsley SD, Rodriguez-Carres M, Kuo A, Wasmann CC, Grimwood J, Schmutz J, Taga M, White GJ, Zhou S, Schwartz DC, Freitag M, Ma LJ, Danchin EG, Henrissat B, Coutinho PM, Nelson DR, Straney D, Napoli CA, Barker BM, Gribskov M, Rep M, Kroken S, Molnár I, Rensing C, Kennell JC, Zamora J, Farman ML, Selker EU, Salamov A, Shapiro H, Pangilinan J, Lindquist E, Lamers C, Grigoriev I V, Geiser DM, Covert SF, Temporini E, Vanetten HD. 2009. The genome of Nectria haematococca: contribution of supernumerary chromosomes to gene expansion. PLoS Genet 5:e1000618.
4. Hacker J, Kaper JB. 2000. Pathogenicity islands and the evolution of microbes. Annu Rev Microbiol 54:641–79.
5. Friesen TL, Stukenbrock EH, Liu Z, Meinhardt S, Ling H, Faris JD, Rasmussen JB, Solomon PS, McDonald BA, Oliver RP. 2006. Emergence of a new disease as a result of interspecific virulence gene transfer. Nat Genet 38:953–6.
6. Akagi Y, Akamatsu H, Otani H, Kodama M. 2009. Horizontal chromosome transfer, a mechanism for the evolution and differentiation of a plant-pathogenic fungus. Eukaryot Cell 8:1732–1738.
7. He C, Rusu AG, Poplawski AM, Irwin JA, Manners JM. 1998. Transfer of a supernumerary chromosome between vegetatively incompatible biotypes of the fungus Colletotrichum gloeosporioides. Genetics 150:1459–1466.
8. Gladieux P, Ropars J, Badouin H, Branca A, Aguileta G, de Vienne DM, Rodríguez de la Vega RC, Branco S, Giraud T. 2014. Fungal evolutionary genomics provides insight into the mechanisms of adaptive divergence in eukaryotes. Mol Ecol 23:753–73.

9. Karasov TL, Horton MW, Bergelson J. 2014. Genomic variability as a driver of plant-pathogen coevolution? Curr Opin Plant Biol 18:24–30.
10. Takken F, Rep M. 2010. The arms race between tomato and Fusarium oxysporum. Mol Plant Pathol 11:309–14.
11. Fitzpatrick DA. 2012. Horizontal gene transfer in fungi. FEMS Microbiol Lett 329:1–8.
12. Mehrabi R, Bahkali AH, Abd-Elsalam KA, Moslem M, Ben M'barek S, Gohari AM, Jashni MK, Stergiopoulos I, Kema GH, de Wit PJ. 2011. Horizontal gene and chromosome transfer in plant pathogenic fungi affecting host range. FEMS Microbiol Rev 35:542–554.
13. Ishikawa FH, Souza EA, Shoji JY, Connolly L, Freitag M, Read ND, Roca MG. 2012. Heterokaryon incompatibility is suppressed following conidial anastomosis tube fusion in a fungal plant pathogen. PLoS One 7:e31175.

DYNAMICS OF ESTABLISHMENT OF MULTINUCLEATE COMPARTMENTS IN *FUSARIUM OXYSPORUM*

Shermineh Shahi[a], Bas Beerens[a], Erik MM Manders[b], Martijn Rep[a]

[a]Molecular Plant Pathology, University of Amsterdam, Amsterdam, The Netherlands
[b]Molecular Cytology, University of Amsterdam, Amsterdam, The Netherlands

Eukaryotic Cell (2015), 14:1 78-85, doi:10.1128/EC.00200-14

ABSTRACT

Nuclear dynamics can vary widely between fungal species and between stages of development of fungal colonies. Here we compared nuclear dynamics and mitotic patterns between germlings and mature hyphae in Fusarium oxysporum. Using fluorescently labeled nuclei and live-cell imaging we show that F. oxysporum is subject to a developmental transition from a uninucleate to a multinucleate state after completion of colony initiation. We observed a special type of hypha that exhibits a faster growth rate, possibly acting as a nutrient scout. The higher growth rate is associated with a higher nuclear count and mitotic waves involving 2-6 nuclei in the apical compartment. Further, we found that dormant nuclei of intercalary compartments can re-enter the mitotic cycle, resulting in multinucleate compartments with up to 18 nuclei in a single compartment.

INTRODUCTION

Cellular growth and the dynamics of organelles in ascomycetous fungi have been studied extensively in different model organisms and several common properties have been described. For example, it is well understood that filamentous fungi grow by hyphal tip extension and that the vesicle-rich Spitzenkörper is the main coordinator of tip growth (1, 2). Further, it has been shown that hyphal compartments are separated from each other by septa, which can be perforated, ensuring cytoplasmic continuity (3–5). Vegetative hyphae have the ability to branch and fuse with each other to form an interconnected mycelial network, which also can have cytoplasmic continuity (6, 7). In some fungi such as *Neurospora crassa*, free nuclear movement between hyphal compartments throughout the interconnected mycelium has been observed (8).

A further common characteristic of the most intensively studied ascomycete species is that hyphal compartments can be multinucleate. For example, compartments of *Ashbya gossypii* can harbor eight to ten nuclei (9). *Aspergillus nidulans* has been shown to have compartments with ten to 60 nuclei (10). The number of nuclei can go up to hundreds of nuclei (in *N. crassa*) or even to thousands of nuclei (in aseptate glomeromycete fungi, 11, 12, for review see 13). Multinucleated hyphae exhibit different modes of mitotic divisions. In synchronous mitosis, all nuclei of a hyphal compartment divide at the same time, as is for instance the case in apical cells of *Ceratocystis fagacearum* (14). An alternative is parasynchronous mitosis, a wave of nuclear divisions that travels along the hypha or hyphal compartment, which has been extensively studied in *A. nidulans* (15). Finally, nuclei of the same compartment can undergo asynchronous mitosis independently of their neighboring nuclei, as has been observed in *N. crassa* and *A. gossypii* (16, 17, for review see 18). *Colletotrichum lindemuthianum* provides an interesting case, in which different mitotic patterns at different developmental stages were observed. Apical compartments of hyphae of mature colonies exhibit synchronous, parasynchronous and asynchronous mitosis, whereas in subapical compartments only synchronous and asynchronous mitosis was observed (19). The mycelium of multinucleate fungi has the potential to contain genetically different nuclei, leading to phenotypic plasticity as well as potentially contributing to fungal virulence (20–23).

Nuclear dynamics in *Fusarium oxysporum* has not been fully resolved. In studies from the 1960s, using microscopic methods including phase contrast and fixed-cell staining, *F. oxysporum* was described as a multinucleate fungus undergoing waves of mitotic nuclear divisions involving several compartments (4, 24). However, in a recent study using modern live-cell imaging techniques and fluorescent labeling Ruiz-Roldán *et al* observed *F. oxysporum* as a

uninucleate fungus, in which only the nucleus of the apical compartment is mitotically active (25).
The aim of this study was to resolve these apparent contradictions and to obtain a fuller understanding of nuclear dynamics of *F. oxysporum* using fluorescently labeled nuclei and live-cell imaging. We found that (i) after completion of colony initiation specialized hyphae with a faster growth rate start to explore the surrounding medium. The higher growth rate is associated with a higher number of nuclei in the apical compartment and mitotic waves involving all nuclei of this compartment; (ii) in intercalary compartments dormant nuclei can be re-activated to enter the mitotic cycle. Apparently, *F. oxysporum* is subject to a developmental change from a uninucleate state in germlings and newly branched hyphae to at least two alternative multinucleate states in hyphae of the mature colony.

RESULTS

The number of nuclei per compartment varies in Fusarium oxysporum.

Studies on nuclear dynamics are often performed in germlings. To obtain a fuller picture of nuclear dynamics, we compared germlings with hyphae of a mature colony using three different Fusarium oxysporum (F. oxysporum) strains (Fol4287, Fom001 and Fo-47) expressing histone H1 tagged with a green fluorescent protein (HH01::GFP). We observed nuclear dynamics and number in germlings after 10 to 15 hours and in mature hyphae after 2 days.

As previously described (25), we saw that during early colony development germlings of *F. oxysporum* have uninucleate compartments (Supplemental Figure S3). This situation changed drastically after 2 days when the number of nuclei per compartment became highly variable. In addition to compartments with a single nucleus, compartments with two or more nuclei were observed (Figure 1). In *Fol*4287, we recorded a distribution in the range of 0 to 18 with an average of 3.1±2.6 (SD) nuclei per compartment after 2 days on minimal medium (Figure 1a and Table 1). Depending on the nuclear count the length of the compartments also varied greatly (48±49 (SD) µm; Supplemental Figure S2 and Table 1). Both odd and even numbers of nuclei per compartment were observed. Multiple nuclei were found in apical and subapical compartments of hyphal tips as well as in intercalary compartments of mature hyphae, in the center as well as at the edge of the colony. Nonetheless, we could classify hyphae into three distinct developmental stages based on several characteristics. First, newly branched hyphae showed the same nuclear dynamics as germlings and usually contained 1 or 2 nuclei per compartment (Figure 1b, upper panel and Figure 1c left panel). Second, we discovered a

specialized hyphal form or developmental stage in *F. oxysporum*, which is relatively thin (2-3 µm diameter compared to 4-6 µm for mature hyphae; Figure 1c, middle panel) and showed a higher growth rate than germlings or newly branched hyphae (Table 1). This newly described hyphal form, referred to here as 'fast growing hyphae', was observed after 2 days but not during early colony initiation and was mostly encountered in the growth front of the colony (Figure 1b, lower panel). With 176±150 (SD) µm, apical compartments of fast growing hyphae were longer than those of germlings and contained 2 to 6 nuclei (Table 1). Hyphae of the third developmental stage displayed a higher nuclear density, manifested in either smaller compartments with a single nucleus or larger compartments with multiple nuclei (up to 18 nuclei were observed; Figure 1c, right panel). Stage III was mostly observed behind the growth front of the colony and represents hyphae of the mature colony (Figure 1b, lower panel).

These distinct developmental stages with their characteristic nuclear dynamics were observed in all three tested strains, suggesting this phenomenon is common in F. oxysporum (Figure 1c). To rule out an effect of histone tagging and microscopic set-up, we performed DNA counter-staining of hyphae grown on PDA plates. After two days stage II and III were clearly distinguishable in colonies of Fol4287 (Supplemental Figure S4).

Fusarium oxysporum shows various patterns of mitosis.

Next, we used live-cell imaging to observe nuclear dynamics after 10 to 15 hours in germlings and after 2 days in hyphae of mature colonies. In germlings only the nucleus of the apical compartment was active and underwent mitosis. This mitosis, then, led to a mitotically inactive nucleus residing in the newly formed first subapical compartment and a mitotically active nucleus in the apical compartment, which entered the next mitotic cycle (Supplemental Figure S3). Again, newly branched hyphae behaved similarly to germlings, where only the apical nucleus was mitotically active (Figure 2). This stage of uninucleate compartments we refer to as stage I. After two days this uniform mitotic pattern changed and became more complicated; hyphae of developing colonies showed two additional mitotic patterns.

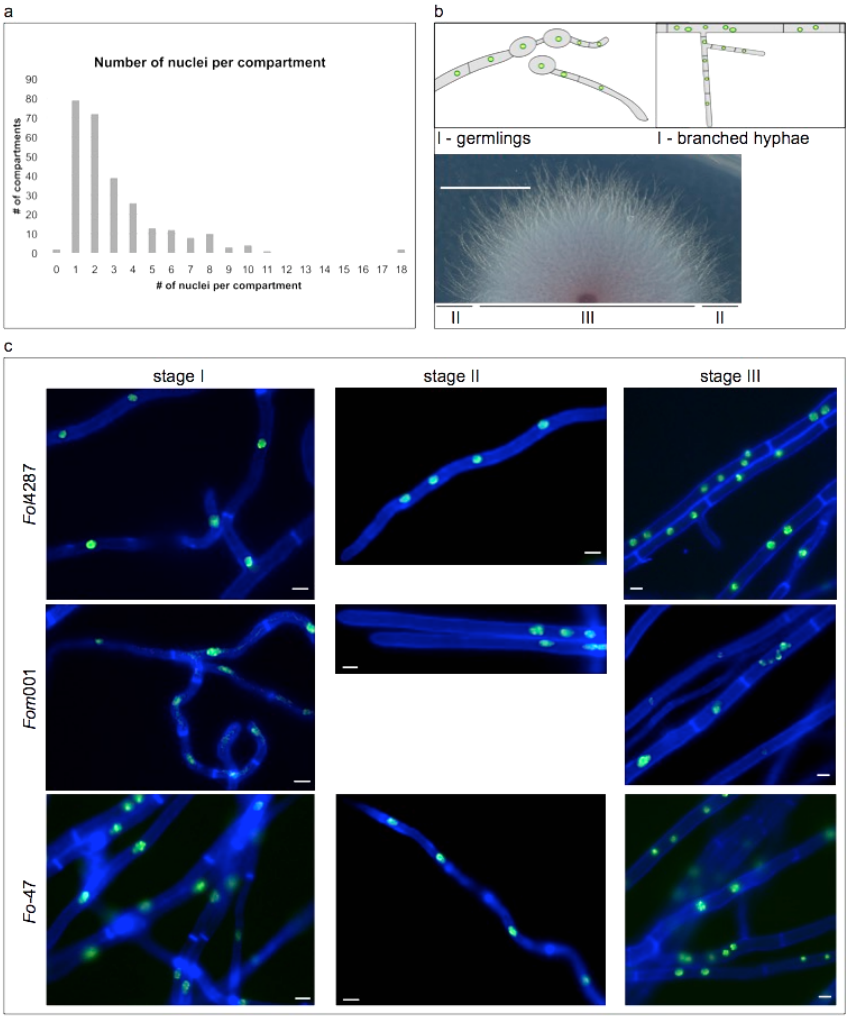

Figure 1: The number of nuclei per compartment is dependent on the hyphal type. a) Range of number of nuclei per compartment. Calculations were based on 65 hyphae from 5 biological replicates. Both odd and even numbers were found. b) Different stages of colony development in *F. oxysporum*. Upper panel shows schematic representation of stage I, in which each compartment harbors 1 nucleus. This stage was found in germlings and in newly branched hyphae. The lower panel shows colony phenotype after 2 days. Stage II, in which fast growing hyphae with multinucleate apical compartments are frequently encountered, can be found in the growth front. Stage III with multinucleate intercalary compartments can usually be found in mature hyphae behind the growth front, where aerial hyphae start to emerge. Scale bar 1 cm. c) The three developmental stages were found in all three strains tested: *F. oxysporum f. sp lycopersici* strain 4287 (*Fol*4287), *F. oxysporum f. sp melonis* strain 001 (*Fom*001), and non-pathogenic *F. oxysporum* strain 47 (*Fo*-47). All strains expressed HH01::GFP and were stained with 1µM calcofluor white. Scale bar: 10 µm.

Table 1: Emergence and characteristics of multinucleate compartments in *Fol*4287 on different media.

Parameter	Minimal medium average±SD (N)	PDA average±SD (N)
Number of nuclei per compartment day 2 [µm]	3.1±2.6 (271)	n.d.
Size of compartment day 2 [µm]	47.5±48.6 (271)	n.d.
Size of apical compartment in fast growing hyphae day 2 [µm]	176.2±149.8 (30)	n.d.
Germination start [h]	10	10
Growth rate at 15h [µm/h]	19.8±7.6 (6)	30.0±7.8 (5)
Appearance of fast growing hyphae [h after germination]	6	10
Growth rate of fast growing hyphae [µm/h]	164.3±64.9 (5)	119.4±35.2 (5)
Appearance of intercalary mitosis [h after germination]	23	26

Values with "±" are means ± SD
n.d., not determined

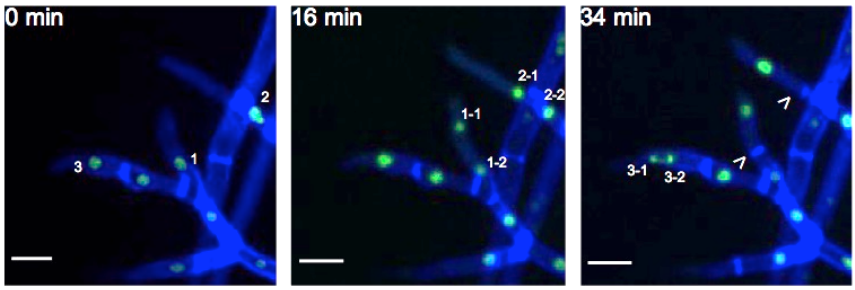

Figure 2: In newly branched hyphae only the apical nucleus is mitotically active. Time-lapse sequences of mitosis of uni-nucleated apical compartments of newly branched hyphae. Numbers indicate nuclei that will undergo mitosis, arrowheads indicate newly formed septa. *Fol*4287 HH01::GFP stained with 1µM calcofluor white. Scale bar: 10µm.

In stage II, apical compartments of fast growing hyphae contained several nuclei and these were all mitotically active. Fast growing hyphae show a rapid parasynchronous mitotic wave of up to 6 nuclei coupled to fast growth, which we refer to as 'hyphal growth spurts' from here on. Typically, a hyphal growth spurt started by extension of the apical compartment and fast migration of the resident nuclei along the growth vector in the direction of the hyphal tip (Figure 3, panels 1 and 2). During this first phase nuclei appear to be elongated, which we attribute to the rapid movement, probably caused by pulling of the nuclei towards the hyphal tip by the cytoskeleton machinery. Next, a mitotic wave including all nuclei of the apical compartment (usually 2-4) occurs, starting with the most apical nucleus. This is followed by formation of the same number of septa resulting mostly in uninucleate subapical compartments, leaving again the original number of nuclei (2-4) in the apical compartment (Figure 3, panels 3 and 4). In some cases, the first subapical compartment with 1 to 3 nuclei was included in the mitotic wave. Interestingly, the same number of nuclei that entered the first mitotic cycle re-enter the next cycle. Always the most apical nuclei of the apical compartment enter the next mitotic cycle, independent of their individual ancestry.

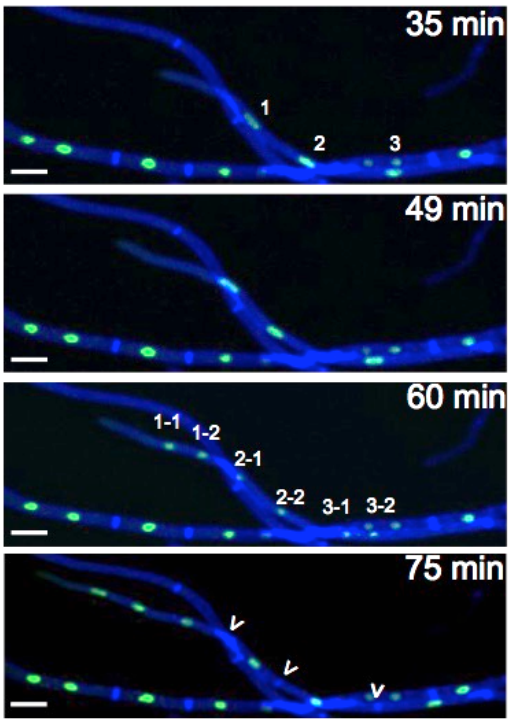

Figure 3: Spurts of mitotic waves occur in fast growing hyphae. Time-lapse sequences of mitotic waves in fast growing hyphae. In fast growing hyphae (164±65 µm/h on minimal medium), nuclei migrate towards the hyphal tip. A mitotic wave follows, starting from the apical nucleus. This mitotic wave can include several compartments and up to six nuclei. The number of septa formed is the same as the number of mitoses and the same number of apical nuclei will enter the next mitotic cycle. Numbers indicate nuclei that will undergo mitosis, arrowheads indicate newly formed septa. Fol4287 HH01::GFP stained with 1µM calcofluor white. Scale bar: 10µm.

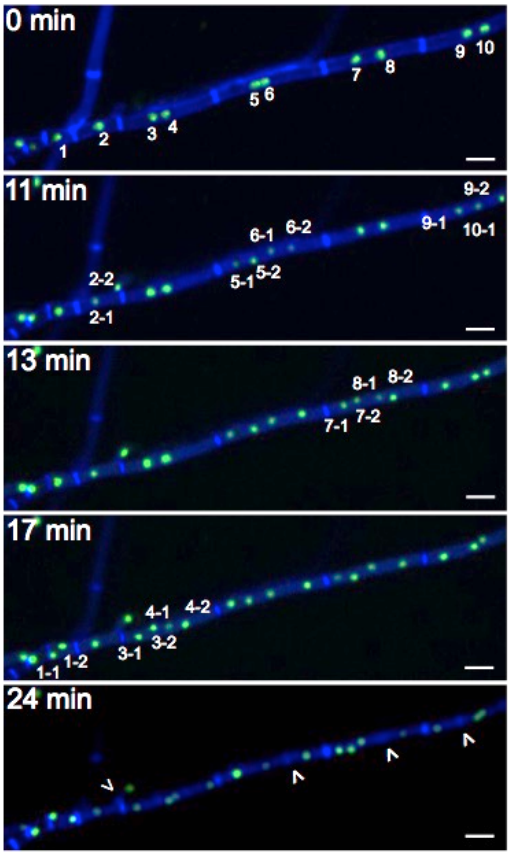

Figure 4: Intercalary compartments undergo asynchronous mitoses. Time-lapse sequences of asynchronous mitoses in intercalary compartments. Nuclei of intercalary compartments can be activated from their dormant state and undergo a mitotic wave, which can include several compartments and a number of nuclei, varying between 1 to 8 or more per compartment. The mitotic wave is asynchronous within and between compartments. Formation of septa does not always occur between daughter nuclei. Numbers indicate nuclei that will undergo mitosis, arrowheads indicate newly formed septa. *Fol*4287 HH01::GFP stained with 1µM calcofluor white. Scale bar: 10µm.

Intercalary compartments represented a further intriguing case. Dormant nuclei of older compartments (so-called intercalary compartments) were in some cases re-activated and underwent mitosis. However, this was not associated with hyphal growth in the form of elongation, extension or branching, resulting in the high nuclear density described above. Intercalary mitosis included one or several compartments, each with one or more nuclei. All nuclei involved showed a mitotic wave that was asynchronous within the compartment as well as between different compartments (Figure 4, panels 1-4). It was previously reported that mitosis is followed by septum formation between the two daughter nuclei (25). However, after intercalary mitoses septum formation took place between some sister nuclei but not all, explaining the occurrence of higher and odd numbers of nuclei per compartment (Figure 4, panel 5 and Supplemental Movie 4). Compartments with a very high nuclear density may result from a progressively lower frequency of septum formation as nuclei multiply within a compartment, which is in accordance with the limited number of cases that we

have observed. Additionally, an intercalary mitotic wave can include some compartments while excluding their neighboring compartments (Supplemental Movie 3 and 4). Within the time frame of our studies, we did not observe the continuation of an intercalary mitotic wave to adjacent compartments. This indicates a strict regulation of the entry point of individual compartments into mitosis, which does not necessarily travel along the hypha.

Emergence and characteristics of fast growing hyphae during colony development depends on medium composition

For a better understanding of the development from a uninucleate to a multinucleate state we monitored nuclear dynamics and mitotic patterns for 48 hours. For our microscope studies we usually use minimal medium, since in this medium hyphal growth is less dense and there is less production of aerial hyphae when compared to PDA medium (Supplemental Figure S5). Additionally, aromatic compounds in PDA medium show a strong autofluorescence in the GFP channel, leading to more background signal. However, to exclude malnutrition as a cause for the distinct nuclear behavior during the different stages of development, we tested nuclear dynamics of hyphae grown on PDA as well as on minimal medium (Table 1).

The different media did not affect germination of microconidia, the most frequently occurring conidia in *F. oxysporum* cultures, and after 10 hours most spores were germinated on both minimal medium and PDA. In general, hyphal growth rate on PDA (30±8 µm/h) was higher than on minimal medium (20±8 µm/h). Fast growing hyphae first emerged after completion of colony initiation, i.e. germination, conidial anastomosis tube (CAT) fusion and maturation of germ tubes into vegetative hyphae (26). The medium composition influenced the timing of the appearance of fast growing hyphae. On minimal medium, the first fast growing hyphae were observed 6 hours after germination, whereas on PDA the first fast growing hyphae were seen 10 hours after germination. The medium composition also influenced the growth rate of fast growing hyphae; with 164±65 µm/h they grew faster on minimal medium than on PDA (119±35 µm/h). Compared to the growth rate of regular hyphae on the respective media, fast growing hyphae grew approximately 8 times faster on minimal medium and 4 times faster on PDA, indicating a role of media composition and perhaps nutrient availability in the development of fast growing hyphae. At this stage, namely where fast growing hyphae appeared on a regular basis on both minimal medium and PDA, multinucleate compartments were almost exclusively observed in the apical compartment of fast growing hyphae. The occurrence of intercalary mitosis was not dependent on medium composition and the first

multinucleate intercalary compartments were observed 23 or 26 hours after germination on minimal medium or PDA, respectively.

DISCUSSION

In this study we showed that within the first 48 hours of colony formation by *Fusarium oxysporum* hyphal characteristics and nuclear dynamics change and these changes can be grouped into three developmental stages. The first stage is colony initiation including germination, CAT fusion, and maturation of germ tubes into vegetative hyphae, which at this stage contain exclusively uninucleate compartments. Depending on the medium composition, this stage can last 16-20 hours after seeding of spores. The second stage is marked by the emergence of fast growing hyphae that fan out with a 4 to 8 times higher growth rate, presumably to sample the surrounding environment for nutrient availability. At this stage, the first multinucleate compartments, the apical compartments of fast growing hyphae, emerge. Fast growing hyphae are present throughout further colony development, in line with a role of these specialized hyphae as scouts. Supporting this idea, we observed that on nutrient-limited medium, fast growing hyphae are formed earlier and show a higher growth rate. In addition to the proposed function as scouts, fast growing hyphae might also play a role in pathogenicity of *F. oxysporum*. The very thin hyphal tips of these specialized hyphae might facilitate the penetration of the host's root surface in the absence of appressoria, as was suggested by Ruiz-Roldán *et al* (25, 27). The third stage is characterized by a dramatic change in nuclear dynamics in intercalary compartments of mature hyphae: dormant nuclei of intercalary compartments are re-activated and undergo mitoses. Not all of these mitoses are followed by septum formation, resulting in highly multinucleated compartments and hyphae with a high nuclear density.

Newly branched hyphae, which appear first during stage II, behave much like germlings. In the cases that we observed the transition from a uninucleate stage to a multinucleate stage was shorter: it is reached after a few mitoses rather than many hours after germination, as is the case for germlings (see Table 1).

One question emerging from these observations is what the benefit could be, if any, of the transition from a uninucleate to a multinucleate state. The answer to this question may well be different for fast growing hyphae versus intercalary compartments. Although in their final form (smaller diameter, long apical compartment and mitotic wave) fast growing hyphae were only found after completion of colony initiation, initial steps towards their formation appear already shortly after germination. As described by Ruiz-Roldán et al, the size of apical compartments increases after each mitosis, which could be a

consequence of accelerating growth (25, Figure 1 and Table 1). To maintain a certain nuclear density in these fast growing apical compartments, we propose that multiple nuclei have to undergo mitosis. A similar model has been suggested for other filamentous fungi with a high growth rate, like *N. crassa*, in which the nuclear population in the growing tip is supported by multiple mitoses and rapid migration of the newly formed nuclei through interconnected hyphae (13, 28).

The advantages of multinuclearity and multiple mitoses in intercalary compartments have been investigated in several fungi, for example in *N. crassa* and *F. moniliforme*. These studies revealed that the same colony contained different nuclear populations (20, 29), demonstrating the potential importance of multinuclearity for fungal diversification and evolution. This is important for two reasons. (i) If only the apical nucleus is mitotically active, propagation of a spontaneous mutation would be limited to few points within a fungal colony and the generation of diversity would mostly occur at the edges of the colony (13). (ii) In previous studies the important role of horizontal gene and chromosome transfer in generating genomic diversity in filamentous fungi was demonstrated (22, 23, 30, 31). Horizontal gene and chromosome transfer requires at least a temporary tolerance for a multinucleate state in the mycelium. To have an effect on genetic diversity, new hyphae and/or spores should emerge from multinucleate compartments to produce offspring. We have not observed this in our study. As far as production of microconidia goes, in *F. oxysporum* this takes place in phialides in which nuclei of all spores originate from a single nucleus (25, Supplemental Movie 5).

Storage of nitrogen and phosphorus could represent a further functional advantage for the transition to multinuclearity in compartments of older mycelium (20). Under starvation conditions, the filamentous fungus *Aspergillus oryzae* is capable of degrading nuclei from compartments of older mycelium through macroautophagy and utilizing the released nutrients to support colony survival and growth (32). Conversely, in *F. oxysporum* compartments of older mycelium might re-activate dormant nuclei to undergo mitosis as a way to store nutrients in the form of DNA.

Another interesting question is how the transitions discussed above are regulated. A strict regulation must be in place to control entry into mitosis in some compartments and exclude the neighboring compartments. *Aspergillus nidulans* displays an elaborate system to regulate cell-to-cell connectivity during the cell cycle. Cytosolic continuity during interphase but not during mitosis is achieved by localization of the NIMA kinase to septal pores from the time of septum formation throughout interphase. During mitosis NIMA transiently

locates to nuclei, where it plays an important role in entry into mitosis as well as in nuclear pore complex disassembly (33–35). A similar system could be in place in *F. oxysporum*, facilitating the inclusion of some compartments and exclusion of others from entry into the next mitotic cycle.

One of the challenges of a multinucleate fungal lifestyle is potential nuclear competition during reproduction and spore dispersal. We propose a model in which *F. oxysporum* essentially follows a multinucleate lifestyle. This multinucleate state would be repressed during sporulation to overcome nuclear competition and is again de-repressed after colony initiation, when a multinucleate lifestyle is advantageous. It will be interesting to see what happens during fusion between older hyphae and whether the post-fusion nuclear degradation described by Ruiz-Roldán (25) is indeed the result of a repression of tolerance of the multinucleate state.

It stands to reason that a similar system as described here for *F. oxysporum* is also in place for other fungi. For example, *Magnaporthe grisea,* which was described as uninucleate, sometimes also exhibits multinucleate compartments in older mycelium (36). A future challenge could be to determine the advantages of this lifestyle, perhaps by finding a way to suppress either the multinucleate state or the uninucleate state through specific mutations.

ACKNOWLEDGEMENTS

This work was made possible by a Vici grant from the Netherlands Organization for Scientific Research (NWO) to MR. We thank Prof. Kück for plasmid pXPcFLPnatFRT which served as template for amplification of the *Penicillium chrysogenum* xylanase promoter. Special thanks to Ronald Breedijk for technical support.

MATERIAL AND METHODS

Strains and culture conditions

Fusarium oxysporum f. sp. lycopersici strain 4287 (*Fol*4287, FGSC9935), *Fusarium oxysporum f. sp. melonis* strain 001 (*Fom*001, FGSC10441), and the non-pathogenic *Fusarium oxysporum* strain 47 (*Fo*-47, FGSC #10445) were used as the parent strains for fungal transformation. They were stored as a monoconidial culture at −80°C and re-vitalized on potato dextrose agar (PDA, Difco) at 25°C. *Agrobacterium tumefaciens* EHA105 (37) was used for *Agrobacterium*-mediated transformation of *F. oxysporum* and was grown in either Luria broth (LB) or 2YT medium (38) containing 20 µg/ml rifampicin at 28°C. Introduction of the plasmids into the *Agrobacterium* strain was performed as previously described (39). *Escherichia coli* DH5 alpha

(Invitrogen) was used for construction, propagation, and amplification of the plasmid and was grown in LB medium at 37°C containing 50 µg/ml kanamycin. For microscopy, the fungus was grown on either PDA supplemented with 2% xylose or on low nutrient or minimal medium (0.17% Yeast Nitrogen Base without amino acids and ammonium sulfate (YNB, Difco), 100mM KNO_3, 2% xylose, 1.2% agarose) at room temperature. If not otherwise indicated, the medium was prepared in the shape of a microscope slide. Spores were collected from either PDA plates or NO3 medium (0.17% YNB, 100mM KNO_3, and 3% sucrose) and filtered with one layer of sterile Miracloth (Calbiochem) and washed with sterile water prior to mounting on agarose slides. These were incubated spore-phase down in a microscope chamber (Nunc) and observed for up to 3 days. To visualize cell walls and septa, 1µM calcofluor white stain (Fluka) was added to the medium (40). To counter-stain DNA the fungus was treated for 1 minute with 1 mg/ml Hoechst 33342 (Life Technologies) and washed with water before microscopy.

Construction of histone H1::GFP fusion protein expressing vector

Binary vector pRW2h suitable for *Agrobacterium*-mediated fungal transformations was used as a backbone for vector construction (41). We constructed a new vector, pRW2h + GFP, in a way that any protein of interest can be expressed as a GFP fusion protein. For this we introduced the GFP gene under the control of a promoter and a terminator with a multiple cloning site between the promoter and the GFP gene. This construct was introduced in the multiple cloning site between the left border and the *hph* resistance cassette. To be able to control expression of the GFP fusion protein, an inducible xylanase promoter from *Penicillium chrysogenum* (42) was used. The promoter region was PCR amplified with the primer combination FP2875 (5'-AAAATTAATTAACTGATGCGAGCAACAGTATG-3') and FP3528 (5'-GATATCTGGTTACCAGATCTTGTTAACAGGGATGGAGGCGATACTTA-3'), using pXPcFLPnatFRT vector (43) as template. The resulting amplicon was cloned in the PacI / EcoRV site in PRW2h. The terminator region of Six1 (44) was PCR amplified with the primer combination FP2877 (5'-AAAAGGTAACCATTATAACCTGCAGGGGGCCCGTTGCGATCCA-3') and FP3704 (5'- TTTTGATATCGGCGCGCCATACCTACGGCATCGAGTTTC-3') using *Fol*4287 genomic DNA (gDNA) as template and cloned in the BstEII / EcoRV site of the vector resulting from previous step, thus introducing five additional restriction sites. Next, the GFP gene was PCR amplified with primer combination FP3510 (5'-AAAAGGTAACCAGCCCGGGCAATTTAAATATGAGTAAAGGAGAAGAACTTTT-3') and FP3513 (5'- TTTTTTATAATTTATTTGTATAGTTCATCCATGC-3') using pGWB451 vector (45) as template and cloned in the BstEII / PsiI site between

promoter and terminator region. To generate a *Fol* histone H1 (HH01, FOXG_12732, http://www.broadinstitute.org/annotation/genome/fusarium_group/) GFP fusion protein, HH01 without a stop codon was PCR amplified with the primer combination FP3516 (5'-AAAAAGATCTAATGCCTCCCAAAGCCGCT-3') and FP3517 (5'-TTTTGGTTACCTTCGCCTTGGCAGCGGCC-3') from *Fol*4287 gDNA and the amplicon was cloned in the BglII / BstEII site in-frame with the GFP gene. The obtained plasmid pRW2h + HH01::GFP (see Supplemental Figure S1 for plasmid map) was transformed into *Agrobacterium tumefaciens* EHA105 and used for subsequent *A. tumefaciens*-mediated *Fusarium* transformation.

Agrobacterium-mediated Fusarium transformation

Agrobacterium-mediated transformation of *F. oxysporum formae specialis* was performed as previously described (46) with minor adjustments (47). Transformants were selected on Czapek Dox agar (CDA, Oxoid) containing 100 µg/ml Hygromycin (Duchefa). Fluorescence was tested on CDA containing 2% xylose.

Microscopic analysis

Successful transformation and DNA counter-staining was tested by localization of fluorescent signal using the AMG Evos FL digital inverted microscope equipped with transmitted light, GFP (470/22-510/42 nm) or DAPI (357/44-447/60 nm) light cubes and driven by built-in software for image acquisition and the inverted agar block method (40).

For confocal microscopy an Eclipse Ti inverted microscope (Nikon) with a FN1 spinning disk and EM-CCD Camera iXon DU897 (Andor) was used with a plan apo VC 40X 1.4 oil objective (Nikon). GFP was excited with 488nm (emission 505-530nm pass filter) and calcofluor with 405nm (emission 420–470 nm pass filter). Pictures were analyzed with the Nikon NIS and Fiji software from imageJ (http://fiji.sc/Fiji).

REFERENCES

1. Riquelme M. 2013. Tip growth in filamentous fungi: a road trip to the apex. Annu Rev Microbiol 67:587–609.
2. Steinberg G. 2007. Hyphal growth: a tale of motors, lipids, and the Spitzenkörper. Eukaryot Cell 6:351–60.
3. Gull K. 1978. Form and function of septa in filamentous fungi, vol III. Edward Arnold, London, United Kingdom.
4. Mouriño-Pérez RR. 2013. Septum development in filamentous ascomycetes. Fungal Biol Rev 27:1–9.

5. Mouriño-Pérez RR, Riquelme M. 2013. Recent advances in septum biogenesis in Neurospora crassa. Adv Genet 83:99–134.
6. Glass NL, Rasmussen C, Roca MG, Read ND. 2004. Hyphal homing, fusion and mycelial interconnectedness. Trends Microbiol 12:135–41.
7. Harris SD. Branching of fungal hyphae: regulation, mechanisms and comparison with other branching systems. Mycologia 100:823–32.
8. Roper M, Simonin A, Hickey PC, Leeder A, Glass NL. 2013. Nuclear dynamics in a fungal chimera. Proc Natl Acad Sci U S A 110:12875–80.
9. Kaufmann A, Philippsen P. 2009. Of bars and rings: Hof1-dependent cytokinesis in multiseptated hyphae of Ashbya gossypii. Mol Cell Biol 29:771–83.
10. Clutterbuck AJ, Roper JA. 2009. A direct determination of nuclear distribution in heterokaryons of Aspergillus nidulans. Genet Res 7:185.
11. Namboodiri AN, Lowry RJ. 1967. Vegetative Nuclear Division in Neurospora. Am J Bot 54:735.
12. Giovannetti M, Sbrana C, Logi C. Microchambers and video-enhanced light microscopy for monitoring cellular events in living hyphae of arbuscular mycorrhizal fungi. Plant Soil 226:153–159.
13. Roper M, Ellison C, Taylor JW, Glass NL. 2011. Nuclear and genome dynamics in multinucleate ascomycete fungi. Curr Biol 21:R786–93.
14. Aist JR. 1969. The mitotic apparatus in fungi, Ceratocystis fagacearum and Fusarium oxysporum. J Cell Biol 40:120–35.
15. Clutterbuck AJ. 1970. Synchronous nuclear division and septation in Aspergillus nidulans. J Gen Microbiol 60:133–5.
16. Minke PF, Lee IH, Plamann M. 1999. Microscopic analysis of Neurospora ropy mutants defective in nuclear distribution. Fungal Genet Biol 28:55–67.
17. Gladfelter AS, Hungerbuehler AK, Philippsen P. 2006. Asynchronous nuclear division cycles in multinucleated cells. J Cell Biol 172:347–62.
18. Gladfelter AS. 2006. Nuclear anarchy: asynchronous mitosis in multinucleated fungal hyphae. Curr Opin Microbiol 9:547–52.
19. Ishikawa FH, Souza EA, Read ND, Roca MG. 2010. Live-cell imaging of conidial fusion in the bean pathogen, Colletotrichum lindemuthianum. Fungal Biol 114:2–9.
20. Maheshwari R. 2005. Nuclear behavior in fungal hyphae. FEMS Microbiol Lett 249:7–14.
21. Jinks JL. 1952. Heterokaryosis: A System of Adaptation in Wild Fungi. Proc R Soc B Biol Sci 140:83–99.
22. Rep M, Kistler HC. 2010. The genomic organization of plant pathogenicity in Fusarium species. Curr Opin Plant Biol 13:420–6.
23. Ma LJ, van der Does HC, Borkovich KA, Coleman JJ, Daboussi MJ, Di

Pietro A, Dufresne M, Freitag M, Grabherr M, Henrissat B, Houterman PM, Kang S, Shim WB, Woloshuk C, Xie X, Xu JR, Antoniw J, Baker SE, Bluhm BH, Breakspear A, Brown DW, Butchko RA, Chapman S, Coulson R, Coutinho PM, Danchin EG, Diener A, Gale LR, Gardiner DM, Goff S, Hammond-Kosack KE, Hilburn K, Hua-Van A, Jonkers W, Kazan K, Kodira CD, Koehrsen M, Kumar L, Lee YH, Li L, Manners JM, Miranda-Saavedra D, Mukherjee M, Park G, Park J, Park SY, Proctor RH, Regev A, Ruiz-Roldan MC, Sain D, Sakthikumar S, Sykes S, Schwartz DC, Turgeon BG, Wapinski I, Yoder O, Young S, Zeng Q, Zhou S, Galagan J, Cuomo CA, Kistler HC, Rep M. 2010. Comparative genomics reveals mobile pathogenicity chromosomes in Fusarium. Nature 464:367–373.

24. Aist JR, Morris NR. 1999. Mitosis in filamentous fungi: how we got where we are. Fungal Genet Biol 27:1–25.
25. Ruiz-Roldán MC, Köhli M, Roncero MI, Philippsen P, Di Pietro A, Espeso EA. 2010. Nuclear dynamics during germination, conidiation, and hyphal fusion of Fusarium oxysporum. Eukaryot Cell 9:1216–1224.
26. Roca GM, Kuo H-C, Lichius A, Freitag M, Read ND. 2010. Nuclear dynamics, mitosis, and the cytoskeleton during the early stages of colony initiation in Neurospora crassa. Eukaryot Cell 9:1171–83.
27. OLIVAIN C, ALABOUVETTE C. 1999. Process of tomato root colonization by a pathogenic strain of Fusarium oxysporum f. sp. lycopersici in comparison with a non-pathogenic strain. New Phytol 141:497–510.
28. Kasuga T, Glass NL. 2008. Dissecting colony development of Neurospora crassa using mRNA profiling and comparative genomics approaches. Eukaryot Cell 7:1549–64.
29. Sidhu GS. 2011. Genetics of Gibberella fujikuroi. III. Significance of heterokaryosis in naturally occurring corn isolates. Can J Bot.
30. Miao VP, Covert SF, VanEtten HD. 1991. A fungal gene for antibiotic resistance on a dispensable (“B”) chromosome. Science (80-) 254:1773–1776.
31. Friesen TL, Stukenbrock EH, Liu Z, Meinhardt S, Ling H, Faris JD, Rasmussen JB, Solomon PS, McDonald BA, Oliver RP. 2006. Emergence of a new disease as a result of interspecific virulence gene transfer. Nat Genet 38:953–956.
32. Shoji J, Kikuma T, Arioka M, Kitamoto K. 2010. Macroautophagy-mediated degradation of whole nuclei in the filamentous fungus Aspergillus oryzae. PLoS One 5:e15650.
33. De Souza CPC, Osmani AH, Hashmi SB, Osmani SA. 2004. Partial nuclear pore complex disassembly during closed mitosis in Aspergillus nidulans. Curr Biol 14:1973–84.

34. De Souza CPC, Osmani SA. 2007. Mitosis, not just open or closed. Eukaryot Cell 6:1521–7.
35. Shen K-F, Osmani AH, Govindaraghavan M, Osmani SA. 2014. Mitotic regulation of fungal cell-to-cell connectivity through septal pores involves the NIMA kinase. Mol Biol Cell 25:763–75.
36. H. Y, T.T. H. 1976. Perithecial development and nuclear behavior in Pyricularia [grisea, Pyricularia oryzae, rice blast, fungus diseases]. Phytopathology.
37. Hood EE, Gelvin SB, Melchers S, Hoekema A. 1993. New Agrobacterium helper plasmids for gene transfer to plants (EHA105). Transgenic Res 2:208–218.
38. Sambrook J, Russel DW. 2001. Molecular Cloning: a Laboratory Manual. Col Spring Harbor Laboratory Press, New York.
39. Mattanovich D, Rüker F, Machado AC, Laimer M, Regner F, Steinkellner H, Himmler G, Katinger H. 1989. Efficient transformation of Agrobacterium spp. by electroporation. Nucleic Acids Res 17:6747.
40. Hickey PC, Swift SR, Roca MG, Read ND. 2004. Live-cell imaging of filamentous fungi using vital fluorescent dyes and confocal microscopy.Methods in Microbiology. Elsevier.
41. Houterman PM, Cornelissen BJ, Rep M. 2008. Suppression of plant resistance gene-based immunity by a fungal effector. PLoS Pathog 4:e1000061.
42. Zadra I, Abt B, Parson W, Haas H. 2000. xylP promoter-based expression system and its use for antisense downregulation of the Penicillium chrysogenum nitrogen regulator NRE. Appl Env Microbiol 66:4810–4816.
43. Kopke K, Hoff B, Kück U. 2010. Application of the Saccharomyces cerevisiae FLP/FRT recombination system in filamentous fungi for marker recycling and construction of knockout strains devoid of heterologous genes. Appl Environ Microbiol 76:4664–74.
44. van der Does HC, Duyvesteijn RGE, Goltstein PM, van Schie CCN, Manders EMM, Cornelissen BJC, Rep M. 2008. Expression of effector gene SIX1 of Fusarium oxysporum requires living plant cells. Fungal Genet Biol 45:1257–64.
45. Nakagawa T, Suzuki T, Murata S, Nakamura S, Hino T, Maeo K, Tabata R, Kawai T, Tanaka K, Niwa Y, Watanabe Y, Nakamura K, Kimura T, Ishiguro S. 2007. Improved Gateway binary vectors: high-performance vectors for creation of fusion constructs in transgenic analysis of plants. Biosci Biotechnol Biochem 71:2095–2100.
46. Mullins ED, Chen X, Romaine P, Raina R, Geiser DM, Kang S. 2001. Agrobacterium-Mediated Transformation of Fusarium oxysporum: An

Efficient Tool for Insertional Mutagenesis and Gene Transfer. Phytopathology 91:173–180.

47. Takken FL, Van Wijk R, Michielse CB, Houterman PM, Ram AF, Cornelissen BJ. 2004. A one-step method to convert vectors into binary vectors suited for Agrobacterium-mediated transformation. Curr Genet 45:242–248.

SUPPLEMENTARIES

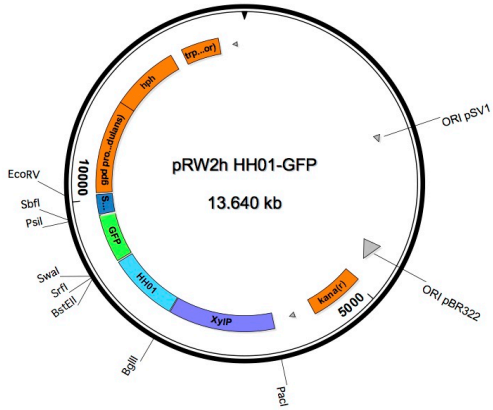

Figure S1: Plasmid map of pRW2h + HH01::GFP used for this study.

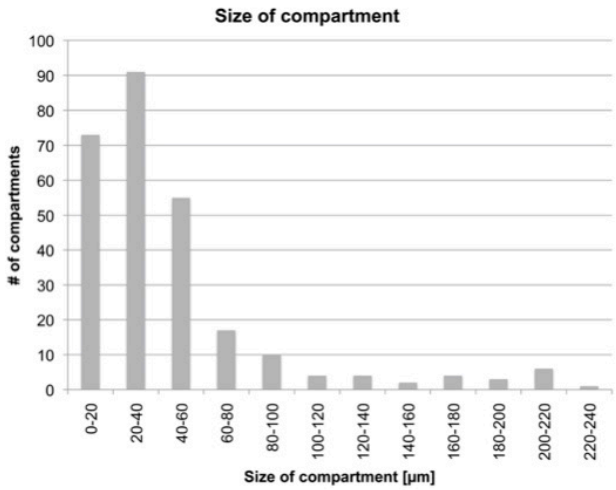

Figure S2: The size of the compartments varies. Number of compartments of the size indicated. Calculations were based in 65 hyphae from 5 biological replicates.

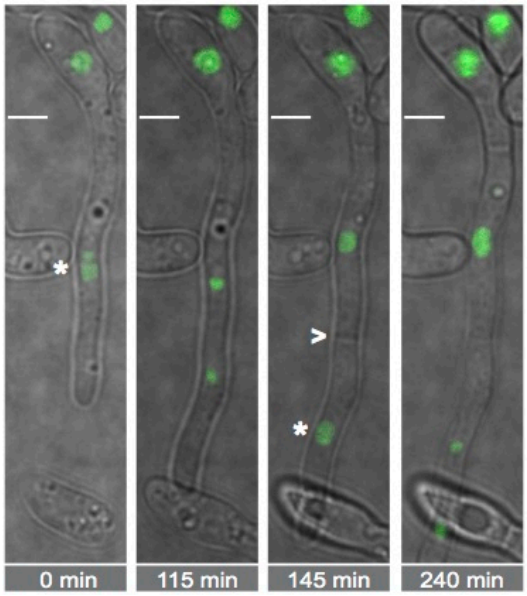

Figure S3: In young germlings only the apical nucleus is active. Time-lapse sequence of mitosis in an 10-hours old germling, Asterisk indicates nucleus that will undergo mitosis, arrowhead indicates newly formed septum. Scale bar: 10 µm.

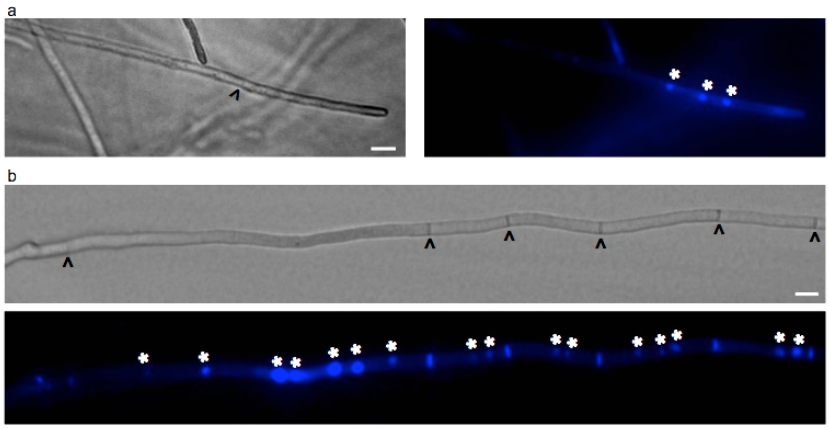

Figure S4: Hoechst 33342 DNA staining of 2-day old hyphae of *Fol*4287 grown on PDA plates. a) Fast growing hyphae harboring 3 nuclei in the apical compartment. Left bright field, right DAPI channel. b) Intercalary compartment of a mature hypha showing various numbers if nuclei per compartment. Top bright field, bottom DAPI channel. Asterisks indicate stained nuclei, arrowheads indicate septa. Scale bar: 10µm.

NUCLEAR DYNAMICS AND GENETIC REARRANGEMENT IN HETEROKARYOTIC COLONIES OF FUSARIUM OXYSPORUM

Shermineh Shahi, Bas Beerens*, Martin Bosch*, Jasper Linmans*, Martijn Rep

* contributed equally

Fungal Genetics and Biology (2016), 91 20-31

ABSTRACT

Recent studies have shown horizontal transfer of chromosomes to be a potential key contributor to genome plasticity in asexual fungal pathogens. However, the mechanisms behind horizontal chromosome transfer in eukaryotes are not well understood. Here we investigated the role of conidial anastomosis in heterokaryon formation between incompatible strains of *Fusarium oxysporum* and determined the importance of heterokaryons for horizontal chromosome transfer. Using live-cell imaging we demonstrate that conidial pairing of incompatible strains under carbon starvation can result in the formation of viable heterokaryotic cells in *F. oxysporum*. Later nuclei of the parental lines presumably fuse as conidia with a single nucleus harboring both marker histones (GFP- and RFP-tagged) are produced. Upon colony formation, this hybrid offspring is subject to progressive and gradual genome rearrangement. The parental genomes appear to become spatially separated and RFP-tagged histones, deriving from one of the strains, *Fol*4287, are eventually lost. With a PCR-based method we showed that markers for most of the chromosomes of this strain are lost, indicating a lack of *Fol*4287 chromosomes. This leaves offspring with the genomic background of the other strain (*Fo*47), but in some cases together with one or two chromosomes from *Fol*4287, including the chromosome that confers pathogenicity towards tomato.

INTRODUCTION

Genome plasticity has been described for a variety of plant-pathogenic fungi, and is considered a driving force in the "arms-race" between pathogen and host. Mutation and meiotic recombination are well-known processes underlying genomic variation. With the increasing availability of genome sequences it has become clear that asexual fungal pathogens also show a high degree of genetic variability (1–4). This has, for example, been demonstrated for *Fusarium oxysporum* (*Fo*) in comparative genome studies using different *Fusarium* species. *Fusarium graminearum* (*Fg*), *Fusarium verticillioides* (*Fv*), *Fusarium solani* (*Fs*), and *Fusarium oxypsorum f. sp. lycopersici* (*Fol*) share a highly conserved core genome harboring all essential housekeeping genes. In addition, *Fs* and *Fol* also carry lineage specific (LS) chromosomes enriched in genes specialized to niche adaptation, such as pathogenicity-related genes (5, 6). In the *Fusarium oxysporum* species complex each *forma specialis* is pathogenic towards a specific plant species. Strains pathogenic towards the same host can be polyphyletic and it has been suggested that horizontal transfer of genetic material might facilitate the emergence of new pathogenic strains (5, 7, 8). Horizontal transfer is defined as non-meiotic transfer of genetic material and the stable integration into the recipient genome. Horizontal chromosome transfer (HCT) is a special case of horizontal transfer where entire chromosomes or sets of chromosomes are transferred between strains (9–12). In the case of *Fo*, it was demonstrated that the two smallest LS chromosomes of strain *Fol*007 can be transferred to a non-pathogenic strain, *Fo*47, leading to the acquirement of pathogenicity towards tomato plants (Ma et al., 2010).

HCT has also been demonstrated for *Colletotrichum gloeosporioides* and *Alternaria alternata* (13, 14), but the underlying mechanisms are not well understood. In the absence of extracellular DNA transfer mechanisms in fungi it is likely that HCT occurs through hyphal fusion (12, 15). In filamentous ascomycetes vegetative hyphal fusion or anastomosis occurs frequently within the same mycelium (self fusion) and presumably ensures the equal distribution of nutrients and facilitates signaling across the mycelium (16, 17). Hyphal fusion between genetically distinct individuals results in formation of heterokaryotic cells, where one or more nuclei from each individual share a continuous cytoplasm. However, genetically distinct fungi differ at vegetative or heterokaryon incompatibility loci and a fusion generally leads to the heterokaryon incompatibility (HI) reaction. The HI reaction includes extreme growth reduction and in most cases compartmentalization of the fused cells and programmed cell death (18–21). It has been suggested that the HI reaction is at least partially suppressed during conidial anastomosis tube (CAT) fusion. CATs

are specialized hyphae interconnecting conidia or germ tubes during early colony initiation (22–25).
In recent years, studies have been conducted to investigate formation of viable heterokaryons. For example, conidial pairing and antidrug resistance testing in *C. gloeosporioides* showed that CAT fusion could generate heterokaryotic colonies with severe growth retardation and it was suggested that slow-growing heterokaryons might act as an intermediate step towards HCT (21). In the bean pathogen *C. lindemuthianum* fluorescently labeled nuclei were used to monitor nuclear fates in heterokaryotic cells. It was demonstrated that heterokaryotic cells formed by CAT fusion are viable and produce uninucleate conidia, which formed colonies with distinct phenotypes from the parental lines (26). The grass endophyte *Epichloë* lacks the HI reaction and vegetative hyphal fusion resulted in stable heterokaryotic cells. Protoplast fusion produced hybrids with genetic markers from both parental lines (27). In addition to their role during colony establishment, nutrient distribution, and signaling, it has been suggested that fungal anastomosis might mediate parasexual or non-meiotic recombination, which could contribute to the high level of genetic variation in the apparent absence of sexual recombination and possibly also enables HCT (28–31).

The aim of this study was to investigate the role of anastomosis in heterokaryon formation between different strains of *F. oxysporum* and determine the importance of heterokaryons for HCT. We observed the fate of fluorescently labeled nuclei during co-cultivation of vegetatively incompatible strains of *F. oxysporum* (32), anastomosis, and early development of heterokaryons, as well as during long-term development of hybrid offspring. In addition, the chromosomal composition of the hybrid offspring during the long-term study was determined using a PCR-based method to detect chromosome-specific markers.

We show that CAT fusion in *F. oxysporum* is greatly increased during carbon starvation and nitrogen limitation and that conidial pairing of the incompatible strains *Fol*4287 and *Fo*47 results in formation of viable heterokaryons. We conclude that CAT fusion of incompatible conidia leads to nuclear fusion and micronuclei formation in the hybrid offspring. During this process *Fol*4287 chromosomes are generally lost, but some chromosomes or parts of chromosomes can apparently be integrated into the *Fo*47 genome, including the “pathogenicity” chromosome that was previously shown to be horizontally transferrable.

RESULTS

Starvation-induced CAT fusion enables heterokaryon formation.

In a first attempt to find viable heterokaryotic cells of *F. oxysporum*, we performed a simple co-cultivation experiment. We mixed conidia of the tomato pathogen *F. oxysporum f. sp. lycopersici* strain 4287 (*Fol*4287) expressing histone H1 fused with red fluorescent protein (H1-RFP) and the hygromycin resistance cassette (*hph*) with conidia of the tomato non-pathogenic *F. oxysporum* strain *Fo*47 expressing histone H1 fused with green fluorescent protein (H1-GFP) and *hph* (Fig S2). The conidial mixture was incubated in nutrient rich medium (PDB), minimal (*i.e.* low carbon) medium, or water for three to five days and then examined microscopically. While we were not able to detect heterokaryotic cells after co-cultivation in rich medium, co-cultivation under carbon starvation resulted in heterokaryotic conidia, germlings, and hyphae. We observed three different types of heterokaryons. In Type I one red nucleus and green cytosolic fluorescence are present in conidia, but the green fluorescence does not continue into the germ tube. This was the most abundant Type. In Type II both red and green nuclei are present in the conidia, but only red nuclei are present in the germ tube. In Type III both red and green nuclei are found in conidia as well as the hyphae (Fig 1a). Type III was the least frequently detected. Interestingly, in all cases observed the dominant (always propagating) nucleus was derived from *Fol*4287, showing as red nuclei.

Table 1: CAT fusion and heterokaryon formation of F. oxysporum strains in different media.

Parameter	Results [%] (n) in			
	H2O	CAT (0.25% xyl)	CAT (0.5% xyl)	CAT (1% xyl)
*Fol*4287				
Conidia	91±5 (1731)	96±4 (2283)	95±3 (718)	99±1 (302)
CATs	8±4	21±10	37±10	4±2
Fol-Fol	*7±4*	19±11	37±11	4±2
Fol-Fo	*1±2*	5±4	2±2	0±0
*Fo*47				
Conidia	87±6 (1265)	97±4 (1091)	98±2 (250)	100±0 (350)
CATs	2±3	6±5	2±2	1±1
Fo-Fo	*1±1*	1±2	0±0	0±1
Fol-Fo	*1±2*	5±4	2±2	0±0

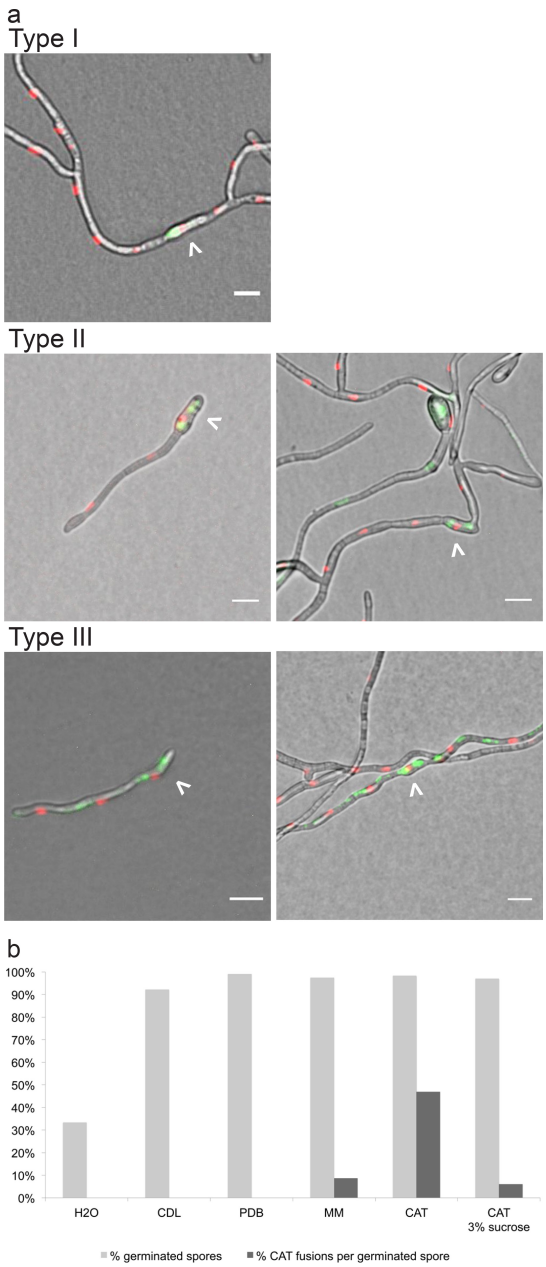

Figure 1: Heterokaryon formation and CAT fusion. a) Under carbon starvation conditions (H2O, minimal medium) incompatible strains of F. oxysporum can produce heterokaryotic conidia, which develop in three distinct ways. Type I: colonies show a red nucleus from the pathogenic strain Fol4287 with green cytosolic signal deriving from the non-pathogenic strain Fo47 in the conidia. Type II: colonies show both red and green nuclei in the conidia, but only the red nucleus proliferates. Type III: colonies harbor red and green foci in the conidia as well as the hyphae. In heterokaryotic colonies nuclei derived from Fol4287 always proliferate and seem dominant. Arrowhead indicates heterokaryotic conidia, scale bar: 10µm. b) CAT fusion in Fol4287 is restricted carbon and nitrogen starvation. Addition of a carbon source decreases the number of CATs formed per germinated conidia. Calculations were based on 300 to 3000 conidia from two to four biological replicates. MM: minimal medium, CAT: CAT medium.

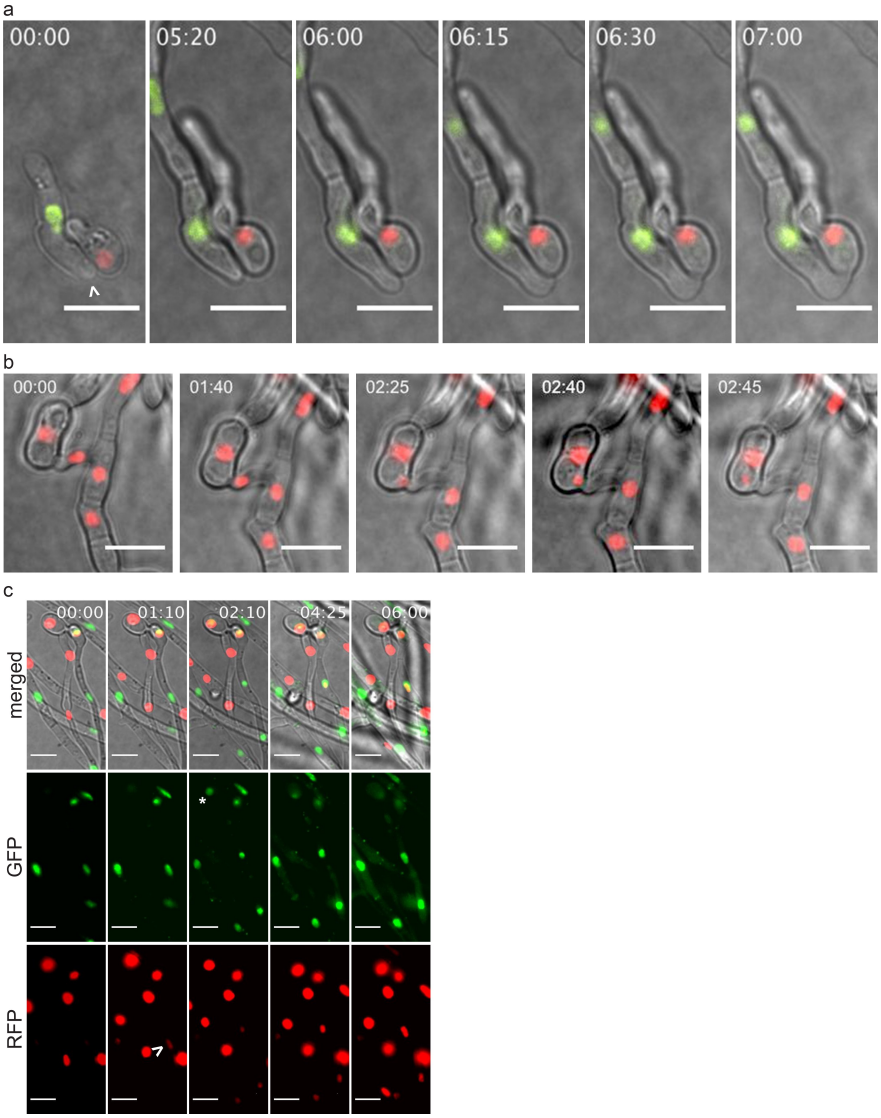

Figure 2: CAT fusion in Fol4287. a) Time-lapse sequence of CAT formation and fusion. In F. oxysporum generally one conidium initiates a CAT and homes toward another conidium. It is neither necessary nor often observed that both conidia form a CAT. Arrowhead marks area where CAT is formed. b) Time-lapse sequence of nuclear migration between two conidia after CAT fusion, showing survival of both nuclei in the same compartment. c) Time-lapse sequence of diffusion of fluorescent signal through CAT. Over time in all nuclei downstream the fused conidia red and green fluorescent signal is detected, showing as yellow nuclei. Top panel: merged, middle panel: GFP, bottom panel: RFP. Arrowhead marks first occurrence of red signal in an originally green nucleus and asterisk first occurrence of green signal in an originally red nucleus. Scale bar: 10µm.

It has been established in *Colletotrichum* species that heterokaryon incompatibility is suppressed during conidial anastomosis tube (CAT) fusion (21, 26). To find out whether the same holds true for *F. oxysporum* we studied CAT fusion in *Fol*4287 in water, czapek dox liquid (CDL), potato dextrose broth (PDB), and minimal medium with no carbon source. Although in our initial experiment co-cultivation of *Fol*4287 and *Fo*47 in water resulted in heterokaryotic cells, we were not able to find CAT fusion in water. This inability may be explained partly by a reduction of germination in water to 33% and partly by aggregation of the conidia to a degree that it was not possible to distinguish whether any CATs had formed. In CDL and PDB CAT fusions occurred in <1% of germinated conidia. However, when incubated in minimal medium 9 % of all germinated conidia showed CAT fusion. Further reduction of nitrate in the minimal medium to 25 mM (referred to as CAT medium from hereon) yielded 47 % CAT fusion (Fig S3). Addition of 3 % sucrose to CAT medium reduced the CAT fusion frequency to 6 % (N= 300-3000, Fig 1b and Fig S3). Neither glutamic acid nor tryptophan had any effect on CAT formation or fusion, unlike as described for *N. crassa* (33). These observations led us to the conclusion that CAT fusion in *F. oxysporum* is stimulated by carbon starvation and limited access to nitrogen. Another interesting observation is that for CAT fusion the formation of a CAT from one of the conidia is sufficient and is in fact the case in the majority of events (85 %, N= 95).

Given that heterokaryon formation and CAT fusion were both detected in medium without a carbon source, we next tested whether an increase of CAT fusion frequency has an effect on heterokaryon formation. For this we introduced H1-RFP with a phleomycin resistance cassette (*ble*) in *Fol*4287 to be paired with the above-mentioned *Fo*47 expressing H1-GFP (*hph*). Conidia from both strains were mixed and co-cultivated for 15-18 hours. We compared CAT fusion frequencies in self-fusion (*Fol*4287-*Fol*4287 and *Fo*47-*Fo*47) and in the incompatible interaction between *Fol*4287 and *Fo*47, the products of which we consider as heterokaryons. Because the expression of the histone H1 fusion protein is under the control of an inducible xylanase promoter, we also tested different concentrations of xylose in the CAT medium, looking for the lowest effective concentration for expression of the H1 fusion genes. We found that CAT fusion frequency between *Fol*4287 conidia is highest in CAT medium with 0,5 % xylose (37±11 %). The highest CAT fusion frequency between *Fol*4287 and *Fo*47 we detected was in CAT medium with 0,25 % xylose (5±4 %) and we therefore decided to use this medium for further co-cultivation studies. CAT fusion between *Fo*47 conidia was virtually absent.

In addition to conidial pairing we also performed hyphal tip pairing to test the effect of hyphal fusion on heterokaryon formation. Hyphal fusion

connects vegetative hyphae throughout the colony, independent of developmental stage. For this we grew *Fol*4287 H1-RFP (*ble*) and *Fo*47 H1-GFP (*hph*) in separate lines side by side on CAT medium supplemented with 0,25% xylose and 1% agarose. We then transferred an agarose block from the area where the hyphae of both strains met onto double selective plates and monitored for hyphal growth. However, no double-resistant outgrowth was observed. Form this we conclude that CAT medium does facilitate heterokaryon formation and that CAT fusion is the main source for heterokaryon formation under the conditions used.

Heterokaryotic germlings show aberrant nuclear behavior during early development.

To better understand the process of CAT fusion we observed nuclear behavior in *Fol*4287 after 15 hours (CAT formation and fusion) and after two days (early development). We followed fusion of *Fol*4287 expressing H1-RFP (*ble*) either with itself or with *Fol*4287 expressing H1-GFP (*hph*). Both CAT fusion and hyphal fusion were frequently observed when cultivated in CAT medium. Again we found that in the majority of cases (85%) the CAT is formed by only one of the conidia (Fig 2a and Movie M1). Furthermore, we observed that migration of the nucleus through a CAT did not result in the degradation of either nucleus, as was observed during hyphal fusion in an earlier study (Fig 2b and Movie M2, 41). However, nuclear migration did not always occur in the process of CAT fusion. In fact in most cases the nuclei remained in the original conidium. After fusion had been established the fluorescent signal traveled through the CAT and it is unknown whether transport of mRNA or protein was responsible. In the hypha of the fusion partner the fluorescent protein was then taken up into the nuclei, showing as yellow nuclei (i.e. red and green). This indicates that after completion of CAT fusion between compatible strains septal pores are open and allow for cytoplasmic continuity (Fig 2c and Movie M3).

Next we investigated the incompatible interaction between *Fol*4287 H1-RFP (*ble*) and *Fo*47 H1-GFP (*hph*) by live-cell imaging. Unfortunately, due to the low frequency of CAT fusion in this interaction we were unable to capture a CAT fusion event by visual prediction of where such an event might occur at 15 hours after co-cultivation. Nonetheless, we detected an apparent attempt and failure of *Fol*4287 CAT to fuse with *Fo*47 conidia. Movie M4 shows how the CAT attempts several times to fuse with the *Fo*47 conidia at different spots, but the fusion never takes place. We were, however, able to find fused CATs after the process had been completed after 24 hours (Fig 3a). In all five cases in which a clear distinction was possible, *Fol*4287 formed the CAT. Remarkably, even after two days we did not observe yellow nuclei (i.e. red and green) in the fused CATs

or the hyphae as a result of transmission of fluorescent signal, contrary to the self-fusion observed in *Fol*4287. However, the co-cultivation had allowed for the production of viable heterokaryotic conidia harboring at least one nucleus of each parental line, visible as distinct red and green nuclei. Further observation of nuclear dynamics in heterokaryotic germlings using live-cell imaging revealed that the red nucleus, originating from *Fol*4287, appeared intact, whereas the green nuclei from *Fo*47 appeared fractionated (two or more) and sometimes bleary. Nonetheless, nuclei from both parental lines proliferated during germination and hyphal growth, but in an asynchronous manner. Surprisingly, exchange of fluorescent protein did not take place in either direction (Fig 3b and Movie M5).

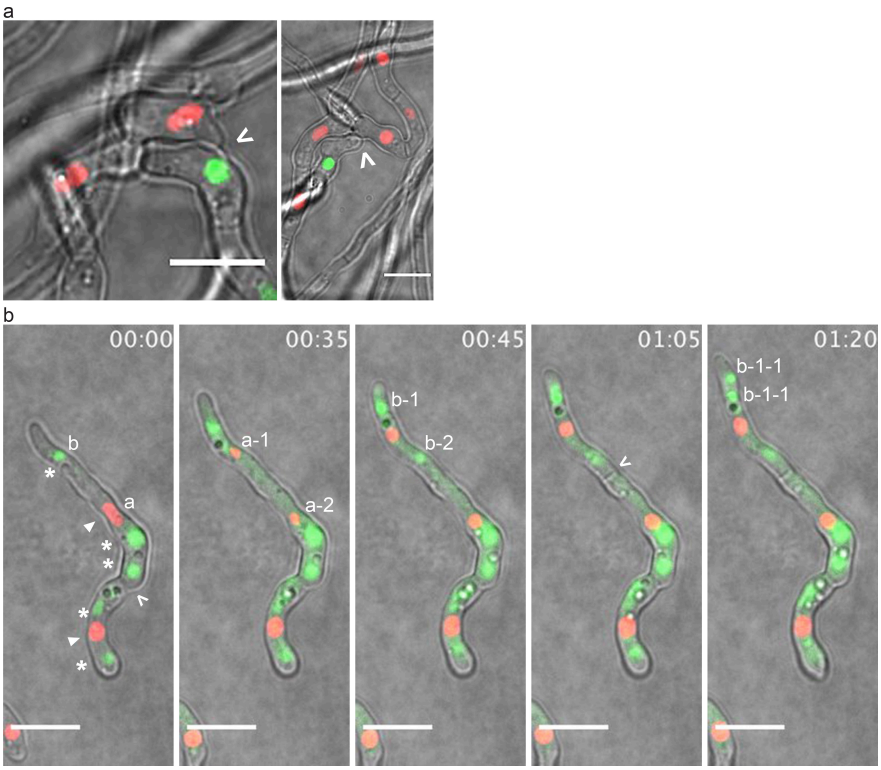

Figure 3: Incompatible interaction. a) CAT fusion between heterokaryotic conidia. Arrowhead marks CAT fusion. b) Proliferation of red and green nuclei in a hybrid offspring. Time-lapse sequence showing mitosis in a heterokaryotic germling. Red nuclei originating from Fol4287 appear intact showing as regular shaped nuclei (filled arrow heads). Green nuclei originating from Fo47 appear fractionated (two or more) and bleary (asterisks). Open arrowheads mark septi. However both red (a) and green (b) nuclei undergo mitosis in an asynchronous manner. Scale bar: 10µm.

Horizontal transfer occurs after heterokaryon formation.
To select heterokaryons for subsequent analysis we allowed the co-cultivation mix to produce conidia for two to five days. Since we did not make use of antifungal drug selection, the majority of the hyphae in the mix were either *Fol*4287 or *Fo*47, with only red or green nuclei, respectively. However, we also found heterokaryotic hyphae. Interestingly, these hyphae produced conidia with a single yellow nucleus, indicating that at some point during development the nuclei of the parental lines must have fused. To better monitor the yellow-nuclei progeny of the heterokaryotic colonies, conidial monosporing was performed. Out of 40 tested single spore colonies, four contained yellow nuclei. Conidia with a yellow nucleus germinated and formed germ tubes with no perceivable morphological differences to either of the parental lines (Fig S4 a). However, in the mature colonies after one to two weeks nuclei seemed fractionated and formed micronuclei (Fig S4 b). We went on to test the stability of the hybrid colonies and incubated the plates for four to six months. Interestingly, the fluorescent signal redistributed over time and a range of green, red and yellow nuclei of different sizes was observed (Fig S4 c). To follow this process further, we transferred an agar block from such plates to a new plate and incubated for two additional weeks. At this time only green nuclei remained (i.e. with histone-GFP from the Fo47 parent). To find out what had happened to the parental genomes during this process, we examined the chromosomal composition of the colonies at different stages. For each chromosome of both parental lines a specific primer pair was designed. Similar to what was found in an earlier study investigating HCT (5), after redistribution of the fluorescent signal and the disappearance of *Fol*4287-derived nuclei, the colonies showed the markers for all chromosomes of *Fo*47 plus the maker for *Fol*4287 chromosome 14. In two cases, the maker for *Fol*4287 chromosome 12 was also detected. In these colonies the marker for the homologous chromosome from *Fo*47 (chromosome 10) was either missing or showed a weaker band (Fig S4 d). Taken together, these results indicate that heterokaryon formation, nuclear fusion in heterokaryons and (mostly uniparental) chromosome loss can lead to apparent horizontal transfer of genetic material from *Fol*4287 to *Fo*47.

We then wished to inspect this process in more detail by observing more examples and gaining a better time resolution. For this purpose we decided to simplify the selection process by using the anti-fungal drug resistance markers. We co-cultivated conidia from each line for two days in CAT medium supplemented with 0,25 % xylose and incubated the mix on a PDA plate to allow for conidium formation for additional two days (= t0). Heterokaryotic conidia were then selected by growth on PDA plates supplemented with both hygromycin and zeocin for five days. About 1 in 300 conidia were double drug

resistant. For microscopical analysis, up to ten colonies were transferred to CDL plates and nuclear composition was determined after one week (= t1). To ensure that always the youngest part of the colony was studied we monitored hyphae from the edge of the colony and transferred an agarose block from this region to a new plate and incubated for one additional week (= t2, t3...). Sixty percent of the double drug resistant colonies showed both red and green signals, either separately or co-localizing to the same nuclei to various degrees (N= 90, eight biological replicates). These were selected for further study. We monitored nuclear and chromosomal composition at each time point until only one single fluorescent signal was observed.

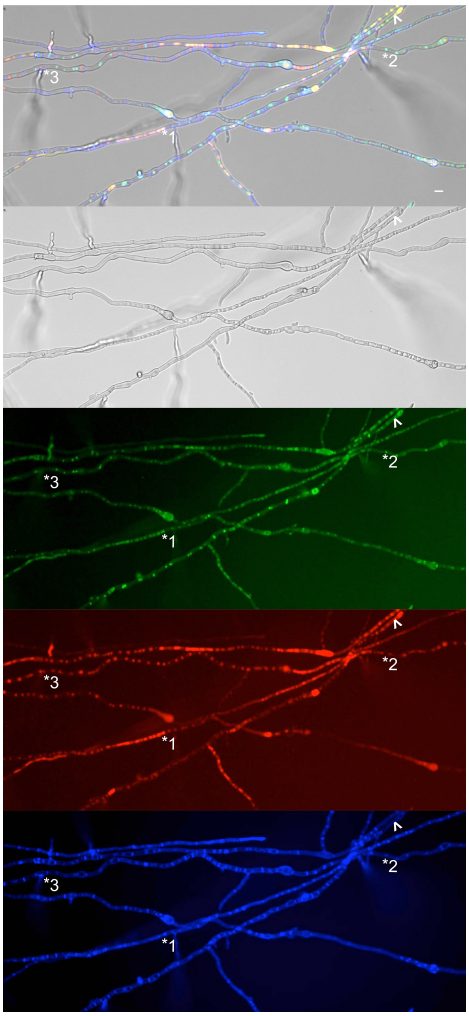

Figure 4: Phenotype and localization of fluorescent histones in a heterokaryotic colony. In heterokaryotic colonies rearrangement of genomes and nuclear shuffling causes stress in the fungus, indicated by highly vacuolated hyphae. During this process nuclei often are smaller and appear as micronuclei. Red and green fluorescent histones co-localize in some cases either into the nucleus (*1) or a vacuole (arrowhead), in other cases only GFP (*2) or rarely RFP (*3) localizes to nuclei. From top to bottom: merged, bright field, GFP, RFP, Hoechst 33342 (DNA) staining. Colony at t1, scale bar: 10 µm.

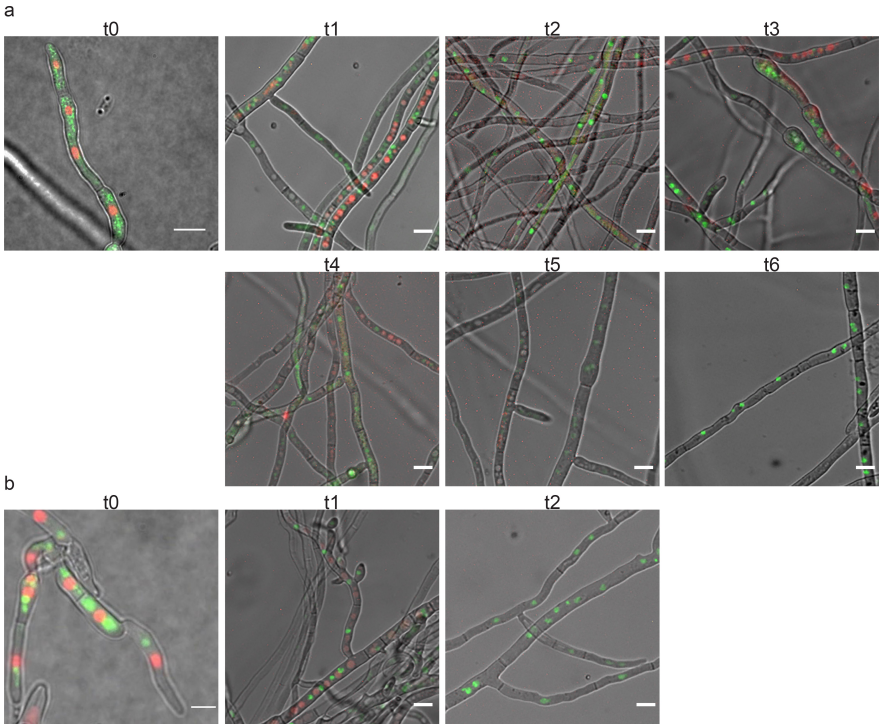

Figure 5: Examples of development of hybrid offspring. Slow (a) and fast (b) transition from heterokaryotic cells with red dominant nucleus to colonies only harboring green nuclei. During this transition often micronuclei are formed (a t1 to t5). After completion green nuclei show a regular shape known from the parental lines (a t5 and b t2). Scale bar: 10µm.

One thing all the offspring had in common, in spite of growing on medium without anti-fungal drugs, is that especially during the first weeks of development the hyphae appeared stressed, showing high levels of vacuolization. In addition, many nuclei appeared fractionated and seemed to form micronuclei (Fig 4, first and second panel). We performed Hoechst 33343 DNA staining at t1 to determine the localization of the H1-RFP and H1-GFP signals. Interestingly, we found that H1-RFP and H1-GFP sometimes co-localized with the DNA stain (Fig 4, *1), sometimes only H1-GFP and rarely only H1-RFP localized with the DNA stain (Fig 4, *2 and *3), and sometimes both co-localized to what seems to be a vacuole (Fig 4, arrow head).

The progeny of heterokaryotic cells displayed a large variety of colony phenotypes. The growth rate of the colonies varied between 1 mm to >3 cm per week (Fig S5a). In addition, some colonies had a patchy phenotype caused by higher branching, accelerated growth, or increased sporulation (Fig S5b, from

left to right). These characteristics are all distinct from the colony morphology of the parental lines. We followed the nuclear composition in 24 individual hybrid colonies on a weekly basis. As described earlier, at time point t1 all colonies showed red and green fluorescence, which either completely or partially co-localized (Fig 4). Surprisingly, this image changed during development of the colonies. Red nuclei derived from *Fol*4287 became less abundant and the red fluorescent signal decreased in intensity. Also, over time H1-RFP co-localized less with DNA and more to what are likely to be vacuoles (Fig 5). By t4 93% of the colonies contained only green nuclei, i.e. with H1-GFP derived from *Fo*47. Interestingly, this development was not always uniform across the colony. Where in one hypha there could still be a mix of red and green nuclei, in other hyphae only green nuclei were present (Fig 5a t2-t5). Once red nuclei had disappeared, the hyphae of the colonies looked healthier, showing regularly shaped nuclei and vacuoles (Fig 5a t6 and 5b t2).

To investigate whether the above-described development of heterokaryotic colonies can indeed lead to horizontal transfer of genetic material, we tested the chromosomal composition of these colonies at different time points by chromosome-specific PCR. Our hypothesis was that during the shift from red to green dominance chromosomes from *Fol*4287 would gradually disappear along with the H1-RFP marker. We tested colonies with only green nuclei and colonies with both red and green nuclei at time point t1. In general, if any were detected at all, bands for *Fol*4287 chromosomes were weaker than bands for *Fo*47 chromosomes (Fig S4 d). In two of the three tested colonies harboring only green nuclei the marker for *Fol*4287 chromosome 14 or both 12 and 14 was detected (colonies #2 and #4, Table 2). This suggests that transfer had already been completed. Alternatively, these chromosomes were still being eliminated at that moment.

We examined five individual colonies from three different pairings showing mixed nuclei at time point t1. In one of these colonies, despite detecting both red and green nuclei at all time points no markers for *Fol*4287 chromosomes were detected (colony #1, Table 2). Two other colonies contained mixed nuclei at time point t1, but only green nuclei were found at time points t2 and t3. Again no *Fol*4287 markers were detected (colonies #5 and #6, Table 2). The other two colonies both showed mixed nuclei at time points after t1. In these colonies markers for *Fol*4287 chromosomes 12 and 14 and chromosomes 10, 12 and 14 were found (colonies #3 and #7, Table 2). In colony #3 the marker for *Fo*47 chromosome 10 was not detected, and was possibly being replaced by the homologous *Fol*4287 chromosome 12. Interestingly, horizontal transfer always took place in one direction, with *Fol*4287 being the donor. Furthermore, horizontal transfer appears to always include at least parts chromosome 14.

Table 2: Presence of chromosome markers in heterokaryotic colonies at one-week intervals.

*Fol*4287	*Fo*47	Colony #	Time point	Growth diameter [cm]	Fluorescence		*Presence/absence of Fol*4287 marker of chromosomes															*Presence/absence of Fo*47 marker of chromosomes											
					GFP	RFP	1	2	3	4	5	6	7	8	9	10	11	12	13	14	15	1	2	3	4	5	6	7	8	9	10	11	12
*Fol*4287 H1-RFP (ble) #3	*Fo*47 H1-GFP (hph) #10		t0				+	+	+	+	+	+	+	+	+	+	+	+	+	+	+	+	+	+	+	+	+	+	+	+	+	+	+
		1	t1	2,8	+	+	-	-	-	-	-	-	-	-	-	-	-	-	-	-	-	+	+	+	+	+	+	+	+	+	+	+	+
			t2		+	+	-	-	-	-	-	-	-	-	-	-	-	-	-	-	-	+	+	+	+	+	+	+	+	+	+	+	+
		2	t1	2	+	-	-	-	-	-	-	-	-	-	-	-	-	-	-	+	-	+	+	+	+	+	+	+	+	+	+	+	+
			t2		+	-	-	-	-	-	-	-	-	-	-	-	-	-	-	-	-	+	+	+	+	+	+	+	+	+	+	+	+
			t3	1,4	+	-	-	-	-	-	-	-	-	-	-	-	-	-	-	-	-		+	+	+	+	+	+	+	+	+	+	+
*Fol*4287 H1-RFP (ble) #3	*Fo*47 H1-GFP (hph) #15		t0				+	+	+	+	+	+	+	+	+	+	+	+	+	+	+	+	+	+	+	+	+	+	+	+	+	+	+
		3	t1	3,9	+	+	-	-	-	-	-	-	-	-	-	-	-	+	-	-	-	+	+	+	+	+	+	+	+	+	-	+	+
			t2		+	+	-	-	-	-	-	-	-	-	-	-	-	-	-	-	-	+	+	+	+	+	+	+	+	+	-	+	+
			t3	2,9	+	+	-	-	-	-	-	-	-	-	-	-	-	-	-	-	-	+	+	+	+	+	+	+	+	+	-	+	+
			t4	2,8	+	+	-	-	-	-	-	-	-	-	-	-	-	-	-	-	-	+	+	+	+	+	+	+	+	+	-	+	+
			t5	3,4	+	-	-	-	-	-	-	-	-	-	-	-	-	+	-	+	-	+	+	+	+	+	+	+	+	+	-	+	+
		4	t1	1,6	+	-	-	-	-	-	-	-	-	-	+	-	-	+	-	+	-	+	+	+	+	+	+	+	+	+	+	+	+
			t2		+	-	-	-	-	-	-	-	-	-	-	-	-	-	-	-	-	+	+	+	+	+	+	+	+	+	+	+	+
			t3	2,1	+	-	-	-	-	-	-	-	-	-	-	-	-	-	-	-	-	+	+	+	+	+	+	+	+	+	+	+	-
*Fol*4287 H1-RFP (ble) #1	*Fo*47 H1-GFP (hph) #15		t0				+	+	+	+	+	+	+	+	+	+	+	+	+	+	+	+	+	+	+	+	+	+	+	+	+	+	+
		5	t1	2,7	+	+	-	-	-	-	-	-	-	-	-	-	-	-	-	-	-	+	+	+	+	+	+	+	+	+	+	+	+
			t2		+	-	-	-	-	-	-	-	-	-	-	-	-	-	-	-	-	+	+	+	+	+	+	+	+	+	+	+	+
		6	t1	3,5	+	+	-	-	-	-	-	-	-	-	-	-	-	-	-	-	-	+	+	+	+	+	+	+	+	+	+	+	+
			t2		+	-	-	-	-	-	-	-	-	-	-	-	-	-	-	-	-	+	+	+	+	+	+	+	+	+	+	+	+
			t3	3,9	+	-	-	-	-	-	-	-	-	-	-	-	-	-	-	-	-		+	+	+	+	+	+	+	+	+	+	+
		7	t1	3,9	+	+	-	-	-	-	-	-	-	-	-	-	-	+	-	+	-	+	+	+	+	+	+	+	+	+	+	+	+
			t2		+	-	-	-	-	-	-	-	-	-	-	+	-	+	-	+	-	+	+	+	+	+	+	+	+	+	+	+	+
			t3	3,5	+	-	-	-	-	-	-	-	-	-	-	+	-	+	-	+	-	+	+	+	+	+	+	+	+	+	+	+	+
			t4	3,7	+	+	-	-	-	-	-	-	-	-	-	-	-	-	-	-	-	+	+	+	+	+	+	+	+	+	+	+	+
			t5	3,8	+	-	-	-	-	-	-	-	-	-	-	-	-	-	-	-	-	+	+	+	+	+	+	+	+	+	+	+	+

DISCUSSION

This study was aimed to improve our understanding of the processes underpinning horizontal chromosome transfer in filamentous ascomycetes. Using live-cell imaging we demonstrated that conidial pairing of incompatible strains under carbon starvation and nitrogen limitation can produce viable heterokaryotic cells in *F. oxysporum*. During development of heterokaryotic hyphae, nuclei of the parental lines presumably fuse as conidia with a single yellow nucleus are produced. This hybrid offspring then undergoes a progressive and gradual genome rearrangement, during which markers for most chromosomes of one parental strain (*Fol*4287) are lost, leaving hybrid offspring with the genomic background of *Fo*47 with the addition of markers for (a) transferred chromosome(s) from *Fol*4287.

We demonstrated that CAT fusion in *Fol* is restricted to carbon starvation and limited access to nitrogen (Fig 1b). On the other hand, we did not observe self-anastomosis in the form of either hyphal or CAT fusion in *Fo*47 (Table1), possibly caused by a loss-of-function mutation in a gene essential for anastomosis in this strain. These observations suggest that during vegetative growth CAT fusion does not play an important role in colony initiation, as is the case for other fungi such as *N. crassa* (17, 24, 25, 35). CAT fusion may be a survival strategy of *Fol* to adapt to limited nutrient availability. One advantage could be a better distribution of nutrients through interconnected germlings. Alternatively, CAT fusion might have an additional and more specialized role in *Fo* by forming heterokaryotic cells to facilitate non-meiotic recombination, from which hybrids can emerge with new properties (e.g. the ability to colonize a certain plant species). Our results support the second role. First, CAT fusion is rarely detected between more than two conidia, which would not add much to the distribution of nutrients. Second, heterokaryon formation is observed during conidial but not hyphal tip pairing experiments (Table 1). Third, we show that new genotypes can emerge from heterokaryons.

In contrast to *Fol-Fol* self interactions, after CAT fusion between *Fol*4287 and *Fo*47 the fluorescently tagged histone proteins were not taken up into the nucleus of the fusion partner and nuclei from each parental strain remained distinct from one another (Fig 2c and 3). We were surprised that despite cytoplasmic continuity, in an incompatible interaction histones encoded in one nucleus are apparently not taken up and integrated into nuclei of the fusion partner. Since during self-anastomosis exchange of nuclear proteins does take place, it appears that having two genetically different nuclei somehow prevents cross-uptake of histones. Asynchronous cell division and asynchronous nucleoprotein synthesis have been proposed as mechanisms for uniparental

chromosome elimination in interspecific plant hybrid cells (36–38). In this study we have seen that in heterokaryotic conidia and germlings nuclei derived from the two different parental lines undergo mitosis in an asynchronous manner (Fig 3b). Similar to interspecies plant hybrids, this might either be the first step towards *Fol*4287 chromosome degradation or alternatively directed degradation of *Fol*4287 chromosomes might be initiated by the asynchronous cell division and/or nucleoprotein synthesis. Supportive of this idea are the differences in nuclear morphology we observed. Where red nuclei deriving from *Fol*4287 at this stage appeared healthy, green nuclei of *Fo*47 were fractionated (two or more nuclei) and sometimes bleary (Fig 1a and 3b). This process may be related to a heterokaryon incompatibility reaction, but the germlings are viable and form colonies that can produce conidia in turn. However, these conidia contain a single yellow (i.e. red and green) nucleus (Fig S4 a), indicating that nuclei must have fused sometime during development. In a previous study we show that *F. oxysporum* essentially follows a multinucleate state after colony initiation but returns to a uninucleate state during sporulation (39). Consistent with these findings, we suggest that prior to conidiation nuclei of *Fol*4287 and *Fo47* can fuse in phialides to produce uninucleate conidia. Nuclear fusion did not take place during sporulation following CAT fusion, perhaps because the suppression of heterokaryon incompatibility reaction allows for multinuclearity also during conidiation. In the mature hyphae emerging from uninucleate spores (with histones from both parents), the multinucleate state is again 'activated' and genome rearrangements are apparently initiated.

In human-mouse hybrid cells spatial separation of the parental genomes takes place prior to the directed elimination of human chromosomes (40–42). We observed formation of micronuclei in mature hyphae of colonies that emerged from yellow (i.e. red and green) nucleus conidia (Fig S4d). In the beginning these micronuclei remain yellow, possibly still having copies of both parental chromosomes or taking up both histone variants. However, during the course of two to six weeks, a redistribution of the red and green fluorescent histones was observed (Fig 5), suggesting that in hybrid offspring of *F. oxysporum* strains spatial separation of parental genomes may also precede chromosome degradation. Supportive of this idea is the decrease of the red signal over time until only green nuclei remain (Fig 5). An interesting question that then arises is how the distinction between core chromosomes highly similar in DNA sequence can be made. As mentioned previously, *Fol*4287 and *Fo*47 share a core genome, which is highly conserved (Ma et al., 2010, Ma, personal communication). We have demonstrated that in the incompatible interaction *Fol*4287 always forms the CAT. The distinction between a "fuser" as the active and a "fusee" as the inactive partner could induce different signaling pathways, one of which might

modify DNA or chromatin, allowing subsequent discrimination between chromosomes from different parents.

We used a PCR-based approach to identify markers for each chromosome of the two parental strains. Although we were able to detect markers for *Fol*4287 chromosome 14 and sometimes also 10 and 12 in the *Fo*47 background, the bands are weak compared to bands for *Fo*47 or *Fol*4287 chromosomes at time point t0 (Fig S4 f). We performed a single round of double drug resistant selection to prevent parental conidia from growing into colonies. Without further selection pressure, however, probably only a minority of the nuclei have incorporated genetic material of *Fol*4287 into the *Fo*47 genome and the detection of the markers appears close to the detection threshold. This would explain the apparent 'loss and gain' of *Fol*4287 markers during development of heterokaryotic colonies. Detection of a marker does not necessarily mean that the entire chromosome is present, but nevertheless indicates horizontal transfer of genetic material. However, in an earlier study, only transfer of entire chromosomes has been observed and chromosome transfer detected by markers was always confirmed by karyotyping (Ma 2010).

As mentioned earlier, a parasexual cycle has been suggested to contribute to the high level of genetic variation in asexual fungi (26, 28, 29, 31). To our knowledge a parasexual cycle in *Fusarium sp*. has only been achieved by protoplast fusion and results in equal distribution of chromosomes from each parental line and recombination between them (30, 43). Our results however, demonstrate that HCT likely occurs through nuclear fusion before conidiation followed by gradual degradation of most chromosomes from the 'donor' parental strain. This suggests that mechanisms underlying HCT are distinct from parasexual recombination.

Heterochromatinization has been demonstrated to play a major role in uniparental chromosome elimination in interspecies plant hybrid cells (44, 45) and directed DNA elimination in *Tetrahymena sp*. (46). A future challenge will be to identify the different steps involved in directed chromosome elimination in *F. oxysporum*. For example, it will be interesting to study the nature and role of micronuclei and chromatin marks in HCT.

ACKNOWLEGDEMENTS

This work was made possible by an Innovational Research Incentives Scheme Vici grant of The Netherlands Organisation for Scientific Research (NWO) to M.R. We thank Erik Manders and Ronald Breedijk for technical support. Special

thanks goes to Li-Jun Ma for provision of *Fo*47 genome sequence and optical map.

MATERIAL AND METHODS

Strains and culture conditions.

Fusarium oxysporum f. sp. *lycopersici* strain 4287 (*Fol*4287, FGSC9935) and the tomato non-pathogenic *Fusarium oxysporum* strain 47 (*Fo*47, FGSC10445) were used as the parental strains for fungal transformation. They were stored as a monoconidial culture at -80 °C and revitalized on potato dextrose agar (PDA) (Difco) at 25 °C. *Agrobacterium tumefaciens* EHA105 (47) was used for *Agrobacterium*-mediated transformation of *F. oxysporum* and was grown in either Luria broth (LB) or 2YT medium (48) containing 20 µg/ml rifampin at 28 °C. Introduction of the plasmids into the *Agrobacterium* strain was performed as previously described (49). *Escherichia coli* DH5α (Invitrogen) was used for construction, propagation, and amplification of the plasmid and was grown at 37 °C in LB medium containing 50 µg/ml kanamycin.

Construction of histone H1 fusion protein-expressing vector and *Agrobacterium*-mediated *Fusarium* transformation.

Construction of pRW2h-H1-GFP and pRW2h-H1-REF was described previously (39, 50). To generate an H1-RFP plasmid with the phleomycin resistance cassette, plasmids pRW2h-H1-RFP and pRW1p (51) were both digested with *Mfe*I and *Blp*I. The resulting fragment from pRW1p containing the phleomycin resistance gene was then ligated into the vector to create pRW2p-H1-RFP. The obtained plasmids pRW2h-H1-GFP, pRW2h-H1-RFP and pRW2p-H1-RFP were transformed into *Agrobacterium tumefaciens* EHA105 and the transformants used for subsequent *A. tumefaciens*-mediated *Fusarium* transformation. *Agrobacterium*-mediated transformation of *F. oxysporum* was performed as previously described (39).

CAT fusion assay.

*Fol*4287 conidia were collected from one-week-old PDA plates in 2 ml of the medium to be tested and filtered through one layer of sterile Miracloth (Calbiochem). 200 µl 7,5x10^5 conidia per ml were incubated in an 8-well microscope chamber slide (Nunc) for 15 to 18 hours. CAT fusion was tested in PDB (Difco), CDL (Oxoid), minimal medium (0.17 % yeast nitrogen base (YNB, Difco) without amino acids and ammonium sulfate, 100 mM KNO3), CAT medium (0.17 % YNB, 25 mM KNO_3), PDB supplemented with 10 µg/ml glutamic acid, minimal medium and CAT medium supplemented with 1 or 10 µg/ml tryptophan, CAT medium supplemented with 3 % sucrose, and water.

Observations were performed, if not otherwise stated, with the AMG Evos FL digital inverted microscope equipped with transmitted light, DAPI (357/44 to 447/60 nm), GFP (470/22 to 510/42 nm), and Texas Red (585/29 to 624/40 nm) light cubes, and driven by built-in software for image acquisition. Images were analyzed with the Fiji software from imageJ (http://fiji.sc/Fiji). CAT fusion frequency was calculated as the percentage of CAT fusions per germinated conidia. 300 to 3000 conidia were counted in two to four biological replicates.

Co-cultivation.
Conidia of *Fol*4287 H1-RFP (*ble*), *Fol*4287 H1-GFP (*hph*), and *Fo*47 H1-GFP (*hph*) were collected from one-week-old PDA plates in 2 ml water, filtered through one layer of sterile Miracloth (Calbiochem), and washed with water. To detect viable heterokaryons in *F. oxysporum,* 10^6 conidia of *Fol*4287 H1-GFP (*hph*) and *Fo*47 H1-GFP (*hph*) were co-incubated in PDB, minimal medium or water for two to five days. After one round of monosporing, single spore colonies were tested for presence of yellow nuclei (i.e. red and green) and incubated for four to six months to monitor nuclear composition (inverted agar block method, Hickey et al., 2004).

Conidial pairing.
To test CAT fusion frequency, 100 µl 7,5x10^5 conidia per ml from each parental strain were incubated in an 8-well microscope chamber slide (Nunc) for 15 to 18 hours. Cat fusion was tested in CAT medium containing 0,25 %, 0,5 %, or 1 % xylose. CAT fusion frequency was calculated based on three to four biological replicates and ~ 300 conidia per replicate. To select heterokaryotic cells, 500 µl 10^6 conidia per ml from each parental strain were incubated in a 1-well microscope chamber slide (Nunc) and after two days 50 µl of the mix was plated on PDA and incubated for two days. Again conidia were collected and washed and 10 µl 10^6 conidia per ml were incubated on PDA buffered with 0,1 M Tris (pH 8) and supplemented with 100 µg/ml hygromycin (Duchefa) and 100 µg/ml zeocin (Invivogen) for five days.

Hyphal tip pairing.
Conidia of *Fol*4287 H1-RFP (*ble*), and *Fo*47 H1-GFP (*hph*) were collected from one-week-old PDA plates in 2 ml water, filtered through one layer of sterile Miracloth (Calbiochem), and washed with water. Conidia of each parental line were applied on CAT medium supplemented with 1 % agarose and 0,25 % xylose in lines 2 cm apart from each other and incubated until the hyphae met. An agarose block from this area was transferred to PDA containing hygromycin and zeocin. Outgrowth of double-selective hyphae was monitored.

Observation of heterokaryotic colonies

Live-cell imaging of CAT fusion and early development of heterokaryotic colonies.

To investigate CAT formation and fusion, conidia of *Fol*4287 H1-RFP (*ble*), *Fol*4287 H1-GFP (*hph*), and *Fo*47 H1-GFP (*hph*) were collected from one-week-old PDA plates in 2 ml water, filtered through one layer of sterile Miracloth (Calbiochem), and washed with water. 100 µl 10^6 conidia per ml from each parental line were mixed and 20 µl was mounted on CAT medium supplemented with 1 % agarose and 0,25 % xylose in the shape of a microscope slide. These were incubated conidia phase down in a 1-well microscope chamber slide (Nunc) and observed after 15 hours. To monitor early development of heterokaryotic cells conidia of the parental lines were co-incubated in CAT medium containing 0,25 % xylose for two days prior to mounting on agarose slides.

Live-cell imaging was performed using an Eclipse Ti inverted microscope (Nikon) equipped with an EM-CCD iXon DU897 camera (Andor), and a plan apo VC 40X 1.4 oil objective (Nikon). GFP was excited with a 488-nm light (emission 525-50 nm BP filter) and RFP with a 561-nm light (emission 600-37 nm BP filter). Pictures were analyzed with the Nikon NIS and Fiji software from imageJ (http://fiji.sc/Fiji).

Development of hybrid offspring.

Double-selective colonies were transferred on CDL plates supplemented with 1 % agarose and 2 % xylose. After one week nuclear composition of young hyphae from the edge of the colony was determined. Nuclear localization was confirmed by DNA counterstaining. For this the mycelium was treated for 1 min with 1 mg/ml Hoechst 33342 (Life Technologies) and washed with water before microscopy. To test chromosomal composition, DNA extraction was performed, and an agarose block from the edge of the colony was transferred to a fresh plate for the next time point. This was repeated until only one of the two fluorescent signals was detected.

Chromosomal composition

To test for the presence of *Fol*4287 and *Fo*47 chromosomes primers based on FOXY insertion sites in *Fol*4287 were used. FOXY transposons are enriched in pathogenic strains of *F. oxysporum*. For each chromosome of *Fol* a locus-specific primer was used together with a FOXY specific primer (5). Similarly, for the same region two specific primers were designed for *Fo*47 (Table S1; for an alignment of *Fol*4287 and *Fo*47 chromosomes see Fig S1)

REFERENCES

1. Gladieux P, Ropars J, Badouin H, Branca A, Aguileta G, de Vienne DM, Rodríguez de la Vega RC, Branco S, Giraud T. 2014. Fungal evolutionary genomics provides insight into the mechanisms of adaptive divergence in eukaryotes. Mol Ecol 23:753–73.

2. Karasov TL, Horton MW, Bergelson J. 2014. Genomic variability as a driver of plant-pathogen coevolution? Curr Opin Plant Biol 18:24–30.

3. Perez-Nadales E, Almeida Nogueira MF, Baldin C, Castanheira S, El Ghalid M, Grund E, Lengeler K, Marchegiani E, Mehrotra PV, Moretti M, Naik V, Oses-Ruiz M, Oskarsson T, Schäfer K, Wasserstrom L, Brakhage AA, Gow NAR, Kahmann R, Lebrun M-H, Perez-Martin J, Di Pietro A, Talbot NJ, Toquin V, Walther A, Wendland J. 2014. Fungal model systems and the elucidation of pathogenicity determinants. Fungal Genet Biol 70:42–67.

4. Takken F, Rep M. 2010. The arms race between tomato and Fusarium oxysporum. Mol Plant Pathol 11:309–14.

5. Ma LJ, van der Does HC, Borkovich KA, Coleman JJ, Daboussi MJ, Di Pietro A, Dufresne M, Freitag M, Grabherr M, Henrissat B, Houterman PM, Kang S, Shim WB, Woloshuk C, Xie X, Xu JR, Antoniw J, Baker SE, Bluhm BH, Breakspear A, Brown DW, Butchko RA, Chapman S, Coulson R, Coutinho PM, Danchin EG, Diener A, Gale LR, Gardiner DM, Goff S, Hammond-Kosack KE, Hilburn K, Hua-Van A, Jonkers W, Kazan K, Kodira CD, Koehrsen M, Kumar L, Lee YH, Li L, Manners JM, Miranda-Saavedra D, Mukherjee M, Park G, Park J, Park SY, Proctor RH, Regev A, Ruiz-Roldan MC, Sain D, Sakthikumar S, Sykes S, Schwartz DC, Turgeon BG, Wapinski I, Yoder O, Young S, Zeng Q, Zhou S, Galagan J, Cuomo CA, Kistler HC, Rep M. 2010. Comparative genomics reveals mobile pathogenicity chromosomes in Fusarium. Nature 464:367–373.

6. Coleman JJ, Rounsley SD, Rodriguez-Carres M, Kuo A, Wasmann CC, Grimwood J, Schmutz J, Taga M, White GJ, Zhou S, Schwartz DC, Freitag M, Ma LJ, Danchin EG, Henrissat B, Coutinho PM, Nelson DR, Straney D, Napoli CA, Barker BM, Gribskov M, Rep M, Kroken S, Molnár I, Rensing C, Kennell JC, Zamora J, Farman ML, Selker EU, Salamov A, Shapiro H, Pangilinan J, Lindquist E, Lamers C, Grigoriev I V, Geiser DM, Covert SF, Temporini E, Vanetten HD. 2009. The genome of Nectria haematococca: contribution of supernumerary chromosomes to gene expansion. PLoS Genet 5:e1000618.

7. Lievens B, Houterman PM, Rep M. 2009. Effector gene screening allows unambiguous identification of Fusarium oxysporum f. sp. lycopersici

races and discrimination from other formae speciales. FEMS Microbiol Lett 300:201–15.

8. Michielse CB, Rep M. 2009. Pathogen profile update: Fusarium oxysporum. Mol Plant Pathol 10:311–24.

9. van der Does HC, Rep M. 2012. Horizontal transfer of supernumerary chromosomes in fungi. Methods Mol Biol 835:427–37.

10. Soanes D, Richards TA. 2014. Horizontal gene transfer in eukaryotic plant pathogens. Annu Rev Phytopathol 52:583–614.

11. Rosewich UL, Kistler HC. 2000. Role of horizontal gene transfer in the evolution of fungi. Annu Rev Phytopathol 38:325–363.

12. Mehrabi R, Bahkali AH, Abd-Elsalam KA, Moslem M, Ben M'barek S, Gohari AM, Jashni MK, Stergiopoulos I, Kema GH, de Wit PJ. 2011. Horizontal gene and chromosome transfer in plant pathogenic fungi affecting host range. FEMS Microbiol Rev 35:542–554.

13. Akagi Y, Akamatsu H, Otani H, Kodama M. 2009. Horizontal chromosome transfer, a mechanism for the evolution and differentiation of a plant-pathogenic fungus. Eukaryot Cell 8:1732–1738.

14. He C, Rusu AG, Poplawski AM, Irwin JA, Manners JM. 1998. Transfer of a supernumerary chromosome between vegetatively incompatible biotypes of the fungus Colletotrichum gloeosporioides. Genetics 150:1459–1466.

15. Fitzpatrick DA. 2012. Horizontal gene transfer in fungi. FEMS Microbiol Lett 329:1–8.

16. Read ND, Lichius A, Shoji J, Goryachev AB. 2009. Self-signalling and self-fusion in filamentous fungi. Curr Opin Microbiol 12:608–15.

17. Simonin A, Palma-Guerrero J, Fricker M, Glass NL. 2012. Physiological significance of network organization in fungi. Eukaryot Cell 11:1345–52.

18. Glass NL, Dementhon K. 2006. Non-self recognition and programmed cell death in filamentous fungi. Curr Opin Microbiol 9:553–8.

19. Glass NL, Kaneko I. 2003. Fatal attraction: nonself recognition and heterokaryon incompatibility in filamentous fungi. Eukaryot Cell 2:1–8.

20. Glass NL, Jacobson DJ, Shiu PKT. 2000. The genetics of hyphal fusion and vegetative incompatibility in filamentous ascomycete fungi. Annu Rev Genet 34:165–186.

21. Manners JM, He C. 2011. Slow-growing heterokaryons as potential intermediates in supernumerary chromosome transfer between biotypes

of Colletotrichum gloeosporioides. Mycol Prog 10:383–388.

22. Ishikawa FH, Souza EA, Read ND, Roca MG. 2010. Live-cell imaging of conidial fusion in the bean pathogen, Colletotrichum lindemuthianum. Fungal Biol 114:2–9.

23. Read ND, Roca GM. 2000. Vegetative Hyphal Fusion in Filamentous Fungi. Landes Bioscience.

24. Roca GM, Arlt J, Jeffree CE, Read ND. 2005. Cell Biology of Conidial Anastomosis Tubes in Neurospora crassa. Eukaryot Cell 4:911–919.

25. Roca GM, Read ND, Wheals AE. 2005. Conidial anastomosis tubes in filamentous fungi. FEMS Microbiol Lett 249:191–8.

26. Ishikawa FH, Souza EA, Shoji JY, Connolly L, Freitag M, Read ND, Roca MG. 2012. Heterokaryon incompatibility is suppressed following conidial anastomosis tube fusion in a fungal plant pathogen. PLoS One 7:e31175.

27. Shoji JY, Charlton ND, Yi M, Young CA, Craven KD. 2015. Vegetative hyphal fusion and subsequent nuclear behavior in Epichloë grass endophytes. PLoS One 10:e0121875.

28. Castro-Prado MAA, Querol CB, Sant'Anna JR, Miyamoto CT, Franco CCS, Mangolin CA, Machado MFPS. 2007. Vegetative compatibility and parasexual segregation in Colletotrichum lindemuthianum, a fungal pathogen of the common bean. Genet Mol Res 6:634–42.

29. Milgroom MG, Sotirovski K, Risteski M, Brewer MT. 2009. Heterokaryons and parasexual recombinants of Cryphonectria parasitica in two clonal populations in southeastern Europe. Fungal Genet Biol 46:849–54.

30. Teunissen HAS, Verkooijen J, Cornelissen BJC, Haring MA. 2002. Genetic exchange of avirulence determinants and extensive karyotype rearrangements in parasexual recombinants of Fusarium oxysporum. Mol Genet Genomics 268:298–310.

31. Clutterbuck AJ. 1996. Parasexual recombination in fungi. J Genet 75:281–286.

32. Puhalla JE. 1985. Classification of strains of Fusarium oxysporum on the basis of vegetative compatibility. Can J Bot 63:179–183.

33. Fischer-Harman V, Jackson KJ, Muñoz A, Shoji J, Read ND. 2012. Evidence for tryptophan being a signal molecule that inhibits conidial anastomosis tube fusion during colony initiation in Neurospora crassa. Fungal Genet Biol 49:896–902.

34. Ruiz-Roldán MC, Köhli M, Roncero MI, Philippsen P, Di Pietro A, Espeso EA. 2010. Nuclear dynamics during germination, conidiation, and hyphal fusion of Fusarium oxysporum. Eukaryot Cell 9:1216–1224.

35. Roca GM, Kuo H-C, Lichius A, Freitag M, Read ND. 2010. Nuclear dynamics, mitosis, and the cytoskeleton during the early stages of colony initiation in Neurospora crassa. Eukaryot Cell 9:1171–83.

36. Gupta SB. 1969. Duration of mitotic cycle and regulation of dna replication in nicotiana plumbaginifolia and a hybrid derivative of n . tabacum showing chromosome instability. Can J Genet Cytol 11:133–142.

37. Laurie DA, Bennett MD. 1989. The timing of chromosome elimination in hexaploid wheat × maize crosses. Genome 32:953–961.

38. Bennett MD, Finch RA, Barclay IR. 1976. The time rate and mechanism of chromosome elimination in Hordeum hybrids. Chromosoma 54:175–200.

39. Shahi S, Beerens B, Manders EMM, Rep M. 2015. Dynamics of the Establishment of Multinucleate Compartments in Fusarium oxysporum. Eukaryot Cell 14:78–85.

40. Sengupta K, Camps J, Mathews P, Barenboim-Stapleton L, Nguyen QT, Difilippantonio MJ, Ried T. 2008. Position of human chromosomes is conserved in mouse nuclei indicating a species-independent mechanism for maintaining genome organization. Chromosoma 117:499–509.

41. Cieplinski W, Reardon P, Testa MA. 1983. Non-random human chromosome distribution in human-mouse myeloma somatic cell hybrids. Cytogenet Cell Genet 35:93–9.

42. Wang Z, Yin H, Lv L, Feng Y, Chen S, Liang J, Huang Y, Jiang X, Jiang H, Bukhari I, Wu L, Cooke HJ, Shi Q. 2014. Unrepaired DNA damage facilitates elimination of uniparental chromosomes in interspecific hybrid cells. Cell Cycle 13:1345–56.

43. Molnár A, Sulyok L, Hornok L. 1990. Parasexual recombination between vegetatively incompatible strains in Fusarium oxysporum. Mycol Res 94:393–398.

44. Sanei M, Pickering R, Kumke K, Nasuda S, Houben A. 2011. Loss of centromeric histone H3 (CENH3) from centromeres precedes uniparental chromosome elimination in interspecific barley hybrids. Proc Natl Acad Sci U S A 108:E498–505.

45. Gernand D, Rutten T, Varshney A, Rubtsova M, Prodanovic S, Brüss C,

Kumlehn J, Matzk F, Houben A. 2005. Uniparental chromosome elimination at mitosis and interphase in wheat and pearl millet crosses involves micronucleus formation, progressive heterochromatinization, and DNA fragmentation. Plant Cell 17:2431–8.

46. Chalker DL. 2008. Dynamic nuclear reorganization during genome remodeling of Tetrahymena. Biochim Biophys Acta 1783:2130–6.

47. Hood EE, Gelvin SB, Melchers S, Hoekema A. 1993. New Agrobacterium helper plasmids for gene transfer to plants (EHA105). Transgenic Res 2:208–218.

48. Sambrook J, Russel DW. 2001. Molecular Cloning: a Laboratory Manual. Col Spring Harbor Laboratory Press, New York.

49. Mattanovich D, Rüker F, Machado AC, Laimer M, Regner F, Steinkellner H, Himmler G, Katinger H. 1989. Efficient transformation of Agrobacterium spp. by electroporation. Nucleic Acids Res 17:6747.

50. Vlaardingerbroek I, Beerens B, Shahi S, Rep M. 2015. Fluorescence Assisted Selection of Transformants (FAST): Using flow cytometry to select fungal transformants. Fungal Genet Biol 76:104–9.

51. Houterman PM, Cornelissen BJ, Rep M. 2008. Suppression of plant resistance gene-based immunity by a fungal effector. PLoS Pathog 4:e1000061.

52. Hickey PC, Swift SR, Roca MG, Read ND. 2004. Live-cell imaging of filamentous fungi using vital fluorescent dyes and confocal microscopy.Methods in Microbiology. Elsevier.

SUPPLEMENTARIES

Table S1: Chromosome–specific primers based Foxy insertion sites in *Fol*4287.

*Fol*4287

Chr #	FP	Sequence forward primer	FP	Sequence reverse primer
1	2330	ATATGAAAGGGGTTCAAGGA	2378	GAGAGAATTCTGGTCGGTG
2	2334	AAAAGAATTGCTCGCGCTCT		
3	2340	GAGCAGATGGGCGTTCCCTA		
4	2344	AGTCCCTTGCGTCCAACCGA		
5	2346	ACCTCCCGAGAAGGTTATCA		
6	2350	ATTCATTGTCACATGCAGCC		
7	2353	GAGGAGATCAAGGACATTTT		
8	2357	ACCTTGGAGGAAATAAACTG		
9	2361	TGAAGTGGACTAAGGAGGAG		
10	4500	TTTTGGGTTCGAGATGGATA		
11	2367	GGACGGAGGGTAACAGGTAC		
12	2371	GAACGCTCGCGTGATGAAGC		
13	4507	GGGCTCCCATGTTTAGGTTC		
14	2374	ATCTCATAATCTGGCGGCTC		
15	2376	ACCGCACAAGACTCAACTAT		

*Fo*47

Chr #	FP	Sequence forward primer	FP	Sequence reverse primer
1	2331	GATCTAATTGAGTTATGAGCC	4483	TCCATGTCATAACCTGGTCT
2	2345	TAGATCCTCCCCTGGTGTCC	4487	AAGCGCTATAATGGGTCCTT
3	4490	TACTCAACGGATACAAAGTCAA	4489	CATGCATGGTTTGGTGGTTC
4	2336	GAATTCCTTGTAGAGGTGCT	4485	ATCGTCAGACTCTGGGGTTG
5	2355	GGAAAGTCTTCCGTGGCTTG	4492	TATCTTGGTGAGTTGACGCC
6	2358	CACTTCGAATACGTAGGCTG	4494	CTGTACCTCATTCATAAGCT GGT
7	4510	CAAAGAGCATGCCACCTATT	4508	ATCGAGGTGCTGTGTTTAGC
8	4497	TGGCAGCTCAGATCATGTTA	4496	CTCCTTACTTCAACGGCGTC
9	2364	GTTCTGAATGTCCTGAGGAA	4499	TATCTTATCGCGGAAGCTCA
10	2371	GAACGCTCGCGTGATGAAGC	4504	TGTCTCCTTCTGCGGGTTAC
11	2366	GGGCATAATTAAGCAGTGAT	4501	TGAGAGGTTAGAGGACGTGA A
12	2373	AGGCATCGTTTAATCGTTGG	4506	CTCCCACTCGACTGGCTAAG

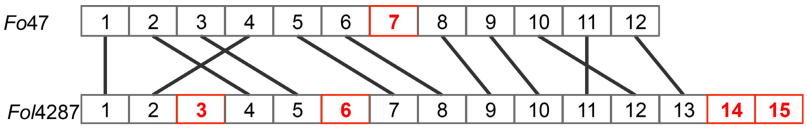

Figure S1: *Fol*4287 and *Fo*47 chromosome alignement. Numbers represent chromosomes. Red numbers represent lineage specific chromosomes. Based on optical mapping (Ma, personal communication).

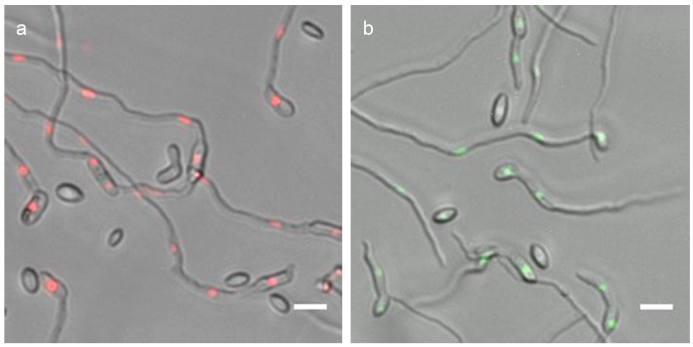

Figure S2: Phenotype of parental lines. a) *Fol*4287 expressing histone H1-RFP fusion protein, b) *Fo*47 expressing H1-GFP. Scale bar: 10µm.

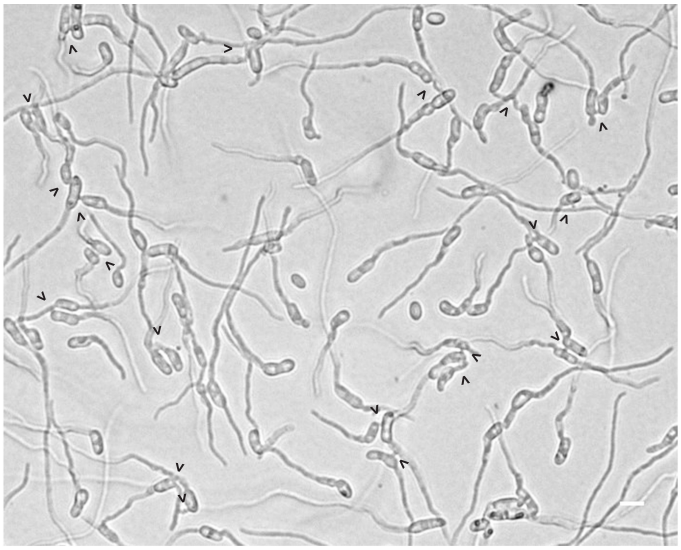

Figure S3: CAT fusion on optimized CAT medium. On medium with no carbon and low nitrate concentration CAT fusion frequency in *Fol*4287 is highly increased. Arrowheads: fused CATs, scale bar: 10µm.

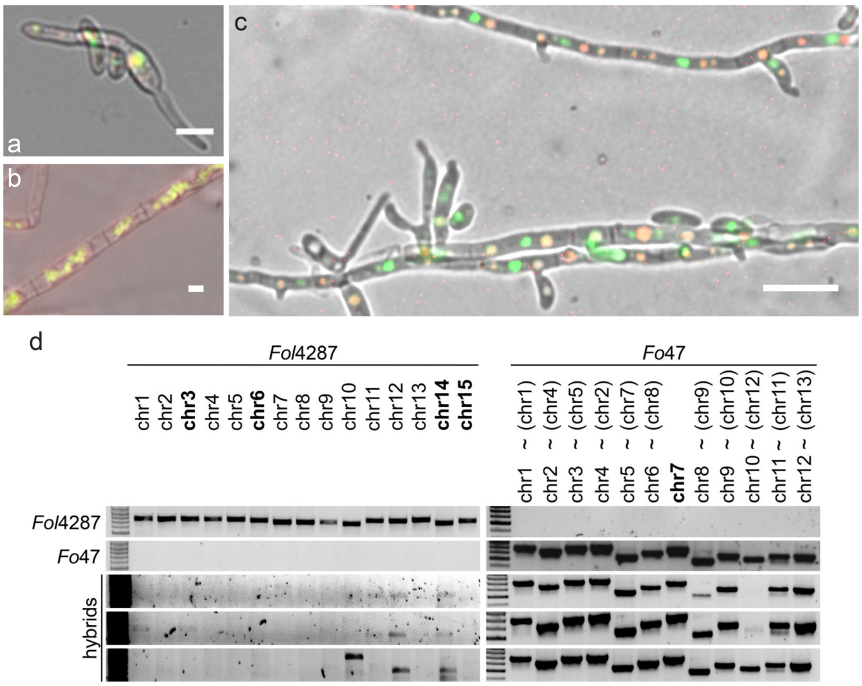

Figure S4: Development and chromosome composition of hybrid colonies. Heterokaryotic colonies produce uni-nucleate conidia that germinate like conidia of the parental lines (a). During further colony development nuclei appear fractionated and form micronuclei (b). After six months the fluorescent signal re-distributes into a mix of red, green, and yellow nuclei of different sizes (c). Scale bar: 10µm. Chromosome composition changes accordingly. A PCR-based test for specific chromosome markers for *Fol*4287 and *Fo*47 shows that at the beginning of the co-cultivation markers for both parental chromosomes are detected (upper PCR panels). After six months hybrid colonies show markers for *Fo*47 chromosomes plus the marker for *Fol*4287 chromosome 14 (middle PCR panel). In some cases also the marker for *Fol*4287 chromosome 12 is present. In theses trains the marker for the corresponding *Fo*47 chromosome (chromosome 10) is either absent or shows a weaker band (lower PCR panels, d). Bold letters mark lineage-specific chromosomes, *Fol*4287 homologous chromosomes of *Fo*47 chromosomes are shown in brackets.

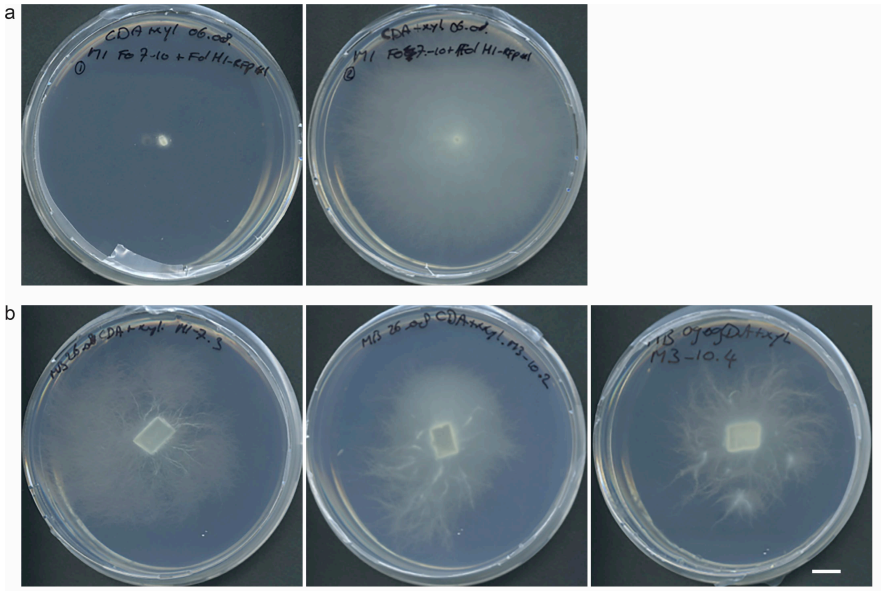

Figure S5: Phenotype of the heterokaryotic hybrid colonies. a) Colony size varies strongly between different colonies. b) Despite of the uniform growth of either of the parental lines, some of the heterokaryotic offspring show a patchy growth caused by increased branching, accelerated growth, or increased conidiation, respectively. Scale bar: 1cm.

SUPPRESSOR OF FUSION, A FUSARIUM OXYSPORUM HOMOLOG OF NDT80, IS REQUIRED FOR NUTRIENT-DEPENDENT REGULATION OF ANASTOMOSIS

Shermineh Shahi, Like Fokkens, Petra M.Houterman and Martijn Rep

ABSTRACT

Heterokaryon formation is an essential step in asexual recombination in *Fusarium oxysporum*. Filamentous fungi have an elaborate nonself recognition machinery to prevent formation and proliferation of heterokaryotic cells, called heterokaryon incompatibility (HI). In *F. oxysporum* the regulation of this machinery is not well understood. In *Neurospora crassa* Vib-1, a putative transcription factor of the p53-like Ndt80 family of transcription factors, has been identified as global regulator of HI. In this study we investigated the role of the *F. oxysporum* homolog of *VIB*-1, *SUF*, in vegetative hyphal and conidial anastomosis tube (CAT) fusion and HI. We identified a novel function for a *NDT80* homolog as a nutrient-dependent regulator of anastomosis. Strains carrying the *SUF* deletion mutation display a hyper-fusion phenotype during vegetative growth as well as germling development. In addition, conidial paring of incompatible *SUF* deletion strains led to more heterokaryon formation, which is independent of suppression of HI. Our data provides further proof for the divergence in the functions of different members *NDT*80 family. We propose that Ndt80 homologs mediate responses to nutrient quality and quantity, with specific responses varying between species.

INTRODUCTION

Filamentous fungi grow by hyphal tip expansion and branching. Hyphae at the growing edge of the colony display a growth pattern described as avoidance, in which hyphal tips show negative autotropism towards each other (1). Behind the growth front ongoing fusions, or anastomoses, between hyphae build a three dimensional network, the mycelium (2). In any given habitat different individuals not only of the same species but also of different species meet and can undergo vegetative hyphal fusion to form heterokaryons (2, 3).

In heterokaryotic cells one or more genetically distinct nuclei from each individual share a common cytoplasm (2). Although there are potential benefits to heterokaryon formation, such as functional polyploidy and mitotic genetic recombination, filamentous ascomycetes display an elaborate nonself recognition system, by which cells with genetically distinct nuclei are compartmentalized and subject to programmed cell death, a process referred to as heterokaryon incompatibility (HI, 4–6). It has been proposed that HI plays a role in restricting the transmission of pathogenic elements such as double-stranded RNAs and the exploitation by aggressive genotypes (7, 8).

Nonself recognition during HI is genetically regulated by allelic specification at *het* (for heterokaryon) loci and individuals that differ at one or more *het* loci are incompatible with each other (2, 3). In *Neurospora crassa* 11 unlinked *het* loci have been described to be involved in nonself recognition and HI, demonstrating the elaborate character of this immune system (2, 9). The *N. crassa HET-c / PIN-c* system has been studied as a model and it has been shown that incompatible interactions at these loci lead to severe growth reduction, decreased conidiation, and programmed cell death of the fusion cell and surrounding cells (2, 4, 5). *het* loci have been shown to encode a variety of products, however the HET domain (Pfam PF06985) is conserved among proteins involved in HI in *N. crassa* and *Podospora anserina* (10, 11). Predicted HET domain genes are common in, and specific to, filamentous ascomycete and basidiomycete genomes (12, 13).

In the past decade, extensive studies have been carried out in *N. crassa* to elucidate molecular mechanisms and genetic regulation of HI. Vib-1 was first identified as a regulator for *HET-c* mediated HI. In incompatible interactions between strains carrying the *VIB-1* deletion the phenotype associated with *HET-c / PIN-c* HI is suppressed (14). Further investigation revealed that Vib-1 is required for the expression of genes involved in HI, and these results collectively lead to the conclusion that Vib-1 is a global mediator of HI in *Neuropora* (9, 14). Furthermore it was established that Vib-1, like its *A. nidulans* homolog XprG, is a positive regulator of extracellular protease

production under carbon and nitrogen starvation (9, 15). *VIB-1* encodes a putative transcription factor of the *p53*-like *NDT*80 / PhoG DNA binding family. It was shown that the Ndt80 / PhoG DNA binding domain (Pfam PF05224) is conserved among ascomycete fungi (9, 16–20).

The filamentous ascomycete *Fusarium oxysporum* is an important plant pathogen and has been studied as a model organism for plant microbe interactions (for reviews see 21, 22). Although no apparent sexual recombination is known, the genomes of *F. oxysporum* species show a high degree of genetic variability (23). Additional comparative genome studies have demonstrated that *Fusarium* species share a conserved core genome, however, *F. oxysporum* and *F. solani* also carry lineage-specific chromosomes (24, 25, Fokkens personal communication). In the case of *F. oxysporum* it was demonstrated that small lineage specific chromosomes harboring essential virulence genes, also known as "pathogenicity" chromosomes, can be horizontally transferred to a non-pathogenic strain, and thereby conferring pathogenicity towards a specific host (25). We have recently described a mechanism in *F. oxysporum* that is likely to enable horizontal chromosome transfer under nutrient-limiting conditions (26). Although this study has added to our knowledge of the mechanics of asexual recombination, the genetic regulation as well as the molecular mechanics of nonself recognition and HI in *F. oxysporum* and their suppression during CAT fusion remain unclear. Given the similarity in phenotypes it was suggested that HI might share a common machinery between different fungal systems (5). The reference *F. oxysporum* genome encodes around 80 putative HET domain proteins (http://www.fungidb.org), yet, to our knowledge, none has been characterized. In this species vegetative compatibility groups (VCG) are determined using nitrate non-utilizing (NIT) mutants (27, 28).

Here we investigate the *F. oxysporum VIB-1* homolog, FOXG_01644 (*f. sp. lycopersici*) and FOMG_05487 (*f. sp. melonis*), for its role in vegetative fusion and nonself recognition. We show that the *F. oxysporum* homolog of Vib-1 is a nutrient-dependent negative regulator of hyphal and CAT fusion. In addition, conidial paring of strains carrying a deletion mutant yielded higher numbers of heterokaryotic cells. However, in contrast to *N. crassa*, the deletion mutant does not overcome HI nor is secretion of proteases affected. We suggest that the increase in heterokaryon formation is a result of increased CAT fusion and propose to rename FOXG_01644 / FOMG_05487 suppressor of fusion (*SUF*).

RESULTS

Fusarium oxysporum has four *NDT*80 homologs

It was previously shown that the number of *NDT80* homologs can vary between different filamentous ascomycetes (9, 29). The reference genome of *F. oxysporum* encodes four predicted proteins with a Ndt80 / PhoG binding domain that fall into three clades described earlier, a *VIB*-1 (vegetative incompatibility blocked, NCU03725) clade, a *FSD*-1 (female sexual development, NCU09915) clade, and a NCU04729 clade (9). *VIB*-1 and NCU04729 each have one ortholog in *F. oxysporum*. Interestingly, even though a sexual cycle is not known for *F. oxysporum*, there is a duplication of *FSD*-1 in *F. oxysporum* but not *F. graminearum* (Fig 1). With the aim to better understand the molecular underpinnings of vegetative fusion and nonself substitutions per amino acid site.
recognition in *F. oxysporum*, we decided to investigate the role of *N. crassa VIB*-1 homologs, FOXG_01644 and FOMG_05487, in these processes.

SUF deletion strains display a hyper-fusion phenotype under nutrient-limiting conditions

To understand the role of *F. oxysporum* homolog of *VIB*-1, we first studied the phenotype of *SUF* deletion mutants. We used a construct based on the flanking regions of *F. oxysporum f. sp. lycopersici* strain 4287 (*Fol*4287) FOXG_01644 to obtain deletion mutants in *Fol*4287, *F. oxysporum f. sp. melonis* strain 001 (*Fom*001), and *F. oxysporum* strain 47 (*Fo*47). None of the deletion mutants showed altered colony morphology or conidiation (data not shown). With around 6.5 x 10^6 conidia / ml the number of conidia produced after three days incubation in NO_3 medium was similar in all strains.

We next investigated the microscopic phenotype of the deletion mutants. For this we grew the wild type strain, two independent *SUF* deletion (*Δsuf*) mutants, and a complemented deletion strain from each background on PDA, CDA, and CAT medium supplemented with 1.5% agarose. PDA is rich in various carbon and nitrogen sources, CDA offers sucrose as the sole carbon and nitrate as the sole nitrogen source, and CAT medium offers no carbon source and limited nitrate (25 mM). Strains grown on PDA did not show any morphological differences between deletion mutant and wild type strains. However, under nutrient-limiting conditions (CDA and CAT medium), hyphae of the *SUF* deletion mutants of *Fol*4287 and *Fom*001, but not *Fo*47 *SUF* deletion strains nor the wild type, exhibited a strong increase in side-to-side fusions. Complemented strains, in which the *SUF* gene was reintroduced *in locus,* displayed a similar phenotype as the wild type strains (Fig 2). Interestingly, not

all hyphae that came into close proximity showed side-to-side fusion nor did we observe a specific pattern, *e.g.* in the distance between the fusions.

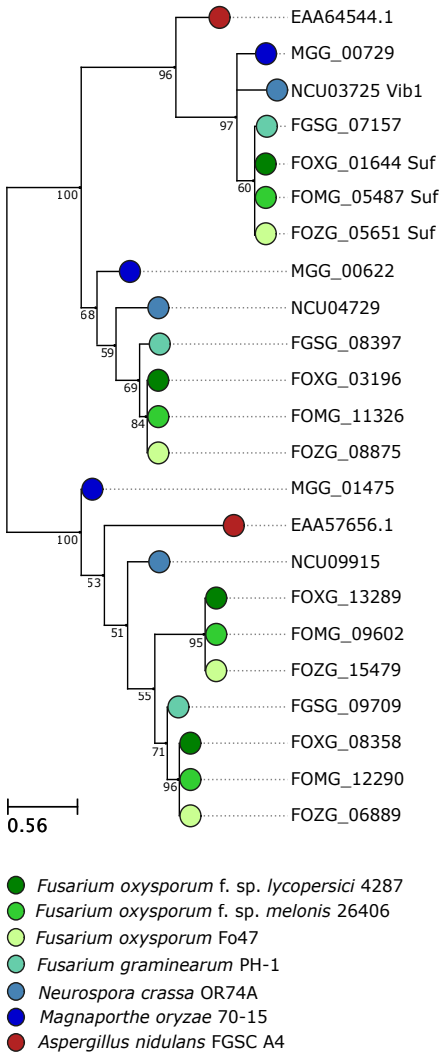

Fig 1: Phylogenetic tree displaying the relationship of *F. oxysporum Ndt*80 homologs to homologs in several other ascomycetes. The tree is based on alignments of NDT80 / PhoG DNA binding domains (PF05224). Each colored circle represents a species. The appearance of the branch illustrates bootstrap values: grey - bootstrap values 50-80, black - bootstrap values 80-90, bold black: bootstrap values > 90. Scale bar indicates number of

→ **Fig 2: *SUF* deletion strains of *Fol*4287 and *Fom*001, but not *Fo47*, display increased vegetative hyphal fusion.** a) In CDA and CAT medium, *Fol*4287 and *Fom*001 strains carrying the *SUF* deletion mutation exhibit higher numbers of hyphal fusion. This phenotype is reversed in the respective complementation strains. *Fo*47 does not undergo vegetative hyphal fusion. Depicted are average and standard errors of hyphal fusion per 0,5 mm^2. The calculation is based on 15 areas from 3 biological replicates. b) *Fol*4287 and *Fom*001 phenotypes on CDA. Arrowheads mark side-to-side fusions. Scale bar: 100 µm.

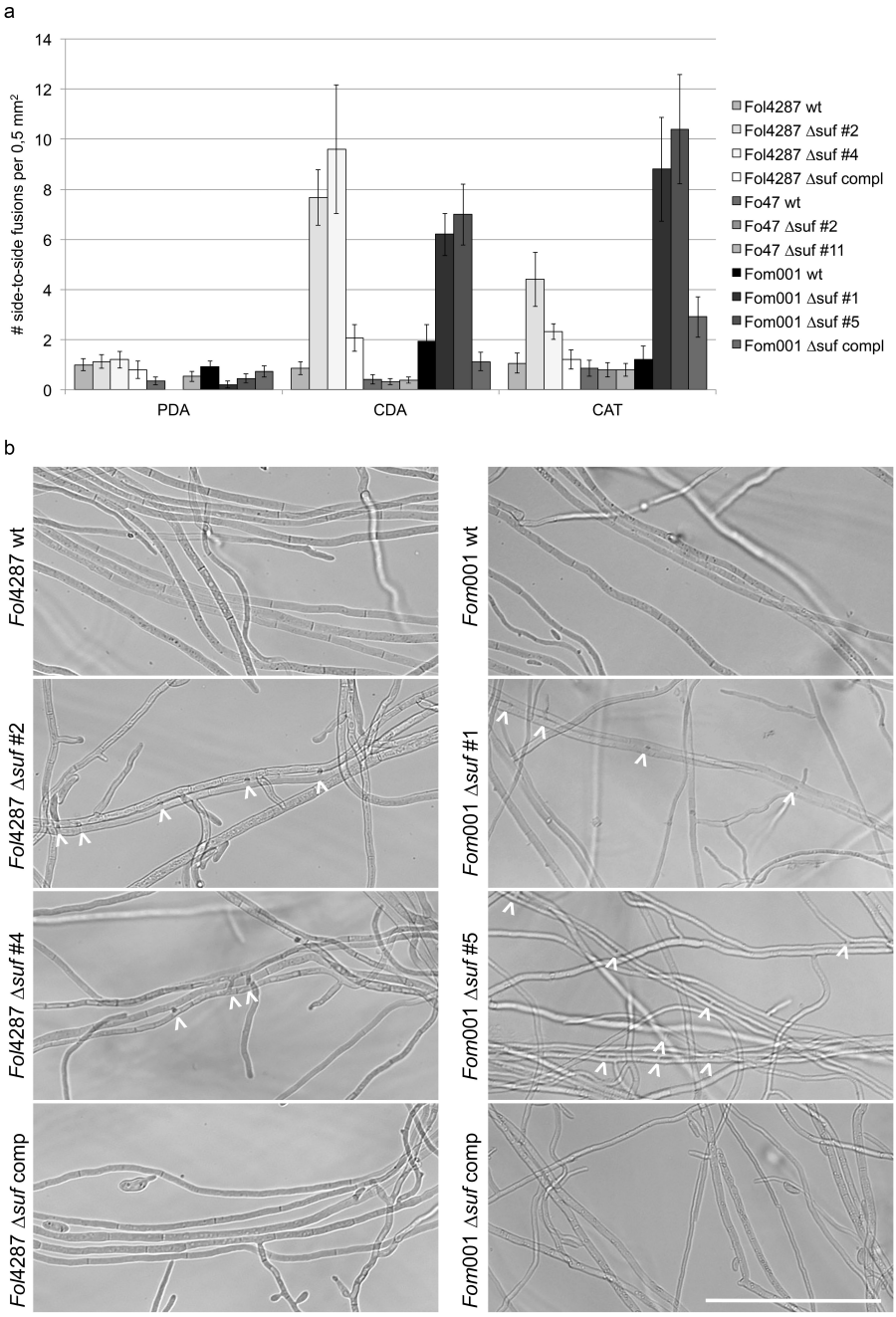
a
side-to-side fusions per 0,5 mm²
14
12
10
8
6
4
2
0
PDA
CDA
CAT
Fol4287 wt
Fol4287 Δsuf #2
Fol4287 Δsuf #4
Fol4287 Δsuf compl
Fo47 wt
Fo47 Δsuf #2
Fo47 Δsuf #11
Fom001 wt
Fom001 Δsuf #1
Fom001 Δsuf #5
Fom001 Δsuf compl
b
Fol4287 wt
Fol4287 Δsuf #2
Fol4287 Δsuf #4
Fol4287 Δsuf comp
Fom001 wt
Fom001 Δsuf #1
Fom001 Δsuf #5
Fom001 Δsuf comp

We examined 15 areas of 0.5 mm² in three biological replicates. In PDA, all strains showed very little or no hyphal fusion (Fig 2a, PDA). In CDA, *Fol*4287 *SUF* deletion mutants peaked at 8 and 10 fusions / area, and *Fom*001 *SUF* deletion mutants at 6 and 7 fusions / area (Fig 2a, CDA). In CAT medium the situation was reversed: *Fol*4287 mutants showed lower numbers of fusion / area (2 and 4) than *Fom*001 mutants (9 and 10 fusions / area, Fig 2a, CAT). *Fo*47 did not show any differences in number of fusions between the different media – the number was low in all cases. This hyper-fusion phenotype is distinct from what has been described for any of the *NDT*80 homologs so far (9, 29–31).

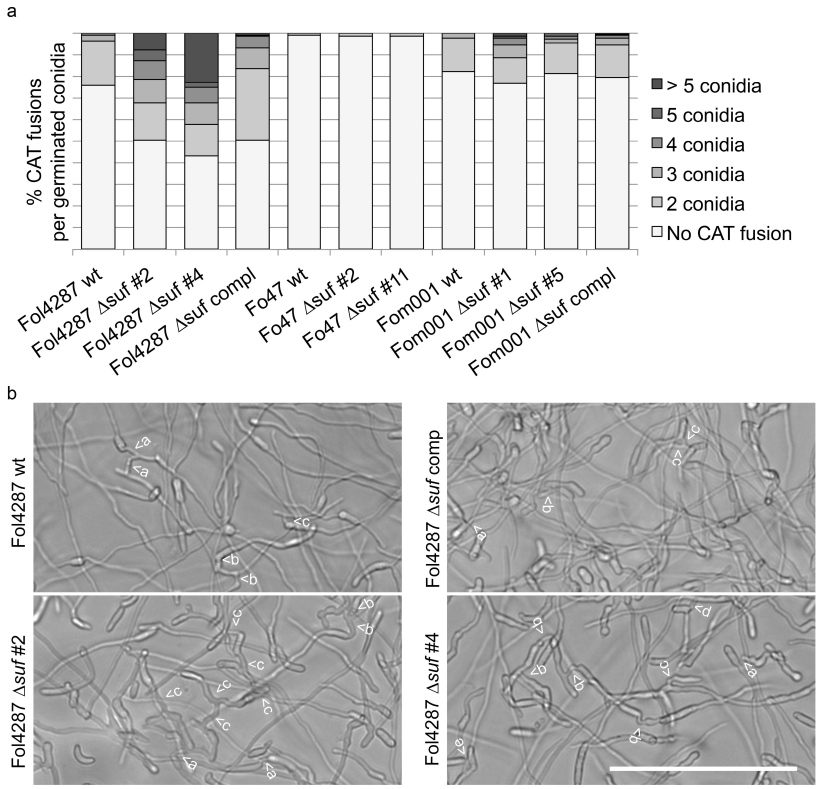

Fig 3: Fol4287 SUF deletion strains exhibit higher fusion rates during germling development. a) Fol4287 SUF deletion strains grown in CAT medium show higher conidial anastomosis tube (CAT) fusion rates. In addition, the number of conidia that are connected increase. Fom001 SUF deletion strains do not exhibit a significant difference to the wild type strain, although a tendency towards more connected conidia was observed. Fo47 does not undergo CAT fusion. Presented are percentages of CAT fusions connecting 1, 2, 3, 4, 5, and >5 conidia per germinated spores. Calculations are based on 1000 to 2500 conidia and 2 biological replicates. b) CAT fusion in Fol4287 wild type (wt) and SUF deletion strain (Δsuf #2). Arrowheads mark CAT fusions. A letter indicates conidia that are interconnected. Scale bar: 100 µm.

We next decided to investigate another type of fusion, CAT (for conidial anastomosis tube) fusion. In contrast to vegetative hyphal fusion that can occur throughout the colony, CAT fusion is restricted to the developmental stage of colony initiation (32, 33). We have observed that CAT fusion in *F. oxysporum* is restricted to carbon starvation and nitrogen limitation and obtained the highest frequency of CAT fusion in a medium with no carbon source and 25 mM nitrate, thus naming this medium CAT medium (26). To test whether *SUF* deletion also has an effect on CAT fusion, we incubated spores of each strain (wild type, two independent deletion mutants, and a complemented strain in each background) in CAT medium for 18 hours. We observed that *Fol*4287 *SUF* deletion mutants exhibit not only an increase CAT fusion, but also an increase in number of conidia that are interconnected (Fig. 3). In the wild type strain we mostly found two conidia and to a much lesser extent three conidia that are connected, whereas in the *SUF* deletion mutant more than five conidia could be part of an interconnected network (Fig 3b). We calculated the percentage of CAT fusions connecting 2, 3, 4, 5 and >5 conidia per germinated conidia based on two biological replicates and 1000 to 2500 conidia. Overall, with *Fol*4287 *SUF* deletion strains the percentage of CAT fusions doubled compared to wild type. About half of the CAT fusions connected more than 3 conidia in the mutants. In the complemented strain the wild type phenotype was partially restored. The percentage of total CAT fusion was not much reduced, but the number of conidia that were connected decreased to wild type level. In *Fom*001 *SUF* deletion mutants the phenotype was less severe, appearing only marginally significant. No increase in percentage of total CAT fusion was detected. However, there was a tendency that more than two conidia are connected through CAT fusions (Fig 3a). *Fo*47 did not show any CAT fusions and *SUF* deletion did not have an effect on this (Fig 3). We decided to continue our further investigations with *Fol*4287 and *Fom*001.

Differential localization of Suf-GFP is regulated by medium composition and nutrient availability

Both Ndt80 and Vib-1 are transcription factors and studies in *N. crassa* detected localization of Vib-1 to the nucleus (9). To test whether Suf also functions in the nucleus, we performed a localization study. Given that the hyper-fusion phenotype of the deletion mutants was specific to nutrient limitation, we considered that Suf localization might also be differentially regulated by nutrient availability. We assessed Suf-GFP localization in three independent transformants grown on PDB, CDL and CAT medium supplemented with 1.5 % agarose and 0.5 % xylose for induction of the xylanase promoter controlling *SUF-GFP* expression. Interestingly, we did not detect any fluorescence in strains grown on PDB (data not shown). Studies in *N. crassa*

demonstrated that Vib-1 localization is independent of the promoter (native or overexpressive, Dementhon et al., 2006). This suggests posttranscriptional regulation of Suf protein levels. Under nutrient-limiting conditions (CDL and CAT) however, Suf-GFP localized to subcellular bodies (Fig 4). Counterstain with the nuclear dye Hoechst 33342, however, did not confirm nuclear localization (data not shown). As was the case with fusions along hyphae in the deletion mutants, localization of Suf-GFP was not uniform (Fig 4). These results stand in contrast to findings in *N. crassa,* where Vib-1-GFP was detected in all nuclei (9).

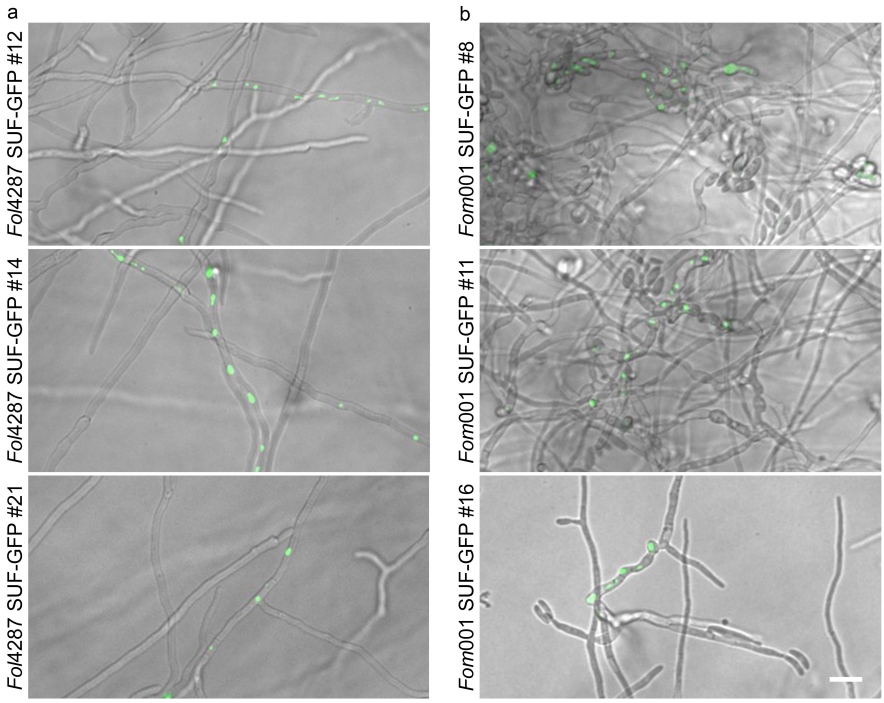

Figure 4: In synthetic medium SUF-GFP accumulates in subcellular bodies. In *Fol*4287 SUF-GFP (a) and *Fom*001 SUF-GFP (b) strains grown on CDA GFP signal was detected in subcellular bodies. Although under the control of a constitutive promoter the phenotype was not uniform and only detected in some hyphae. Scale bar: 10 µm.

SUF deletion strains display increased heterokaryon formation but no suppression of HI-associated cell death

Under nutrient-limiting conditions CAT fusion between incompatible strains of *F. oxysporum* allows heterokaryon formation (Shahi et al, submitted). *N. crassa* Vib-1 has been described as a global regulator of HI (9). We investigated the

effect of *SUF* deletion on heterokaryon formation between *Fol*4287 and *Fom*001 during conidial pairing. For this we co-cultivated *Fol*4287 expressing phleomycin resistance and *Fom*001 expressing hygromycin resistance and allowed for conidium formation. 10^4 conidia emerging from the mixed incubation were plated on double-selection PDA plates (*i.e.* containing both hygromycin and zeocin) and the percentage of emerging colonies was calculated. Co-cultivation of *Fol*4287 and *Fom*001 wild type (at the *SUF* locus) yielded no double-selective colonies. We tested four different combinations of *Fol*4287 Δ*suf* and *Fom*001 Δ*suf* strains. In all combinations double drug-resistant colonies emerged: *Fol*4287 Δ*suf* #2 and *Fom*001 Δ*suf* #1 (9.4 ± 2.1 %), *Fol*4287 Δ*suf* #2 and *Fom*001 Δ*suf* #5 (2.5 ± 1.3 %), *Fol*4287 Δ*suf* #4 and *Fom*001 Δ*suf* #1 (14.1 ± 3.5 %), and *Fol*4287 Δ*suf* #4 and *Fom*001 Δ*suf* #5 (1.4 ± 0.9 %, average and standard deviation based on 10 replicates). This demonstrates that, similar to *N. crassa*, deletion of *SUF* increases heterokaryon formation.

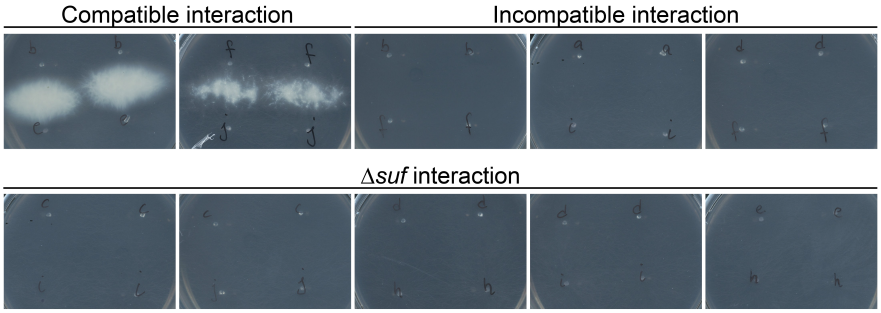

Figure 5: *SUF* deletion does not overcome heterokaryon incompatibility. In *F. oxysporum* vegetative compatibility is tested using nitrate non-utilizing (NIT) mutants. Compatible strains carrying different NIT mutations can complement the NIT phenotype (thin growth on nitrate medium) resulting in formation of aerial hyphae. Pairing of complementing *Fol*4287 and *Fom*001 NIT mutants resulted in production of aerial hyphae (compatible interaction), whereas the pairing of *Fol*4287 with *Fom*001 did not complement the NIT phenotype (incompatible interaction). The same results were obtained in different pairings between *Fol*4287 and *Fom*001 *SUF* deletion strains (Δ*suf* interaction). a: *Fol*4287 Nit1, b: *Fol*4287 NitM, c: *Fol*4287 Δ*suf* Nit1, d: *Fol*4287 Δ*suf* NitM, e: *Fol*4287 Δ*suf* Nit3, f: *Fom*001 Nit1, h: *Fom*001 Δ*suf* Nit1, i: *Fom*001 Δ*suf* Nit3, j: *Fom*001 Δ*suf* NitM.

We next tested whether the increase in heterokaryon formation is caused by a general suppression of HI-mediated cell death, as was described for *N. crassa*. As mentioned earlier, the mechanisms underlying nonself recognition and HI are not well understood in *F. oxysporum*. In species in which allelic interactions of HI are not known, heterokaryon formation can be tested using nitrate non-utilizing (NIT) mutants. NIT mutants display thin growth on media containing nitrate as a sole nitrogen source. Strains with different NIT mutations are able

to complement each other only when they are able to form heterokaryons and are thus compatible with each other (27, 28). Complementation is apparent from aerial hyphae formation where hyphae of the two strains meet. We used the VCG testing system to determine whether *SUF* deletion mutants can overcome HI during vegetative growth. For this we selected at least one NIT mutant per strain (*Fol*4287 wt, *Fol*4287 Δ*suf* #2, *Fom*001 wt, and *Fom*001 Δ*suf* #1, for phenotype on nitrate medium see Fig S2). As was expected, the positive control, *i.e.* interaction between compatible strains or selfing, resulted in formation of aerial hyphae (Fig 5, upper left panel). Neither the interaction between *Fol*4287 and Fom001 wild type nor *SUF* deletion strains resulted in formation of aerial hypha, thus marking these strains as incompatible (Fig 5, upper right and bottom panel). We conclude that the increase in heterokaryon formation observed upon mixing of conidia is caused by the increase in CAT fusion and that, unlike *N. crassa Vib*-1, Suf is not involved in regulation of HI.

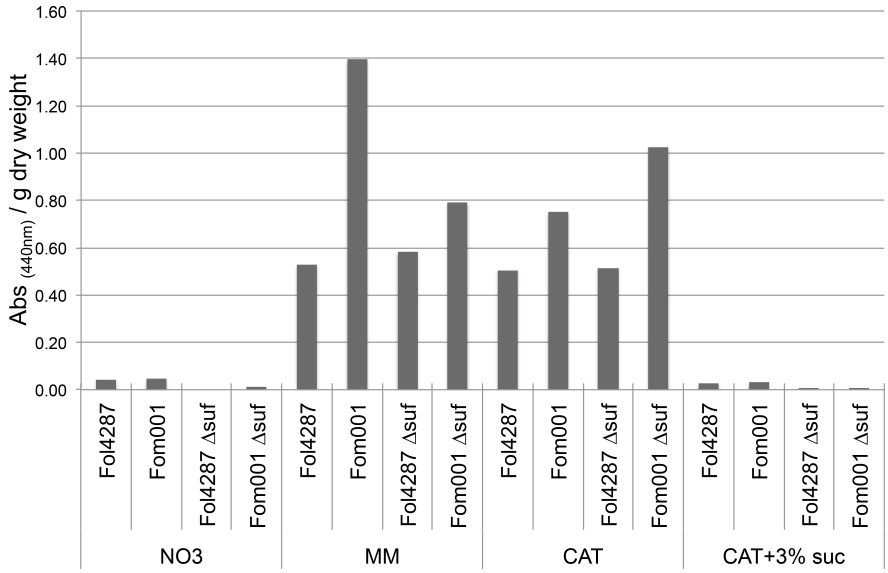

Figure 6: In *F. oxysporum* the production of extracellular proteases in response to carbon and nitrogen starvation is independent of *SUF*. *Fol*4287 and *Fom*001 wild type and *SUF* deletion strains were assessed for extracellular protease activity. Protease activity was determined by measuring the release of the trichloroacetic acid (TCA)-soluble orange sulfanilamide component of azocasein upon proteolysis at 440nm. Results are displayed as absorbance per gram dry weight. *F. oxysporum* extracellular protease production is, similar to *N. crassa* and *A. nidulans*, triggered by carbon source starvation (MM and CAT medium) but the *F. oxysporum Ndt*80 homolog Suf deletion does not suppress the induction of protease production.

Suf is not important for secretion of proteases or for carbon utilization.

Another phenotype that has been associated with *NDT*80 homologs *VIB*-1 and *XprG* is absence of extracellular proteases in the culture medium in the respective deletion mutants. In *N. crassa* and *A. nidulans* extracellular protease production is induced upon carbon or nitrogen starvation (9, 16). We examined culture supernatants of *Fol*4287 and *Fom*001 wild type and *SUF* deletion mutants for protease activity in different media (NO_3, minimal medium (MM), CAT, and CAT + 3 % sucrose). Similar to *N. crassa* and *A. nidulans*, extracellular protease production is strongly induced under nutrient-limiting condition in *F. oxysporum* (MM and CAT). However, *SUF* deletion had no effect on protease production (Fig 6). We also found no major differences in culture supernatant protein profiles using SDS-PAGE between wild type and *SUF* deletion mutants in any of the media (Fig S3). We conclude that Suf does not play a major role in protease production in *F. oxysporum* in response to carbon or nitrogen starvation.

In another study a link between Vib-1 and carbon utilization was demonstrated (30). We analyzed carbon source utilization using BIOLOG FF MicroPlates, which contain a different carbon source in each of the 96 wells. The ratios between *Fol*4287 *SUF* deletion strain and wild type strain growth rates were calculated. Values higher than 1.5 or lower than 0.5 are considered a substantial difference in growth rate (34). In our assay, the *SUF* deletion strain performed similar to the wild type strain on all tested carbon sources. Thus, Suf is not required for utilization of these carbon sources.

DISCUSSION

In this study we present a novel role for the F. oxysporum *NDT80* homolog suppressor of fusion (*SUF*) as a nutrient-dependent negative regulator of vegetative hyphal and CAT fusion. *Fol*4287 and *Fom*001 strains carrying a *SUF* deletion show increased vegetative hyphal fusion and in case of *Fol*4287 also increased CAT fusion (Fig 2 and 3). Genes negatively regulating fusion have rarely been characterized. To our knowledge only two genes have been identified, the *N. crassa* NCU006362, a predicted GTPase activating protein, and *SPR7*, a secreted serine protease (35). In both cases the deletion strain exhibits higher CAT fusion frequencies and higher numbers of connected conidia. It was suggested that both genes are involved in fungal communication prior to fusion (35).

We also established that the localization of Suf-GFP to subcellular bodies is triggered by nutrient limitation. in no other *NDT*80 homolog studied so far, a differential localization as a response to nutrient availability has been reported.

In our experiment Suf-GFP was under the control of an inducible promoter, and although constitutively expressed, in rich medium (PDA and CAT + 3 % sucrose) no Suf-GFP signal was detected. This indicates that Suf localization and/or accumulation is post-transcriptionally regulated. The *N. crassa* Vib-1 exhibits dynamic localization during asexual differentiation and HI and it was suggested that this also is post-transcriptionally regulated (9). Another striking difference to other *NDT*80 homologs is that in *F. oxysporum* the localization of Suf-GFP, similar to hyphal fusions in the *SUF* deletion mutant, is not uniform (Fig 4). We propose that under nutrient-limiting conditions Suf is post-transcriptionally altered and accumulates to these subcellular bodies, where it in turn negatively regulates hyphal and CAT fusion. Further research will be needed to elucidate what these bodies are and how the accumulation of Suf-GFP is regulated.

Despite (almost) identical protein sequences of the *SUF* homologs in the three *F. oxysporum* strains analyzed in this study, the deletion strains show different phenotypes. We have previously observed that *Fo*47 has a fusion defect and does not undergo vegetative fusion in form of hyphal or CAT fusion and confirmed this phenotype in this study (27 and Fig 2 and 3). *SUF* deletion does not overcome this fusion defect, indicating that either the two processes are unlinked or that the fusion defect of *Fo*47 is caused by a protein downstream of Suf, maybe even a target of Suf. The differences in phenotype between *Fol*4287 and *Fom*001 *SUF* deletion strains could also be caused by differences in Suf targets.

We show that *SUF* deletion increases heterokaryon formation but does not suppress HI. The increase in heterokaryon formation could be caused by the observed increase in CAT fusion frequency. Studies in other ascomycete fungi have shown that *NDT*80 homologs play different roles in ascomycete fungi. *Saccharomyces cerivisiae NDT*80, the founder of this family of p53-like transcription factors, is a transcriptional activator of ~150 genes involved in completion of meiosis (31). In *Candida albicans* one *NDT*80 homolog has been characterized, which is involved in drug resistance, biofilm formation, and virulence (36–39). The filamentous ascomycete *A. nidulans* has two *NDT*80 homologs. The closer homolog to *NDT*80 is involved in sexual reproduction. The second homolog, *XprG*, which is more closely related to *N. crassa VIB*-1, has been shown to be a transcriptional activator of a large number of genes in response to carbon limiting conditions (29). The *N. crassa* Vib-1 was characterized as a global regulator of heterokaryon incompatibility (HI) and a positive regulator of extracellular protease production under carbon and nitrogen starvation (9, 30). A second *NDT*80 homolog, *FSD*-1, is involved in

female sexual development, a process that is initiated under nitrogen limiting conditions (20). The one apparent commonality across these diverse functions is activation under nutrient-limiting conditions. Although this has not been tested for *N. crassa VIB*-1, in *P. anserina* HI is associated with the response to starvation (40). It was suggested that nutrient sensing might represent one of the ancestral roles for Ndt80 family of proteins (9, 19, 29). Our data provides further support for this hypothesis.

Phylogenetic analyses revealed that the Ndt80 DNA-binding domain (DBD) is conserved among ascomycete fungi, but the proteins have diverged outside this domain (Fig 1). The question that arises is how these different *NDT*80 homologs can respond to the same environmental cues. It is possible that the proteins are activated through a conserved mechanism despite sequence divergence. Alternatively, the expression of *NDT*80 and its homologs could be triggered by nutritional cues. In *S. cerivisiae* Ime1 and Ime2 are positive regulators of expression of *NDT*80 (41). *N. crassa* and *A. nidulans* both have a homolog of *IME*2, but not *IME*1 and Ime2 homologs have been shown to be negative regulators of Vib-1 and XprG, respectively (20, 29, 42). It was suggested that the regulation of *NDT*80 homologs by Ime2 homologs might be conserved among ascomycete fungi (42). *F. oxysporum* also has a *IME*2 homolog, FOXG_13813 (http://www.fungidb.org), and it will be interesting to study its function in regulation of *SUF*.

We have shown that both deletion mutant phenotype and Suf-GFP localization to the subcellular bodies is triggered in CDA. CDA contains sucrose as sole carbon and nitrate as sole nitrogen source but both in adequate quantities, thus the medium is not causing starvation. Apparently, then, it is the absence of complex compounds in CDA (present in PDA) that triggers accumulation of Suf and (in its absence) increased hyphal fusion. That may also hold true for other *NDT*80 homologs, possibly regulated by Ime2 homologs. Depending on the fungal species, different developmental processes are then activated. In addition, conidial pairing of strains with a *SUF* deletion show an increase in heterokaryon formation, the first step towards horizontal chromosome transfer (26).

Continued work will be required to elucidate the role of *NDT*80 homologs in fungal development as well as asexual recombination and horizontal chromosome transfer in *F. oxysporum*. This might include the identification of downstream targets of Suf by transcriptome analysis, characterization of other *F. oxysporum NDT*80 homologs and regulators of Suf.

ACKNOWLEDGEMENTS
This work was made possible by an Innovational Research Incentives Scheme Vici grant of The Netherlands Organisation for Scientific Research (NWO) to M.R. We thank Bas Beerens, Martin Bosch and Ido Vlaardingerbroek for their assistance with experiments.

MATERIAL AND METHODS

Strains and culture conditions.

Fusarium oxysporum f. sp. lycopersici strain 4287 (*Fol*4287, FGSC9935), *Fusarium oxysporum f. sp. melonis* strain 001 (*Fom*001, FGSC10441), and the non-pathogenic *Fusarium oxysporum* strain 47 (*Fo*47, FGSC10445) were used as the parental strains for fungal transformation. They were stored as a monoconidial culture at -80 °C and revitalized on potato dextrose agar (PDA) (Difco) at 25 °C. *Agrobacterium tumefaciens* EHA105 (43) was used for *Agrobacterium*-mediated transformation of *F. oxysporum* and was grown in either Luria broth (LB) or 2YT medium (44) containing 20 µg/ml rifampin at 28 °C. Introduction of the plasmids into the *Agrobacterium* strain was performed as previously described (45). *Escherichia coli* DH5α (Invitrogen) was used for construction, propagation, and amplification of the plasmid and was grown at 37 °C in LB medium containing 50 µg/ml kanamycin.

Construction of vectors and *Agrobacterium*-mediated *Fusarium* transformation.

Suf-GFP

Construction of pRW2h-H1-GFP containing the hygromycin (hph) resistance cassette and under the control of the xylanase promoter was described previously (46). To generate a Suf-GFP fusion protein, *SUF* (FOXG_01644) without a stop codon was PCR amplified with the primer combination FP6365 (5'-agatctATGACAACCGCAACGG-3') and FP6566 (5'-ggttacctGTTCCCATTCCAGGAATATTG-3') from *Fol*4287 gDNA and the amplicon was cloned in the *Bgl*II / *Bst*EII site in-frame with the GFP gene.

SUF deletion

To generate *SUF* deletion (Δ*suf*) mutants, we used plasmids pRW2h-H1-GFP and pRW2p-H1-RFP (26, 46). These plasmids have either the hygromycin resistance cassette (hph) and histone-GFP under the control of the xylanase promoter or the phleomycin resistance cassette (tested with zeocin, ble) and histone-RFP under the control of the xylanase promoter as selection marker. We introduced an ~1 kb sequence upstream (left flank) and downstream (right flank) of *SUF* open reading frame (ORF) for homologous recombination. For this we PCR amplified the left flank with primer combination FP4278 (5'-

cggaattcGCCGTGCCGTTCACTCC-3') and FP4279 (5'-ggggtaccGCCTACGAAGTAGAAGATGAGCTT-3') and the right flank with primer combination FP4280 (5'-tgctctagaCGATATACAAAAGTTGCCATCAAA-3') and FP4281 (5'-cccaagcttGAACAGATCTATTAACAAAGCCATCC-3'). The right flank was cloned in the *Xba*I site upstream the right border and the left flank in the *Pac*I site downstream the left border.

***SUF* complementation**

Binary vectors pRW2h (hph) and pRW2p (ble) were used as a backbone for vector construction (26, 47). We introduced an ~1 kb sequence upstream (left flank) plus the ORF and an ~1 kb sequence downstream (right flank) of *SUF* for homologous recombination. For this we PCR amplified the left flank plus *SUF* ORF with primer combination FP6455 (5'-ttaattaaGCCGTGCCGTTCACTC-3') and FP6456 (5'-ttaattaaCTAGTTCCCATTCCAGGAATATTG-3') and the right flank as described before. The right flank was cloned in the *Xba*I site upstream the right border and the left flank plus *SUF* ORF in the *Pac*I site downstream the left border. pRW2h-*SUF* (hph) was used to complement H1-RFP Δ*suf* (ble) and pRW2p-*SUF* (ble) to complement H1-GFP Δ*suf* (hph, for plasmid maps see Fig S1).

***Agrobacterium*-mediated *Fusarium* transformation**

The obtained plasmids Suf-GFP (hph), H1-GFP Δ*suf* (hph), H1-RFP Δ*suf* (ble), pRW2h-*SUF* (hph) and pRW2p-*SUF* (ble) were transformed into *Agrobacterium tumefaciens* EHA105 and the transformants were used for subsequent *A. tumefaciens*-mediated *Fusarium* transformation. *Agrobacterium*-mediated transformation of *F. oxysporum* was performed as previously described (46).

Localization studies

*Fol*4287 and *Fom*001 strains carrying the Suf-GFP fusion gene were grown on potato dextrose broth (PDB, Difco), Czapek Dox liquid (CDL, Oxoid), and conidial anastomosis tube (CAT) medium (0.17 % YNB, 25 mM KNO_3) supplemented with 1.5 % agarose and 0.5 % xylose for one week at 25°C. Observations were performed with the AMG Evos FL digital inverted microscope equipped with transmitted light, GFP (470/22 to 510/42 nm), and DAPI DAPI (357/44-447/60 nm) light cubes, and driven by built-in software for image acquisition using the inverted agar method (48). To counter-stain DNA the fungus was treated for 1 minute with 1 mg/ml Hoechst 33342 (Life Technologies) and washed with water before microscopy. Images were analyzed with the Fiji software from imageJ (http://fiji.sc/Fiji).

CAT and hyphal fusion assays.

For CAT fusion assay, conidia of *Fol*4287 H1-RFP Δ*suf*, *Fom*001 H1-GFP Δ*suf*, and *Fo*47 H1-GFP Δ*suf* were collected from one-week-old PDA plates in 2 ml of the medium to be tested and filtered through one layer of sterile Miracloth (Calbiochem). 200 µl 7.5x10^5 conidia per ml were incubated in an 8-well microscope chamber slide (Nunc) for 15 to 18 hours in CAT medium and observed with the AMG Evos FL digital inverted microscope. 1000 to 2500 conidia were counted in two biological replicates. CAT fusion frequency was calculated as the percentage of CAT fusions per germinated conidia.

For hyphal fusion assays, *Fol*4287 H1-RFP Δ*suf*, *Fom*001 H1-GFP Δ*suf*, and *Fo*47 H1-GFP Δ*suf* were grown on PDA, CDA, or CAT medium supplemented with 1.5 % agarose for one week at 25°C. Side-to-side fusion between hyphae behind the growth front were counted per area (0.5 mm^2). 15 technical in 3 biological replicates were performed.

Co-cultivation.

Conidia of *Fol*4287 wild type (wt), *Fol*4287 H1-RFP Δ*suf*, *Fom*001 wt, and *Fom*001 H1-GFP Δ*suf* were collected from one-week-old PDA plates in 2 ml water, filtered through one layer of sterile Miracloth (Calbiochem), and washed with water. To select heterokaryotic cells, 1 ml with 10^6 conidia from each parental strain were incubated in a 1-well microscope chamber slide (Nunc). After two days conidia were collected and 50 µl was plated on PDA and incubated for additional two days. Again conidia were collected and washed and 10^4 conidia per ml were incubated on PDA buffered with 0.1 M Tris (pH 8.0) and supplemented with 100 µg/ml hygromycin (Duchefa) and 100 µg/ml zeocin (Invivogen) for five days. The number of double drug-resistant colonies was counted.

Selection of Nit mutations and complementation testing

The screen was performed as previously described (Puhalla, 1985). We selected different nitrate non-utilizing (NIT) mutants for each strain (*Fol*4287 wt, *Fol*4287 H1-RFP Δ*suf*, *Fom*001 wt, and *Fom*001 H1-GFP Δ*suf*) and tested compatibility in different combinations.

Analysis of culture supernatant

Conidia of *Fol*4287 wt, *Fol*4287 H1-RFP Δ*suf*, *Fom*001 wt, and *Fom*001 H1-GFP Δ*suf* were collected from 3-day old liquid culture, filtered through one layer of sterile Miracloth (Calbiochem), and washed with water. Conidia concentration was adjusted to 10^8 conidia / ml. 20 ml NO_3 (0.17 % YNB, 100 mM KNO_3, 3% sucrose) were inoculated with 5x10^7 conidia and grown at 25°C shaking. After 2 days the mycelium was pelleted and washed with CAT medium. One pellet

each was transferred to 20ml NO_3, minimal medium (MM, 0.17 % YNB, 100 mM KNO_3), CAT, and CAT +3% sucrose media, with (induction for protease activity assay) or without (for SDS-PAGE) 1% BSA and incubated for another 2 days. The culture was again filtered through one layer of sterile Miracloth and the filtrate was centrifuged. The supernatant used for further testing. The mycelial pellet was dried and the dry weight was measured. Protease activity in the culture supernatant was determined by measuring the release of the trichloroacetic acid (TCA)-soluble orange sulfanilamide component of azocasein upon proteolysis, as previously described (4).
Further, SDS-PAGE was conducted to visualize protein patterns of culture supernatant. For this 20 µl of culture supernatant was loaded on a 15% sodium dodecyl sulfate (SDS) polyacrylamide gel followed by protein silver staining (50).

Carbon utilization assay
To analyze carbon utilization of the *Fol*4287 *SUF* deletion mutant, BIOLOG FF MicroPlates containing in each well a different carbon source were used, as described (34).

Phylogenetic analysis
Complete proteomes of *F. oxysporum* f. sp. *lycopersici* 4287, *F. oxysporum* f. sp. *melonis* 26406, *F. graminearum* PH1, *Magnaporthe oryzae* 70-15 and *N. crassa* OR74a were obtained *via* the Broad institute and the genome of *Apergillus nidulans* was obtained from GenBank. Proteins that have a Ndt80 domain were identified by searching all proteomes with a hmmer model for PF05224 (51) using hmmsearch from the Hmmer package (52). The domain sequences were cut out using a custom python script and a multiple sequence alignment for the domain sequences was constructed using Clustal Omega with default settings (53). The alignment was inspected but no changes were performed. The alignment was trimmed using trimAl (-strictplus) (54). Finally, PhyML (55) with 4 substitution rate categories and estimated proportion of invariable sites and gamma distribution was used to infer the phylogeny.

REFERENCES

1. Prosser JI. 1995. Kinetics of Filamentous Growth and Branching, p. 301–318. *In* Gow, NAR, Gadd, GM (eds.), The Growing Fungus. Springer Netherlands, Dordrecht.
2. Glass NL, Jacobson DJ, Shiu PKT. 2000. The genetics of hyphal fusion and vegetative incompatibility in filamentous ascomycete fungi. Annu Rev Genet 34:165–186.

3. Saupe SJ. 2000. Molecular genetics of heterokaryon incompatibility in filamentous ascomycetes. Microbiol Mol Biol Rev 64:489–502.
4. Glass NL, Dementhon K. 2006. Non-self recognition and programmed cell death in filamentous fungi. Curr Opin Microbiol 9:553–8.
5. Glass NL, Kaneko I. 2003. Fatal attraction: nonself recognition and heterokaryon incompatibility in filamentous fungi. Eukaryot Cell 2:1–8.
6. Pontecorvo G. 1956. The parasexual cycle in fungi. Annu Rev Microbiol 10:393–400.
7. Debets AJM, Griffiths AJF. 1998. Polymorphism of het-genes prevents resource plundering in Neurospora crassa. Mycol Res 102:1343–1349.
8. Cortesi P, McCulloch CE, Song H, Lin H, Milgroom MG. 2001. Genetic control of horizontal virus transmission in the chestnut blight fungus, Cryphonectria parasitica. Genetics 159:107–18.
9. Dementhon K, Iyer G, Glass NL. 2006. VIB-1 is required for expression of genes necessary for programmed cell death in Neurospora crassa. Eukaryot Cell 5:2161–73.
10. Smith ML, Micali OC, Hubbard SP, Mir-Rashed N, Jacobson DJ, Glass NL. 2000. Vegetative incompatibility in the het-6 region of Neurospora crassa is mediated by two linked genes. Genetics 155:1095–104.
11. Espagne E, Balhadère P, Penin M-L, Barreau C, Turcq B. 2002. HET-E and HET-D belong to a new subfamily of WD40 proteins involved in vegetative incompatibility specificity in the fungus Podospora anserina. Genetics 161:71–81.
12. Fedorova ND, Badger JH, Robson GD, Wortman JR, Nierman WC. 2005. Comparative analysis of programmed cell death pathways in filamentous fungi. BMC Genomics 6:177.
13. Van der Nest MA, Olson A, Lind M, Vélëz H, Dalman K, Brandström Durling M, Karlsson M, Stenlid J. 2014. Distribution and evolution of het gene homologs in the basidiomycota. Fungal Genet Biol 64:45–57.
14. Xiang Q, Glass NL. 2002. Identification of vib-1, a locus involved in vegetative incompatibility mediated by het-c in Neurospora crassa. Genetics 162:89–101.
15. Katz ME, Gray K-A, Cheetham BF. 2006. The Aspergillus nidulans xprG (phoG) gene encodes a putative transcriptional activator involved in the response to nutrient limitation. Fungal Genet Biol 43:190–9.
16. Montano SP, Coté ML, Fingerman I, Pierce M, Vershon AK, Georgiadis MM. 2002. Crystal structure of the DNA-binding domain from Ndt80, a transcriptional activator required for meiosis in yeast. Proc Natl Acad Sci U S A 99:14041–6.
17. Sopko R, Stuart DT. 2004. Purification and characterization of the DNA binding domain of Saccharomyces cerevisiae meiosis-specific

transcription factor Ndt80. Protein Expr Purif 33:134–44.
18. Lamoureux JS, Stuart D, Tsang R, Wu C, Glover JNM. 2002. Structure of the sporulation-specific transcription factor Ndt80 bound to DNA. EMBO J 21:5721–32.
19. Katz ME, Braunberger K, Yi G, Cooper S, Nonhebel HM, Gondro C. 2013. A p53-like transcription factor similar to Ndt80 controls the response to nutrient stress in the filamentous fungus, Aspergillus nidulans. F1000Research 2:72.
20. Hutchison EA, Glass NL. 2010. Meiotic regulators Ndt80 and ime2 have different roles in Saccharomyces and Neurospora. Genetics 185:1271–82.
21. de Sain M, Rep M. 2015. The Role of Pathogen-Secreted Proteins in Fungal Vascular Wilt Diseases. Int J Mol Sci 16:23970–93.
22. Takken F, Rep M. 2010. The arms race between tomato and Fusarium oxysporum. Mol Plant Pathol 11:309–14.
23. Rep M, Kistler HC. 2010. The genomic organization of plant pathogenicity in Fusarium species. Curr Opin Plant Biol 13:420–6.
24. Coleman JJ, Rounsley SD, Rodriguez-Carres M, Kuo A, Wasmann CC, Grimwood J, Schmutz J, Taga M, White GJ, Zhou S, Schwartz DC, Freitag M, Ma LJ, Danchin EG, Henrissat B, Coutinho PM, Nelson DR, Straney D, Napoli CA, Barker BM, Gribskov M, Rep M, Kroken S, Molnár I, Rensing C, Kennell JC, Zamora J, Farman ML, Selker EU, Salamov A, Shapiro H, Pangilinan J, Lindquist E, Lamers C, Grigoriev I V, Geiser DM, Covert SF, Temporini E, Vanetten HD. 2009. The genome of Nectria haematococca: contribution of supernumerary chromosomes to gene expansion. PLoS Genet 5:e1000618.
25. Ma LJ, van der Does HC, Borkovich KA, Coleman JJ, Daboussi MJ, Di Pietro A, Dufresne M, Freitag M, Grabherr M, Henrissat B, Houterman PM, Kang S, Shim WB, Woloshuk C, Xie X, Xu JR, Antoniw J, Baker SE, Bluhm BH, Breakspear A, Brown DW, Butchko RA, Chapman S, Coulson R, Coutinho PM, Danchin EG, Diener A, Gale LR, Gardiner DM, Goff S, Hammond-Kosack KE, Hilburn K, Hua-Van A, Jonkers W, Kazan K, Kodira CD, Koehrsen M, Kumar L, Lee YH, Li L, Manners JM, Miranda-Saavedra D, Mukherjee M, Park G, Park J, Park SY, Proctor RH, Regev A, Ruiz-Roldan MC, Sain D, Sakthikumar S, Sykes S, Schwartz DC, Turgeon BG, Wapinski I, Yoder O, Young S, Zeng Q, Zhou S, Galagan J, Cuomo CA, Kistler HC, Rep M. 2010. Comparative genomics reveals mobile pathogenicity chromosomes in Fusarium. Nature 464:367–373.
26. Shahi S, Beerens B, Bosch M, Linmans J, Rep M. 2016. Nuclear dynamics and genetic rearrangement in heterokaryotic colonies of Fusarium oxysporum. Fungal Genet Biol 91:20–31.
27. Puhalla JE. 1985. Classification of strains of Fusarium oxysporum on the

basis of vegetative compatibility. Can J Bot 63:179–183.
28. Correll J C, Klittich C J R, Leslie J F. 1987. Nitrate Nonutilizing Mutants of Fusarium oxysporum and their use in vegetative compatibility tests. Phytopathology 77:1640–1646.
29. Katz ME, Cooper S. 2015. Extreme Diversity in the Regulation of Ndt80-Like Transcription Factors in Fungi. G3 (Bethesda) 5:2783–92.
30. Xiong Y, Sun J, Glass NL. 2014. VIB1, a link between glucose signaling and carbon catabolite repression, is essential for plant cell wall degradation by Neurospora crassa. PLoS Genet 10:e1004500.
31. Chu S, Herskowitz I. 1998. Gametogenesis in yeast is regulated by a transcriptional cascade dependent on Ndt80. Mol Cell 1:685–96.
32. Roca GM, Read ND, Wheals AE. 2005. Conidial anastomosis tubes in filamentous fungi. FEMS Microbiol Lett 249:191–8.
33. Roca GM, Arlt J, Jeffree CE, Read ND. 2005. Cell Biology of Conidial Anastomosis Tubes in Neurospora crassa. Eukaryot Cell 4:911–919.
34. Michielse CB, van Wijk R, Reijnen L, Manders EMM, Boas S, Olivain C, Alabouvette C, Rep M. 2009. The nuclear protein Sge1 of Fusarium oxysporum is required for parasitic growth. PLoS Pathog 5:e1000637.
35. Palma-Guerrero J, Hall CR, Kowbel D, Welch J, Taylor JW, Brem RB, Glass NL. 2013. Genome wide association identifies novel loci involved in fungal communication. PLoS Genet 9:e1003669.
36. Wang J-S, Yang Y-L, Wu C-J, Ouyang KJ, Tseng K-Y, Chen C-G, Wang H, Lo H-J. 2006. The DNA-binding domain of CaNdt80p is required to activate CDR1 involved in drug resistance in Candida albicans. J Med Microbiol 55:1403–11.
37. Chen C-G, Yang Y-L, Shih H-I, Su C-L, Lo H-J. 2004. CaNdt80 is involved in drug resistance in Candida albicans by regulating CDR1. Antimicrob Agents Chemother 48:4505–12.
38. Nobile CJ, Fox EP, Nett JE, Sorrells TR, Mitrovich QM, Hernday AD, Tuch BB, Andes DR, Johnson AD. 2012. A recently evolved transcriptional network controls biofilm development in Candida albicans. Cell 148:126–38.
39. Sellam A, Askew C, Epp E, Tebbji F, Mullick A, Whiteway M, Nantel A. 2010. Role of transcription factor CaNdt80p in cell separation, hyphal growth, and virulence in Candida albicans. Eukaryot Cell 9:634–44.
40. Pinan-Lucarré B, Balguerie A, Clavé C. 2005. Accelerated cell death in Podospora autophagy mutants. Eukaryot Cell 4:1765–74.
41. Winter E. 2012. The Sum1/Ndt80 transcriptional switch and commitment to meiosis in Saccharomyces cerevisiae. Microbiol Mol Biol Rev 76:1–15.
42. Hutchison EA, Bueche JA, Glass NL. 2012. Diversification of a protein

kinase cascade: IME-2 is involved in nonself recognition and programmed cell death in Neurospora crassa. Genetics 192:467–82.

43. Hood EE, Gelvin SB, Melchers S, Hoekema A. 1993. New Agrobacterium helper plasmids for gene transfer to plants (EHA105). Transgenic Res 2:208–218.
44. Sambrook J, Russel DW. 2001. Molecular Cloning: a Laboratory Manual. Col Spring Harbor Laboratory Press, New York.
45. Mattanovich D, Rüker F, Machado AC, Laimer M, Regner F, Steinkellner H, Himmler G, Katinger H. 1989. Efficient transformation of Agrobacterium spp. by electroporation. Nucleic Acids Res 17:6747.
46. Shahi S, Beerens B, Manders EMM, Rep M. 2015. Dynamics of the Establishment of Multinucleate Compartments in Fusarium oxysporum. Eukaryot Cell 14:78–85.
47. Houterman PM, Cornelissen BJ, Rep M. 2008. Suppression of plant resistance gene-based immunity by a fungal effector. PLoS Pathog 4:e1000061.
48. Hickey PC, Swift SR, Roca MG, Read ND. 2004. Live-cell imaging of filamentous fungi using vital fluorescent dyes and confocal microscopy.Methods in Microbiology. Elsevier.
49. Klittich C J R, Leslie J F. 1988. Nitrate reduction mutants of Fusarium moniliforne (Gibberella fujikuroi). Genet Soc Am 118:417–423.
50. Shevchenko A, Wilm M, Vorm O, Mann M. 1996. Mass spectrometric sequencing of proteins silver-stained polyacrylamide gels. Anal Chem 68:850–8.
51. Finn RD, Bateman A, Clements J, Coggill P, Eberhardt RY, Eddy SR, Heger A, Hetherington K, Holm L, Mistry J, Sonnhammer ELL, Tate J, Punta M. 2014. Pfam: the protein families database. Nucleic Acids Res 42:D222–30.
52. Eddy SR. 2009. A new generation of homology search tools based on probabilistic inference. Genome Inform 23:205–11.
53. Sievers F, Wilm A, Dineen D, Gibson TJ, Karplus K, Li W, Lopez R, McWilliam H, Remmert M, Söding J, Thompson JD, Higgins DG. 2011. Fast, scalable generation of high-quality protein multiple sequence alignments using Clustal Omega. Mol Syst Biol 7:539.
54. Capella-Gutiérrez S, Silla-Martínez JM, Gabaldón T. 2009. trimAl: a tool for automated alignment trimming in large-scale phylogenetic analyses. Bioinformatics 25:1972–3.
55. Guindon S, Dufayard J-F, Lefort V, Anisimova M, Hordijk W, Gascuel O. 2010. New algorithms and methods to estimate maximum-likelihood phylogenies: assessing the performance of PhyML 3.0. Syst Biol 59:307–21.

SUPPLEMENTARIES

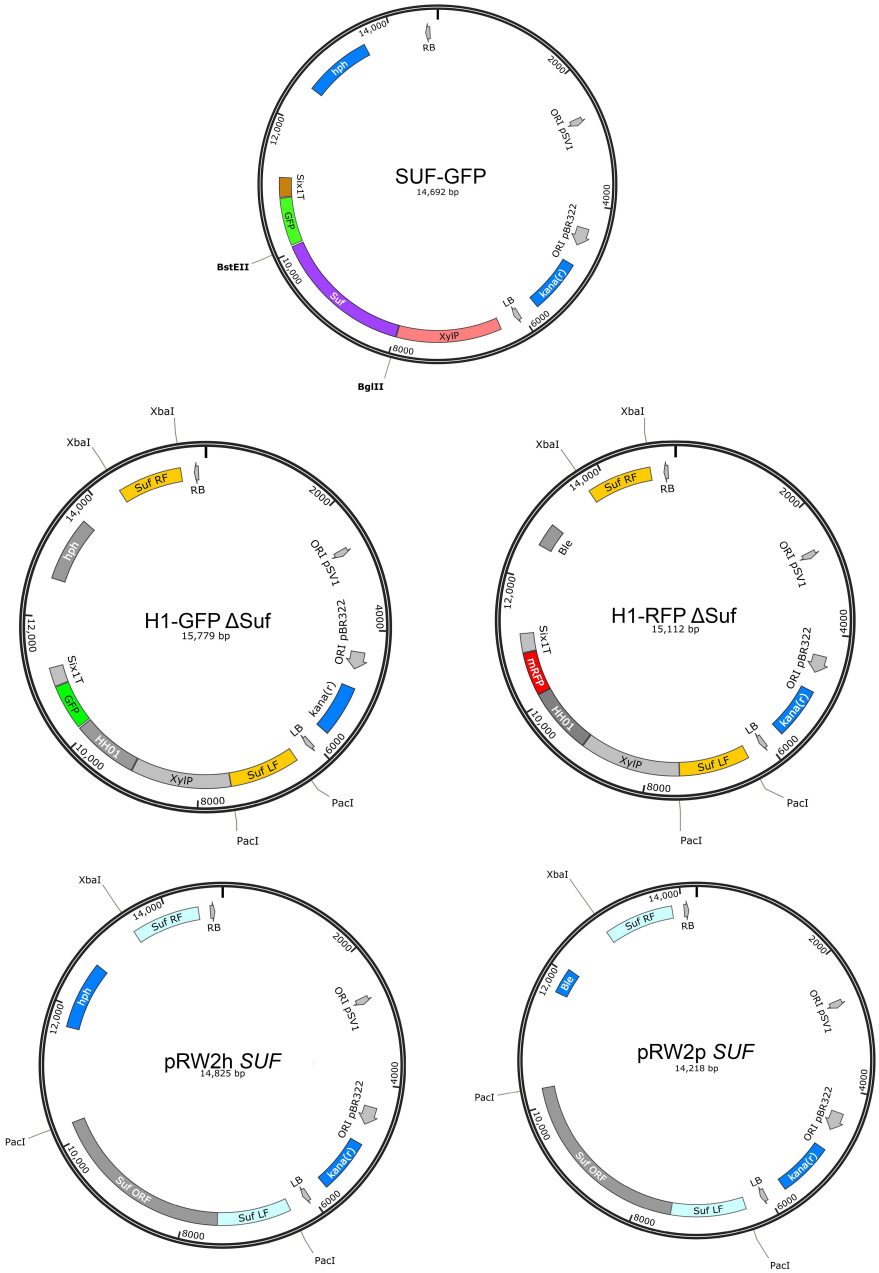

Figure S1: Maps of plasmids used for this study.

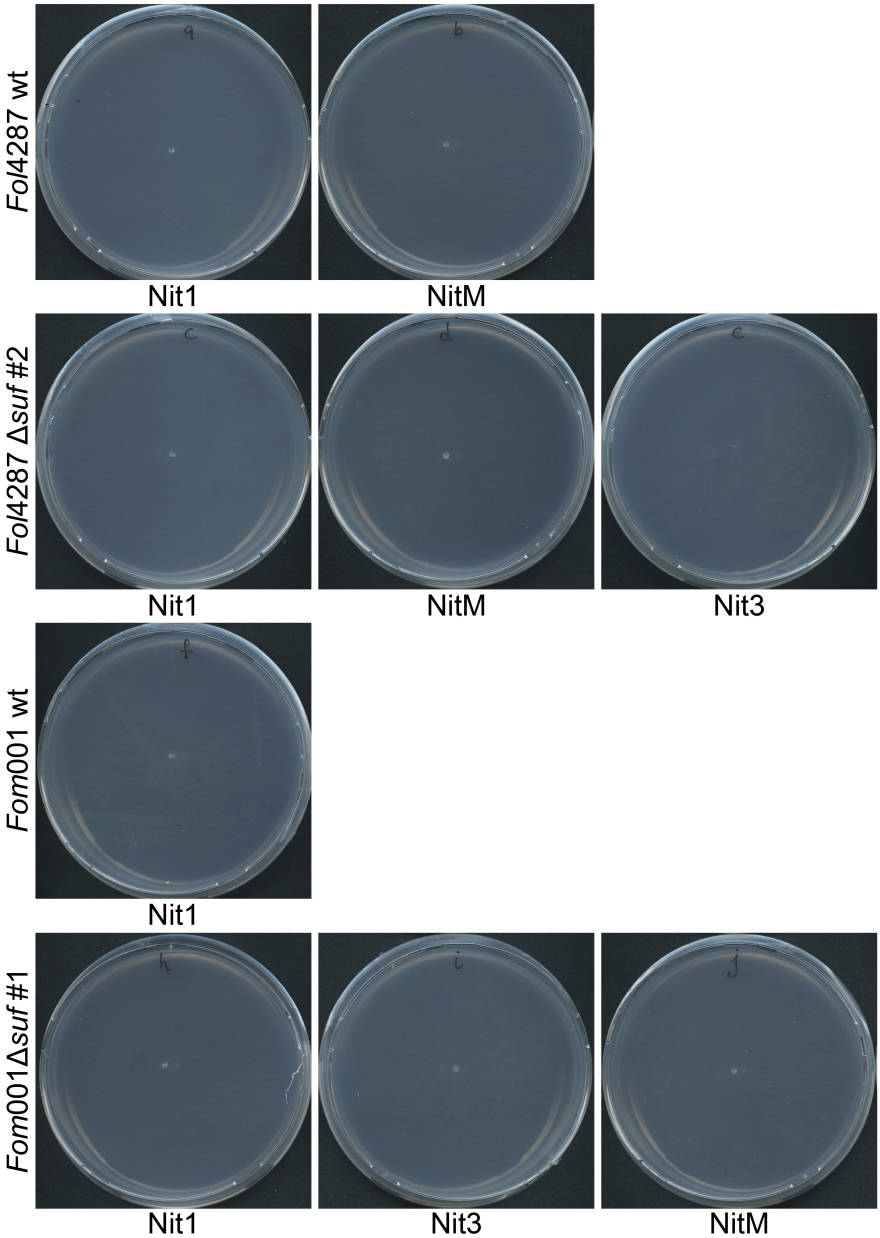

Figure S2: Phenotype of Nit mutants on nitrate medium. On medium containing nitrate as sole nitrogen medium nitrate non-utilizing mutants show a very thin growth pattern.

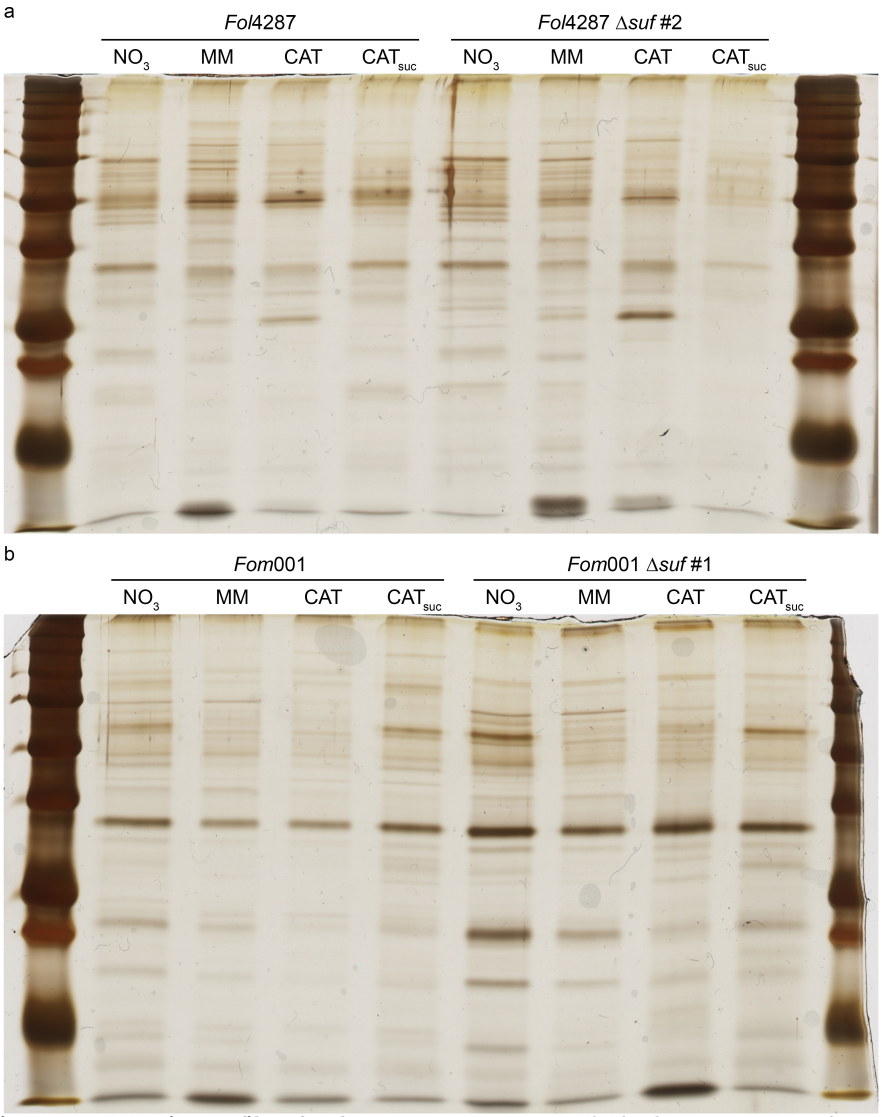

Figure S3: Protein profile of culture supernatant. 20 µl of culture supernatant from a) *Fol*4287 and b) *Fom*001 wild type and *suf* deletion mutants separated on SDS-PAGE and silver-stained. Culture supernatant was collected as described in material and methods. No major differences between wild type and deletion mutant in any of the tested media was observed.

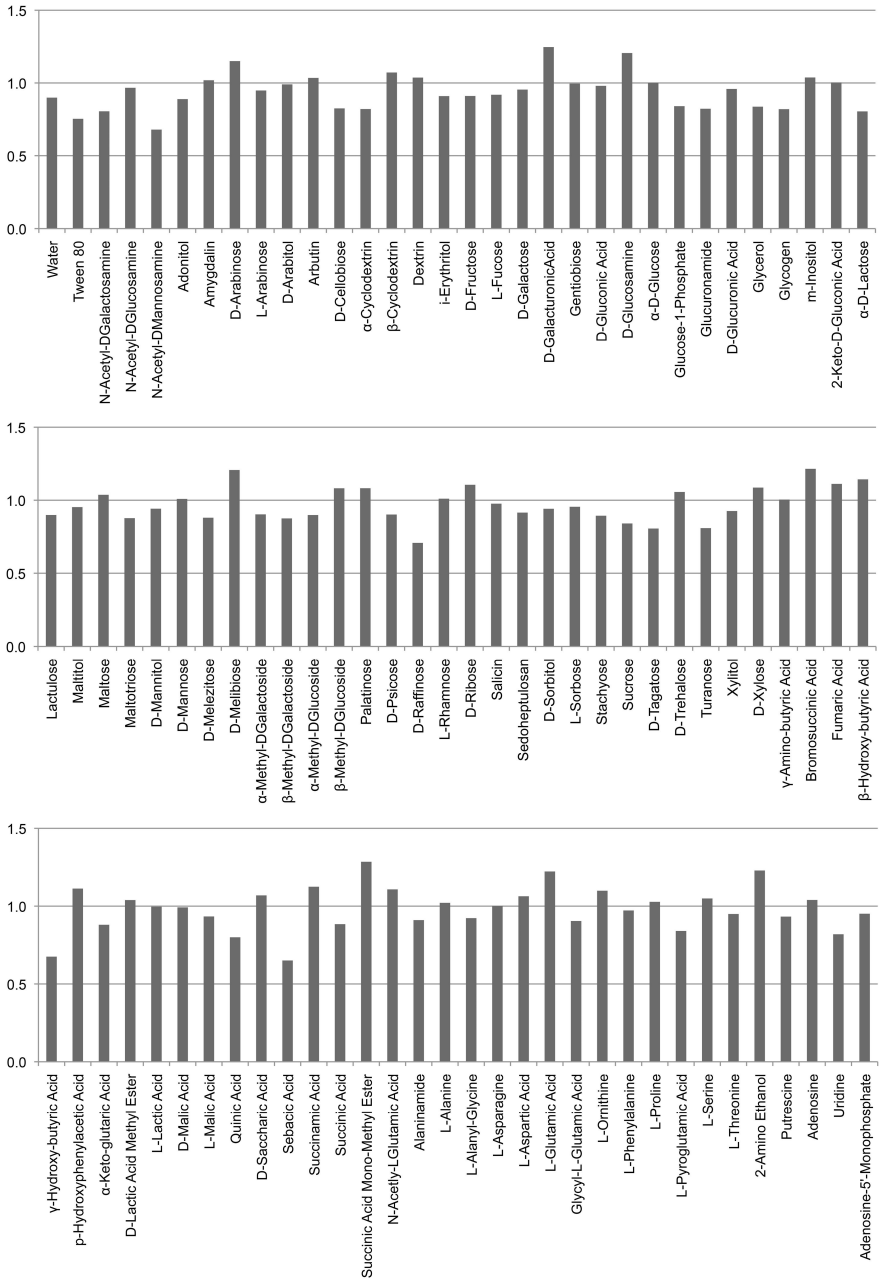

Figure S4: *Suf* is not involved in carbon source utilization. Shown are the ratios of growth rate between *Fol*4287 *suf* deletion and wild type strain. Values higher than 1.5 or lower that 0.5 are considered a substantial difference in growth rate. In all tested carbon sources deletion mutant and wild type strain performed similarly.

General Discussion

Horizontal transfer, *i.e.* non-meiotic transfer of genetic material and stable integration into the recipient genome, plays an important role in evolution of filamentous fungi (for a review see 1, 2). Studies carried out in the past two decades and the increasing availability of genome data has allowed a better understanding of fungal evolution. An intriguing insight coming from these studies is the concept of the "two-speed" genome, in which the genome consists of a conserved core and a variable part that harbors virulence genes embedded in otherwise gene poor regions and transposable elements. These regions are proposed to serve as hotspots for adaptive evolution (3, 4). In *F. oxysporum* (*Fo*) virulence genes are located on a lineage-specific (LS) chromosome – chromosome 14 in the reference strain *Fol*4287 – hence the designation "pathogenicity" chromosome. It was demonstrated that this pathogenicity chromosome can be horizontally transferred to the non-pathogenic strain *Fo*47, leading to newly acquired pathogenicity towards tomato plants (2, 5). Although horizontal chromosome transfer (HCT) has also been observed in *Colletotrichum gloeosporioides* and *Alternaria alternata*, little is known about the mechanism (6, 7). It has been proposed that HCT takes place in slow-growing heterokaryons, *via* nuclear fusion or *via* selective transfer, *i.e.* active transport from one nucleus into the other (6, 8).

Using *Fusarium oxysporum* as a model, the studies presented in this thesis lay groundwork for understanding HCT in filamentous fungi. Firstly, for horizontal transfer of genetic material to occur most likely nuclei of the transfer partners have to be present in the same cellular compartment. For this *Fo* has to be able to allow a - at least temporary - multinucleate state. In **Chapter two** we demonstrate that *Fo* can be considered a multinucleate organism and that this multinucleate state is only suppressed during conidiation and early colony development. In **chapter three**, we provide evidence for a mechanism leading to horizontal transfer of genetic material. We show that conidial anastomosis tube (CAT) fusion can lead to the formation of viable heterokaryons. During further development of the heterokaryotic colony, nuclei of the parental lines may fuse and undergo genome rearrangement by forming micronuclei. The parental genomes are then spatially separated and chromosomes of the pathogenic line are selectively eliminated. In some nuclei, however, the pathogenicity chromosome apparently escapes this elimination process and is stably integrated in the genome of the previously non-pathogenic strain (see Figure 1).

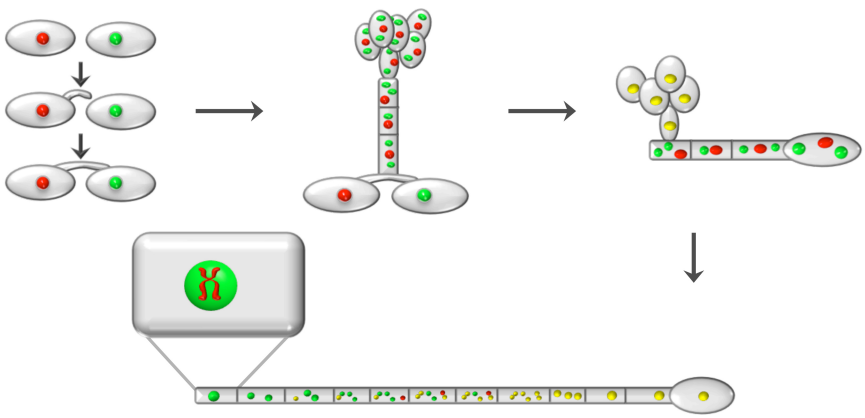

Figure 1: Model for horizontal chromosome transfer in *F. oxysporum*. Under carbon starvation conidial pairing of incompatible strains can result in the formation of viable heterokaryotic cells. During further development, nuclei of the parental lines presumably fuse to produce conidia with a single nucleus harboring both GFP- and RFP-histone H1 fusion proteins, shown as yellow nuclei. Upon colony formation, this hybrid offspring is subject to progressive and gradual genome rearrangement. The parental genomes are spatially separated and RFP-tagged histones, derived from the *Fol*4287 strain, are eventually lost. The resulting cells have the chromosomal background of *Fo*47 with sometimes the addition of *Fol*4287 chromosomes, in all cases including the pathogenicity chromosome (**Chapter three** and 2, 5).

Since HCT takes place in heterokaryons that are genetically unstable and in which nuclear organization and – presumably – content are irregular, we

considered that processes related to vegetative incompatibility might affect the "success rate" of HCT. We therefore set out to investigate the role of heterokaryon incompatibility (HI) in HCT in *Fo* using a targeted mutation approach. In *N. crassa*, deletion of the Vegetative Incompatibility Blocked 1 (VIB-1) gene suppresses HI. In **chapter four** we show that fusion in *Fo* is regulated by "suppressor of fusion" (SUF), the ortholog of VIB-1 and a putative transcription factor of the Non-Dityrosine 80 (Ndt80) family of transcription factors that in other ascomycetes is involved in HI and / or sexual development (9–11). Taken together, these findings raise new interesting questions that I will discuss in further detail.

MICRONUCLEI FORMATION - A PROCESS FOR UNIPARENTAL CHROMOSOME ELIMINATION

In **Chapter three** we provide evidence that fusion of nuclei likely take place in heterokaryons of *Fol*4287 and *Fo*47. This fusion launches a series of events that ultimately lead to the selective loss of *Fol*4287 chromosomes. Such a phenomenon is not unique to fungi: uniparental chromosome loss has been observed in interspecific hybrids of diverse organisms. In somatic hybrid cells formed by artificial cell fusion between human and mouse cells, extensive elimination of human chromosomes occurs (12). In interspecies fish hybrids formed by sexual hybridization, elimination of uniparental chromosomes occurs during embryonic development (13). In flowering plants, interspecies crosses are used to produce haploids through uniparental chromosome elimination (14).

Several processes underlying uniparental chromosome elimination have been suggested. In interspecific grass hybrids, for example, asynchronous mitosis and asynchronous nucleoprotein synthesis have been proposed to initiate loss of chromosomes from one parental line (15–17). In interspecific fish, lagging chromosomes have been discussed as a possible mechanism. Lagging chromosomes are chromosomes that are not correctly attached to the kinetochores during meitosis and thus lag behind at anaphase (13). In human-mouse somatic cell hybrids a progressive loss of human chromosomes was suggested to be preceded by spatial segregation of the parental genomes (18). However, the exact mechanism of uniparental chromosome elimination, especially in fungi, is still poorly understood. Many efforts are being made in mammals and plants to help understand this phenomenon. One commonality that has been observed across kingdoms is the formation of micronuclei (18, 19). These are mostly formed at the end of mitosis. It was proposed that chromosomes lagging behind during mitosis are sequestered in micronuclei and that these chromosomes are either acentric or carry inactivated centromeres

(19, 20). In human-mouse somatic hybrid cells, as well as in plants, a variable number of chromosomes of one parental line were found in micronuclei (18, 19). Whether micronuclei serve to spatially separate parental genomes after nuclear fusion or are solely a stage in the degradation of nuclei is not clear – it may be a combination of both. DNA fragmentation in micronuclei has been demonstrated in grass hybrids (19). In human-mouse somatic cell hybrids it appears that human chromosomes are sorted into micronuclei in a progressive manner and it was suggested that fragmentation of human chromosomes is initiated in the main nucleus (18).

Gernand and coworkers already pointed out the similarities in the processes of micronucleus formation in plants and mammals and suggested that the process allowing for uniparental chromosome loss is evolutionary conserved (19). In **Chapter three** we show that this might in fact also apply to fungi. In *Fol*4287 / *Fo*47 hybrid cells fluorescent histones of one fusion partner are not taken up by nuclei of the other fusion partner, which already indicates that mitosis is either not synchronous in nuclei from the different parental lines or that "autonomous" cytoplasm surrounds each nucleus. Our findings support at least the former. In the cases observed by live-cell imaging, we were able to confirm asynchronous mitosis. During development of the heterokaryons nuclear fusion presumably takes place before conidiation, producing conidia with a single nucleus. Colonies emerging from these conidia undergo a major genome rearrangement after apparent micronucleus formation, resulting in loss of *Fol*4287 chromosomes. This may involve spatial segregation of *Fol*4287 chromosomes into micronuclei followed by their degradation. Uniparental chromosome loss in hybrids has been shown to be a progressive process that in grass hybrids takes 6 to 23 days before completion (18, 19). Our own observations also support a gradual and progressive loss of *Fol*4287 chromosomes.

The question that now arises is how – and which - chromosomes in micronuclei are degraded. Again there are some indications from previous studies. For example, micronuclei in mammalian cells have been shown to be removed via macroautophagy (referred to as autophagy from hereon, 21, 22). Autophagic removal of whole nuclei has been observed in fungi. During starvation periods *Aspergillus oryzae* uses autophagy of whole nuclei in intercalary compartments to obtain nutrients necessary for vegetative growth (23). In a recent study Corral-Ramos and coworkers have demonstrated that the autophagy machinery is conserved in *Fo* and is also involved in degradation of whole nuclei during vegetative growth (24). It stands to reason that autophagic removal of micronuclei could serve to eliminate chromosomes from *Fol*4287.

Future research should concentrate on the nature of micronuclei in *Fol*4287 / *Fo*47 hybrids. For example, it will be interesting to study chromosome content and ploidy level in nuclei / micronuclei during development of hybrid colonies. For this, nuclei could be isolated and after staining with propidium iodide sorted using FACS (fluorescence-activated cell sorting). Additionally, the TUNEL (Terminal deoxynucleotidyl transferase dUTP nick end labeling) assay and counter staining with a vacuolar dye will help to determine whether DNA is fragmented in micronuclei and / or micronuclei are removed via autophagy.

HETEROCHROMATINIZATION AND ITS PUTATIVE ROLE IN UNIPARENTAL CHROMOSOME ELIMINATION

Ma and coworkers demonstrated horizontal transfer of the two smallest LS chromosomes of *Fol*007 (the pathogenicity chromosome and the smallest chromosome, 5). This suggests there are features that distinguish between transferrable and non-transferrable chromosomes. Given that entire chromosomes are horizontally transferred, prominent candidates for such distinguishing marks are chromatin modifications (25). In order to investigate unique chromatin features that might distinguish LS / transferrable from core / non-transferrable chromosomes, we performed ChIP-sequencing and generated a whole genome chromatin map for several well-known modifications of histone H3.

We found that in *Fo* subtelomeric as well as LS regions (*i.e.* chromosomes 1b, 2b, 3, 6, 14, and 15 of *Fol*4287) are associated with the histone mark H3K27me3 (Fig 2). This is in agreement with findings from studies performed in other filamentous fungi. Galazka and Freitag have described that while fungal LS chromosomes are heterochromatic, they are mostly associated with H3K27me3, a facultative heterochromatin mark that can be activated under certain circumstances (26). Classical B chromosomes (extra chromosomes) from plants have also been shown to be heterochromatic (27), but the chromatin mark mostly used there is H3K9me3, known for constitutive silencing (28). Galazka and Freitag proposed a cooperation between the constitutive and facultative silencing markers H3K9- and H3K27-methylation and that different fungi might use different combinations for silencing (26). Indeed, the density of H3K9me3 in *Fo* is very low, especially in the larger core chromosomes. The involvement of H3K9me3 in HCT has been tested by co-cultivation of strains carrying a deletion in Defective In Methylation 5 (DIM5), an H3K9-specific methyl transferase, without showing any effects on HCT (van der Does, personal communication).

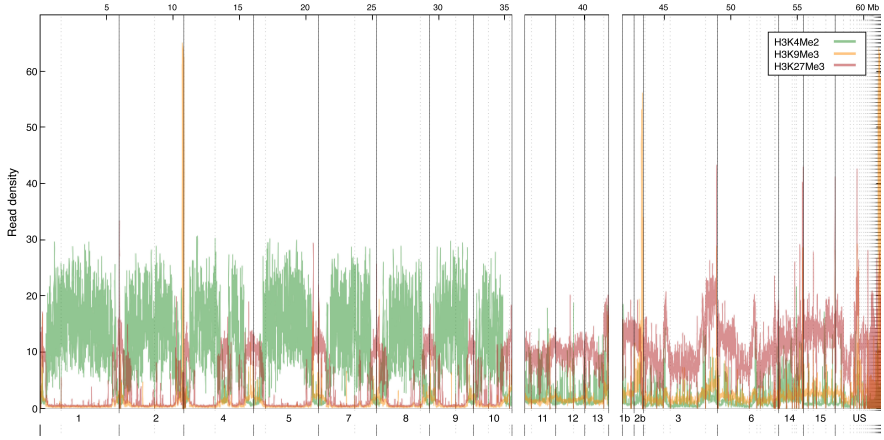

Figure 2. Whole genome chromatin map reveals that LS chromosomes in *Fo* are associated with H3K27 methylation. In the *Fol*4287 reference genome LS regions and subtelomeric regions are enriched for the silencing mark H3K27me3, which is typically associated with facultative heterochromatin. In addition to the LS chromosomes, the three smallest core chromosomes 11, 12 and 13 are also associated with facultative heterochromatin. The mark for constitutive heterochromatin, H3K7me3, is by comparison very low on the core genome and moderate in LS regions. *Fol*4287 chromosomes are shown at the bottom and genome size at the top. ChIP-seq results (read density) are shown for H3K4me2, a marker for active genes (green), H3K9me3 (orange), and H3K27me3 (red). US: Unaligned Supercontig; for methods see (29).

Studies in *F. graminearum* have revealed that subtelomeric regions associated with H3K27me3 show the highest variability in DNA sequence having the highest frequency of single nucleotide polymorphisms (SNPs) (29). Furthermore, it was demonstrated that genes for niche adaptation in *F. solani* (27) and *Fol* (5) are located on LS chromosomes and in subtelomeric regions in other fungi (27). Taken together, these findings suggest that the facultative silencing marker H3K27me3 is associated with adaptation (26, 27). A surprising finding from our study, however, is that not only LS regions are associated with the facultative heterochromatin mark, but also the smallest three core chromosomes (chromosomes 11, 12 and 13 in *Fol*4287, Fig 2). We have earlier mentioned the model of the "two-speed genome", a bipartite genome with a conserved or "slow" evolving core and variable or "fast" evolving LS regions, which are rich in virulence genes and transposable elements (3, 4). Considering our own data, we propose a "three-speed genome" for *Fo*, including a conserved core, the "fast" evolving LS part, and an in-between part consisting of regions that are syntenic with related species, but still prone to variability in sequence and marked with H3K27me3 (Fokkens and Shahi, unpublished data). Supporting this idea is that at least one of these chromosomes, chromosome 12 of *Fol*4287, is conditionally dispensable (**chapter three** and 2).

In conclusion, we have found a histone mark, H3K27me3, which distinguishes between core and LS chromosomes and identified a third "chromosome type" (fast evolving core) in a filamentous ascomycete (Fokkens and Shahi, unpublished). However, extensive investigations to identify chromosomes amenable for transfer has revealed that of the *Fol*4287 LS chromosomes only chromosome 14 is "transferrable" and even in the studies that used *Fol*007 as a donor, where both the equivalent of chromosomes 14 and the smallest chromosome have been shown to be transferred, transfer of larger LS chromosomes was never observed (2, 5). Can this solely be attributed to chromosome size or are there different and / or additional features that determine the potential for transfer / protection from elimination?

Studies of grass hybrids have shown that chromosomes that are eliminated are highly condensed and heterochromatinized (19). Gernand and coworkers proposed a model in which selective elimination of chromosomes involves spatial separation followed by micronucleus formation, heterochromatinization and DNA fragmentation in micronuclei (19). In addition, heterochromatinization by H3K9 and H3K27 methylation has been shown to play a major role in uniparental chromosome elimination by specifically marking chromosomes for elimination (18, 19). Whether a change in chromatin structure during hybrid development in *Fo* takes place and guides directed chromosome elimination, will be a challenge for future research.

Another intriguing question is how heterochromatinization is regulated. In the case of uniparental chromosome elimination in *Fo* a distinction between nearly identical chromosomes has to be made. Here we might find an indication by looking at sexual development and macronucleus formation in ciliates. The ciliate *Tetrahymena* has two different nuclei in the same cytoplasm: a transcriptionally inactive diploid micronucleus with 10 chromosomes and a transcriptionally active macronucleus with over 20,000 chromosomes. The macronucleus is formed from a micronucleus during sexual reproduction by selectively removing more than 6,000 internal DNA sequences and it was demonstrated that this directed DNA elimination is epigenetically regulated (30, 31). Mochizuki proposed the "scan RNA model", in which the entire micronuclear genome is transcribed in both directions to form double-stranded RNA that is processed to small scanning RNAs (scRNA) *via* an RNAi-related machinery. During macronucleus development scRNA are transferred to the macronucleus, where scRNA with a homologous sequence are degraded. The remaining scRNA represent the internal sequences of the micronucleus that have to be degraded from the new macronucleus. In the new macronucleus the scRNA serve as a scaffold for heterochromatinization (31).

Small non-coding RNAs (ncRNA) have also been associated with the recruitment of the machinery needed for heterochromatinization in plants, *Caenorhabditis elegans* and *Drosophila melanogaster* (32–34). In the fungal kingdom heterochromatinization induced by RNA-related machinery has been extensively studied in *Schizosaccharomyces pombe* (for review see 27). These studies show that the targeting mechanism for heterochromatin formation and proteins involved in the RNAi-induced degradation pathway, including dicer and argonaute, are conserved among eukaryotic kingdoms. More research is needed to reveal whether *Fo* employs a RNAi-related machinery to distinguish between nearly identical chromosomes.

HORIZONTAL CHROMOSOME TRANSFER IN *F. OXYSPORUM* IS THE RESULT OF ASEXUAL RECOMBINATION

Fo is considered to be an asexual fungus. Strains infecting the same host are polyphyletic but share the same virulence genes that are located on a so-called pathogenicity chromosome. It was demonstrated that this pathogenicity chromosome can be transmitted horizontally or non-meiotically (2, 5). This raised the question how such a non-meiotic transfer of genetic material takes place in an (presumably) asexual fungus. In the studies presented in this thesis we have shown that conidial paring leads to nuclear fusion and ultimately to integration of the *Fol*4287 pathogenicity chromosome (chromosome 14) and sometimes also chromosome 10 or 12 into the genome of *Fo*47 (**chapter three and four**).

When comparing with well-known basic principles of sexual recombination, namely formation of gametes *via* meiosis, mate recognition, cell-cell fusion and ploidy change, the process leading to horizontal transfer of genetic material in *Fo* is similar in several respects: Finding a fusion partner, undergoing conidial anastomosis tube (CAT) fusion, and nuclear fusion leading to ploidy change (36). However, *Fo* does not form gametes and chromosomes are selectively eliminated instead and we suggest using the term "**asexual recombination**". Although there are some similarities with the parasexual cycle described for other filamentous fungi, *i.e.* cell fusion, non-sexual recombination, and ploidy change, the defining criterion is not fulfilled, namely that the loss of chromosomes occurs in a stochastic manner (**chapter three** and 2, 37)

Heitman and coworkers described the advantages of sex in generating genetic diversity to accelerate adaptation. But as everything in life, it comes at a cost of - amongst others - finding a suitable partner (36). Like uniparental sexual recombination and the parasexual cycle, asexual recombination is independent of mating type and can even occur between different strains (38).

In filamentous ascomycetes vegetative hyphal fusion or anastomosis occurs frequently within the same mycelium (self fusion) and presumably facilitates the distribution of nutrients as well as signaling across the mycelium (39, 40). We have shown that CAT fusion is a rare event in *Fo* but increases in frequency under carbon starvation conditions. In addition, one of the strains used in our study, *Fo*47, has a defect in self-fusion without showing any further phenotypic traits under laboratory conditions (**chapter three and four**). Also, in *Fol*4287 a deletion of Soft (SO), a gene essential for fusion, did not result in a growth phenotype (Vlaardingerbroek, personal communication). These findings indicate that fusion in general and CAT fusion in particular does not play an important role in vegetative growth in *Fo*. Furthermore, we showed that CAT fusion is regulated by a putative transcription factor (SUF1) that in other fungi regulates expression of genes involved in sexual development in a nutrient-dependent manner (**chapter four** and 38–40). Starvation often serves as a signal for a drastic change in development, for example in several organisms starvation is used as signal to enter a sexual cycle (31, 41). In *Fo* starvation may be a key stimulator for initiating asexual recombination *via* conidial pairing. CAT fusion in *Fo* shows another novel feature in that the formation of an anastomosis tube from one of the fusion partners is sufficient for anastomosis. This would allow a distinction between a "fuser" as the active partner (*Fol*4287 in our studies) and a "fusee" as the inactive partner (*Fo*47), leading to early signaling cascades that might activate some kind of self-preservation or "immune response" in *Fo*47. This could for example include embellishment of chromosomes of the "intruder" with a certain chromatin mark in order to distinguish between "self" and "non-self" chromosomes. After nuclear fusion and recombination the hybrid colony returns to its haploid state and since meiosis does not take place in *Fo*, one copy of the homologous chromosomes is degraded. In contrast to a parasexual cycle, however, the signaling initiated *via* CAT fusion may have differentiated "self" and "nonself" chromosomes, so that only *Fol*4287 chromosomes are lost. This would explain why transfer of chromosomes 3, 6, and 15 of *Fol*4287 has never been detected. Chromosomes 3 and 6 contain large duplications within and between each other and chromosome 15 is largely duplicated in another part of the genome (Fokkens and Rep, personal communication and 5). In a sense, the pathogenicity chromosome can be viewed as a non-recombining chromosome, as has been previously suggested (6). It was observed that horizontal transfer and exchange of genetic material always involves transfer of the pathogenicity chromosome (chromosome 14 of *Fol*4287, this thesis, 2, 5). It remains possible that along with the repertoire to infect a new host, the pathogenicity chromosome could also harbor a specific genetic element that initiates or otherwise regulates asexual recombination (2, 42).

REFERENCES

1. Mehrabi R, Bahkali AH, Abd-Elsalam KA, Moslem M, Ben M'barek S, Gohari AM, Jashni MK, Stergiopoulos I, Kema GH, de Wit PJ. 2011. Horizontal gene and chromosome transfer in plant pathogenic fungi affecting host range. FEMS Microbiol Rev 35:542–554.
2. Vlaardingerbroek I, Beerens B, Rose L, Fokkens L, Cornelissen BJC, Rep M. 2016. Exchange of core chromosomes and horizontal transfer of lineage-specific chromosomes in Fusarium oxysporum. Environ Microbiol Epub ahead.
3. Dong S, Raffaele S, Kamoun S. 2015. The two-speed genomes of filamentous pathogens: Waltz with plants. Curr Opin Genet Dev 35:57–65.
4. Croll D, McDonald BA. 2012. The accessory genome as a cradle for adaptive evolution in pathogens. PLoS Pathog 8:e1002608.
5. Ma LJ, van der Does HC, Borkovich KA, Coleman JJ, Daboussi MJ, Di Pietro A, Dufresne M, Freitag M, Grabherr M, Henrissat B, Houterman PM, Kang S, Shim WB, Woloshuk C, Xie X, Xu JR, Antoniw J, Baker SE, Bluhm BH, Breakspear A, Brown DW, Butchko RA, Chapman S, Coulson R, Coutinho PM, Danchin EG, Diener A, Gale LR, Gardiner DM, Goff S, Hammond-Kosack KE, Hilburn K, Hua-Van A, Jonkers W, Kazan K, Kodira CD, Koehrsen M, Kumar L, Lee YH, Li L, Manners JM, Miranda-Saavedra D, Mukherjee M, Park G, Park J, Park SY, Proctor RH, Regev A, Ruiz-Roldan MC, Sain D, Sakthikumar S, Sykes S, Schwartz DC, Turgeon BG, Wapinski I, Yoder O, Young S, Zeng Q, Zhou S, Galagan J, Cuomo CA, Kistler HC, Rep M. 2010. Comparative genomics reveals mobile pathogenicity chromosomes in Fusarium. Nature 464:367–373.
6. Akagi Y, Akamatsu H, Otani H, Kodama M. 2009. Horizontal chromosome transfer, a mechanism for the evolution and differentiation of a plant-pathogenic fungus. Eukaryot Cell 8:1732–1738.
7. He C, Rusu AG, Poplawski AM, Irwin JA, Manners JM. 1998. Transfer of a supernumerary chromosome between vegetatively incompatible biotypes of the fungus Colletotrichum gloeosporioides. Genetics 150:1459–1466.
8. Manners JM, He C. 2011. Slow-growing heterokaryons as potential intermediates in supernumerary chromosome transfer between biotypes of Colletotrichum gloeosporioides. Mycol Prog 10:383–388.
9. Katz ME, Cooper S. 2015. Extreme Diversity in the Regulation of Ndt80-Like Transcription Factors in Fungi. G3 (Bethesda) 5:2783–92.
10. Dementhon K, Iyer G, Glass NL. 2006. VIB-1 is required for expression of genes necessary for programmed cell death in Neurospora crassa. Eukaryot Cell 5:2161–73.

11. Winter E. 2012. The Sum1/Ndt80 transcriptional switch and commitment to meiosis in Saccharomyces cerevisiae. Microbiol Mol Biol Rev 76:1–15.
12. Nabholz M, Miggiano V, Bodmer W. 1969. Genetic analysis with human--mouse somatic cell hybrids. Nature 223:358–63.
13. Sakai C, Konno F, Nakano O, Iwai T, Yokota T, Lee J, Nishida-Umehara C, Kuroiwa A, Matsuda Y, Yamashita M. 2007. Chromosome elimination in the interspecific hybrid medaka between Oryzias latipes and O. hubbsi. Chromosome Res 15:697–709.
14. Dunwell JM. 2010. Haploids in flowering plants: origins and exploitation. Plant Biotechnol J 8:377–424.
15. Gupta SB. 1969. Duration of mitotic cycle and regulation of dna replication in nicotiana plumbaginifolia and a hybrid derivative of n . tabacum showing chromosome instability. Can J Genet Cytol 11:133–142.
16. Bennett MD, Finch RA, Barclay IR. 1976. The time rate and mechanism of chromosome elimination in Hordeum hybrids. Chromosoma 54:175–200.
17. Laurie DA, Bennett MD. 1989. The timing of chromosome elimination in hexaploid wheat × maize crosses. Genome 32:953–961.
18. Wang Z, Yin H, Lv L, Feng Y, Chen S, Liang J, Huang Y, Jiang X, Jiang H, Bukhari I, Wu L, Cooke HJ, Shi Q. 2014. Unrepaired DNA damage facilitates elimination of uniparental chromosomes in interspecific hybrid cells. Cell Cycle 13:1345–56.
19. Gernand D, Rutten T, Varshney A, Rubtsova M, Prodanovic S, Brüss C, Kumlehn J, Matzk F, Houben A. 2005. Uniparental chromosome elimination at mitosis and interphase in wheat and pearl millet crosses involves micronucleus formation, progressive heterochromatinization, and DNA fragmentation. Plant Cell 17:2431–8.
20. Wang J-S, Yang Y-L, Wu C-J, Ouyang KJ, Tseng K-Y, Chen C-G, Wang H, Lo H-J. 2006. The DNA-binding domain of CaNdt80p is required to activate CDR1 involved in drug resistance in Candida albicans. J Med Microbiol 55:1403–11.
21. Rello-Varona S, Lissa D, Shen S, Niso-Santano M, Senovilla L, Mariño G, Vitale I, Jemaá M, Harper F, Pierron G, Castedo M, Kroemer G. 2012. Autophagic removal of micronuclei. Cell Cycle 11:170–6.
22. Huang Y, Jiang L, Yi Q, Lv L, Wang Z, Zhao X, Zhong L, Jiang H, Rasool S, Hao Q, Guo Z, Cooke HJ, Fenech M, Shi Q. 2012. Lagging chromosomes entrapped in micronuclei are not “lost” by cells. Cell Res 22:932–935.
23. Shoji J, Kikuma T, Arioka M, Kitamoto K. 2010. Macroautophagy-

mediated degradation of whole nuclei in the filamentous fungus Aspergillus oryzae. PLoS One 5:e15650.

24. Corral-Ramos C, Roca MG, Di Pietro A, Roncero MIG, Ruiz-Roldán C. 2015. Autophagy contributes to regulation of nuclear dynamics during vegetative growth and hyphal fusion in Fusarium oxysporum. Autophagy 11:131–44.
25. Calero-Nieto F, Hera C, Di Pietro A, Orejas M, Roncero MIG. 2008. Regulatory elements mediating expression of xylanase genes in Fusarium oxysporum. Fungal Genet Biol 45:28–34.
26. Galazka JM, Freitag M. 2014. Variability of chromosome structure in pathogenic fungi--of "ends and odds". Curr Opin Microbiol 20:19–26.
27. Coleman JJ, Rounsley SD, Rodriguez-Carres M, Kuo A, Wasmann CC, Grimwood J, Schmutz J, Taga M, White GJ, Zhou S, Schwartz DC, Freitag M, Ma LJ, Danchin EG, Henrissat B, Coutinho PM, Nelson DR, Straney D, Napoli CA, Barker BM, Gribskov M, Rep M, Kroken S, Molnár I, Rensing C, Kennell JC, Zamora J, Farman ML, Selker EU, Salamov A, Shapiro H, Pangilinan J, Lindquist E, Lamers C, Grigoriev I V, Geiser DM, Covert SF, Temporini E, Vanetten HD. 2009. The genome of Nectria haematococca: contribution of supernumerary chromosomes to gene expansion. PLoS Genet 5:e1000618.
28. Schotanus K, Soyer JL, Connolly LR, Grandaubert J, Happel P, Smith KM, Freitag M, Stukenbrock EH. 2015. Histone modifications rather than the novel regional centromeres of Zymoseptoria tritici distinguish core and accessory chromosomes. Epigenetics Chromatin 8:41.
29. Connolly LR, Smith KM, Freitag M. 2013. The Fusarium graminearum histone H3 K27 methyltransferase KMT6 regulates development and expression of secondary metabolite gene clusters. PLoS Genet 9:e1003916.
30. Feng X, Guang S. 2013. Non-coding RNAs mediate the rearrangements of genomic DNA in ciliates. Sci China Life Sci 56:937–43.
31. Mochizuki K. DNA rearrangements directed by non-coding RNAs in ciliates. Wiley Interdiscip Rev RNA 1:376–87.
32. Grewal SIS, Elgin SCR. 2007. Transcription and RNA interference in the formation of heterochromatin. Nature 447:399–406.
33. Huettel B, Kanno T, Daxinger L, Bucher E, van der Winden J, Matzke AJM, Matzke M. 2007. RNA-directed DNA methylation mediated by DRD1 and Pol IVb: A versatile pathway for transcriptional gene silencing in plants. Biochim Biophys Acta - Gene Struct Expr 1769:358–374.
34. Cui M, Kim EB, Han M. 2006. Diverse chromatin remodeling genes antagonize the Rb-involved SynMuv pathways in C. elegans. PLoS Genet 2:e74.

35. Goto DB, Nakayama J. 2012. RNA and epigenetic silencing: insight from fission yeast. Dev Growth Differ 54:129–41.
36. Ni M, Feretzaki M, Sun S, Wang X, Heitman J. 2011. Sex in fungi. Annu Rev Genet 45:405–30.
37. Schardl CL, Craven KD. 2003. Interspecific hybridization in plant-associated fungi and oomycetes: a review. Mol Ecol 12:2861–2873.
38. Ni M, Feretzaki M, Li W, Floyd-Averette A, Mieczkowski P, Dietrich FS, Heitman J. 2013. Unisexual and heterosexual meiotic reproduction generate aneuploidy and phenotypic diversity de novo in the yeast Cryptococcus neoformans. PLoS Biol 11:e1001653.
39. Read ND, Lichius A, Shoji J, Goryachev AB. 2009. Self-signalling and self-fusion in filamentous fungi. Curr Opin Microbiol 12:608–15.
40. Simonin A, Palma-Guerrero J, Fricker M, Glass NL. 2012. Physiological significance of network organization in fungi. Eukaryot Cell 11:1345–52.
41. Chu S, Herskowitz I. 1998. Gametogenesis in yeast is regulated by a transcriptional cascade dependent on Ndt80. Mol Cell 1:685–96.
42. Rosewich UL, Kistler HC. 2000. Role of horizontal gene transfer in the evolution of fungi. Annu Rev Phytopathol 38:325–363.

Summary

SUMMARY

Genome plasticity and adaptive evolution are considered a driving force in the "arms-race" between a pathogen and its host. The advancement in bioinformatics and increasing availability of new genome sequences has revealed that not only meiotic recombination is responsible for the rather fast evolution of fungal pathogens. Comparative studies has allowed for a better understanding of fungal evolution. One striking finding from these studies is that fungal pathogens often show a "two-speed" genome, a bipartite genome in which virulence factors or effector genes have been accumulated in otherwise gene-poor and transposon-rich regions. For several fungal species it has now been established that these regions are heterochromatinized with the facultative chromatin mark H3K27me3. In special cases the "fast" evolving part of the genome is organized into small chromosomes. In the asexual ascomycete *F. oxysporum* (*Fo*) one such chromosome houses all effector genes and is thus referred to as the "pathogenicity" chromosome. For some years we have the knowledge that this pathogenicity chromosome can be horizontally transferred to a non-pathogenic strain, conferring pathogenicity to this strain. We have since used *Fo* as a model organism to address fundamental questions like how horizontal transfer of whole chromosomes is accomplished. Results of an investigation of this question are presented in this thesis.

In **chapter two** we investigate nuclear dynamics and mitotic patterns in different strains of *Fo* during several developmental stages using fluorescently labeled nuclei and live-cell imaging. We established that after completion of colony initiation *Fo* undergoes a developmental transition from a uninucleate to a multinucleate state and that dormant nuclei in intercalary compartments can be reactivated to enter the mitotic cycle. We propose a model in which *Fo* follows a multinucleate life style, but this multinucleate state is temporarily suppressed during conidiation and early colony development. This fulfills the first pre-requisite for horizontal chromosome transfer, namely that nuclei have to be able come into close proximity before transfer can take place.

We next focused on possible mechanics underlying horizontal chromosome transfer. In **chapter three** we describe studies performed to understand the role of anastomosis in heterokaryon formation between different strains of *F. oxysporum* and determined the importance of heterokaryons for horizontal chromosome transfer. A combination of live-cell imaging of fluorescently labeled nuclei during co-cultivation of vegetatively incompatible strains of *Fo,* heterokaryon formation and development of hybrid colonies and a PCR-based method to determine the chromosomal composition of the hybrid offspring helped us to shed some light into the mysteries that surround the phenomenon of horizontal chromosome transfer.

We demonstrate that starvation-induced CAT fusion between two strains of *Fo* results in formation of viable heterokaryons. During further development of these heterokaryotic colonies nuclear fusion apparently precedes conidiation. Upon colony formation, the hybrid offspring is subject to progressive and gradual genome rearrangement. The parental genomes appear to become spatially separated and *Fol*4287 chromosomes are eventually lost. The offspring shows the genomic background of *Fo*47, in some cases with the addition of one or two chromosomes from *Fol*4287, including the "pathogenicity" chromosome.

Finally, we dedicated some effort in understanding the regulation of heterokaryon formation in *Fo* (**chapter four**). We investigated the role of "suppressor of fusion" (SUF), a putative transcription factor of the p53-like Ndt80 family of transcription factors, in vegetative hyphal and conidial fusion and heterokaryon formation. We identified a novel function for a *NDT80* homolog as a nutrient-dependent regulator of anastomosis. Strains carrying the *SUF* deletion display a hyper-fusion phenotype during vegetative growth as well as germling development. In addition, co-incubation of incompatible *SUF* deletion strains led to more heterokaryon formation.

We have laid the groundwork for understanding the mechanics underlying horizontal chromosome transfer. In **chapter five** I discuss the results in a wider context and conclude that horizontal transfer of "pathogenicity" chromosomes is the product of asexual recombination followed by uniparental or directed chromosome elimination from which "transferrable" chromosomes can escape.

SAMENVATTING

Genoomplasticiteit en adaptieve evolutie worden beschouwd als een drijvende krachten in de “wapenwedloop” tussen een pathogeen en zijn gastheer. De vooruitgang in de bioinformatica en de toegenomen beschikbaarheid van nieuwe genoomsequenties hebben laten zien dat de relatief snelle evolutie van pathogene schimmels niet alleen is toe te schrijven aan meiotische recombinatie. Vergelijkende genoomstudies hebben geleid tot een beter begrip van de evolutie van schimmels. Een opvallende vondst uit deze studies is dat pathogene schimmels vaak een “two-speed” genoom hebben, een tweeledig genoom waarin virulentiefactoren of effector-genen zijn verzameld in anderszins gen-arme en transposon-rijke regio’s. Voor verschillende pathogene schimmelsoorten is nu aangetoond dat deze regio’s zijn gekenmerkt door de facultatieve H3K27me3 chromatine modificatie. In speciale gevallen is het “snel” evoluerende deel van het genoom georganiseerd in kleine chromosomen. In de asexuele ascomyceet *Fusarium oxysporum* (*Fo*) huisvest een dergelijk chromosoom alle effector-genen en wordt daarom “pathogeniteits-chromosoom” genoemd. Sinds een aantal jaar is bekend dat dit chromosoom horizontaal kan worden overgedragen naar een niet-pathogene stam en daarmee deze stam pathogeniteit kan verlenen. Sindsdien hebben we *Fo* gebruikt als modelorganisme om fundamentele vragen te adresseren, zoals hoe horizontale overdracht van een heel chromosoom wordt bewerkstelligd. De resultaten van onderzoek naar dit vraagstuk worden in dit proefschrift gepresenteerd.

In **hoofdstuk twee** onderzoeken we de nucleaire dynamiek en mitotische patronen in verschillende stammen van *Fo* tijdens verschillende stadia van ontwikkeling, gebruik makend van fluorescent gelabelde kernen en 'live-cell imaging'. We laten zien dat *Fo* na het voltooien van kolonie-initiatie een transitie in ontwikkeling ondergaat van enkelkernig naar meerkernig en dat inactieve kernen in tussencompartimenten tot een mitotische cyclus gereactiveerd kunnen worden. We stellen een model voor waarin *Fo* een veelkernige levensstijl heeft, maar deze veelkernige staat tijdelijk onderdrukt wordt gedurende sporulatie en vroege kolonie vorming. Dit vervult de eerste vereiste voor horizontale overdracht, namelijk dat kernen dicht bij elkaar in de buurt moeten kunnen komen voordat overdracht plaats kan vinden.

Vervolgens richten we ons op de mogelijke mechanismen waardoor horizontale overdracht plaats vindt. In **hoofdstuk drie** beschrijven we studies bedoeld om de rol van anastomose in heterokaryonvorming tussen verschillende *Fo* stammen te begrijpen en bepalen we het belang van heterokaryons voor horizontale chromosoom-overdracht. Een combinatie van 'live-cell imaging' van fluorescent gelabelde kernen tijdens co-cultivatie van vegetatief incompatibele stammen van *Fo*, de vorming van heterokaryons en de ontwikkeling van hybride kolonies en een PCR gebaseerde methode om de chromosoom-compositie van hybride nageslacht te bepalen heeft ons geholpen om enig licht te laten schijnen op het fenomeen van horizontale chromosoom-overdracht.

We laten zien dat fusie van 'conidial anastomosis tubes' (CAT fusie), geïnduceerd door nutriënt-depletie (uithongering), resulteert in de vorming van levensvatbare heterokaryons. In de verdere ontwikkeling van deze heterokaryotische kolonies blijkt nucleaire fusie vooraf te gaan aan conidiatie (sporevorming). Tijdens kolonievorming is het hybride nageslacht onderworpen aan voortschrijdende en geleidelijke herorganisatie van het genoom. De ouder-genomen lijken fysiek gescheiden te raken en *Fol4287* chromosomen verdwijnen uiteindelijk. Het nageslacht heeft de genomische achtergrond van *Fo47*, in enkele gevallen met toevoeging van een of twee chromosomen van *Fol4287*, inclusief het "pathogeniteits-chromosoom".

Tenslotte richten we onze aandacht op het begrijpen van de regulatie van heterokaryon-formatie in *Fo* (**hoofdstuk vier**). We onderzoeken de rol van "suppressor of fusion" (*SUF*), een lid van de p53-like Ndt80 familie van transcriptiefactoren, in vegetatieve hyphen en tijdens fusie van conidia en heterokaryon vorming. We identificeren een nieuwe functie als nutriënt afhankelijke regulator van anastomose voor een *NDT80* homoloog. Stammen met een *SUF* deletie hebben een hyper-fusie fenotype zowel tijdens vegetatieve groei als tijdens de ontwikkeling van pas ontkiemde microconidia. Daarbij leidt

coïncubatie van incompatibele *SUF* deletie-stammen tot de vorming van meer heterokaryons.

We hebben hiermee de basis gelegd voor het begrijpen van het mechanisme dat ten grondslag ligt aan de horizontale overdracht van chromosomen. In **hoofdstuk vijf** bediscussieer ik de resultaten in een bredere context en concludeer dat horizontale overdracht van pathogeniteits-chromosomen het product is van asexuele recombinatie gevolgd door asymetrische (van één ouder) of gerichte eliminatie van chromosomen waaraan "overdraagbare" chromosomen kunnen ontsnappen

ZUSAMMENFASSUNG

Es wird angenommen, dass Genomplastizität und adaptive Evolution die treibenden Kräfte hinter dem Wettrüsten zwischen einem Pathogen und seinem Wirt sind. Der Fortschritt in der Bioinformatik und die zunehmende Verfügbarkeit an Genomsequenzen haben ein besseres Verständnis der Pilzevolution ermöglicht und gezeigt, dass nicht nur meiotische Rekombination für die schnelle Evolution von pathogenen Pilzen verantwortlich ist. Eine bemerkenswerte Folgerung aus vergleichenden Genomstudien ist, dass pathogene Pilze oft ein „Zwei-Speed-Genom“ aufweisen. In solchen Fällen sind Virulenzfaktoren oder Effektoren in einem Teil des Genoms angereichert, das sonst arm an essentiellen Genen und reich an Transposons ist. Für mehrere Pilzspezies wurde bisher bereits veranschaulicht, dass diese Regionen heterochromatinisiert sind und mit dem sogenannten fakultativen Chromatinmarker, H3K27 Methylierung, versehen sind. Weiterhin wurde gezeigt dass in besonderen Fällen, diese schnell-evolvierenden Regionen sich in separate Chromosomen zusammengeschlossen haben. In dem asexuellem Fadenpilz *Fusarium oxysporum* (*Fo*) liegen alle Virulenzgene auf einem solchen Chromosomen, was dazu veranlasste diesen als den „Pathogenitätschromosomen“ zu bezeichnen. Seit einigen Jahren wissen wir nun, dass dieser Pathogenitätschromosom horizontal, also nicht sexuell, auf einen nichtpathogenen Stamm übertragen werden kann und in diesem zur Aneignung von Pathogenität führt. Wir benutzen *Fo* als ein Modelsystem um grundlegende Fragen über den horizontalen Chromosomentransfer zu beantworten. Die Ergebnisse und Folgerungen dieser Untersuchungen, sind in dieser Dissertation zusammengefasst.

In **Kapitel Zwei** untersuchen wir mittels der Live-Cell-Imaging Technologie und fluoreszenzmarkierter Kerne die Dynamik von Kernteilung während verschiedenen Entwicklungsabschnitten in unterschiedlichen *Fo*-Stämmen. Wir konnten zeigen, dass *Fo* nach der Kolonieinitiierung einen Übergang von einem einkernigen zu einem mehrkernigen Zustand erfährt. Weiterhin konnten wir feststellen, dass inaktive Kerne älterer Zellen wieder aktiviert werden können und erneut der Kernteilung unterliegen. Wir schlagen daher ein Modell vor, indem *Fo* eigentlich eine mehrkernige Lebensform darstellt, diese aber während der Konidienbildung kurzzeitig unterdrückt wird. Somit wäre die Grundvoraussetzung für den horizontalen Chromosomentransfer, nämlich die räumliche Nähe von Zellkernen innerhalb einer Zelle, erfüllt.

In **Kapitel Drei** beschäftigen wir uns mit Mechanismen, die zur horizontalen Chromosomentransfer führen und haben die Rolle von Hyphenfusion und Heterokaryonformation in Bezug auf horizontalen Chromosomentransfer untersucht. Hierzu haben wir zunächst mittels Live-Cell-Imaging von fluoreszenzmarkierten Kernen das Verhalten dieser während der Kultivierung inkompatibler Stämme, der Heterokaryonformation und der Entwicklung sogenannter Hybride beobachtet. Des Weiteren haben wir eine PCR-basierte Methode benutzt um die chromosomale Zusammensetzung in den Hybriden zu identifizieren. Wir haben beobachtet, dass nach einer Hungerphase sogenannte CAT Fusionen (für conidial anastomosis tube) zwischen unterschiedlichen *Fo*-Stämmen zur Formation von überlebensfähigen Heterokaryons führen können. Während der weiteren Entwicklung dieser heterokaryotischen Kolonien kommt es vermutlich zu einer Kernfusion. So entstandenen Hybride unterziehen sich dann einer schrittweisen Genomumstrukturierung. Hierbei werden die elterlichen Genome räumlich voneinander getrennt, wobei Chromosomen eines Elternstammes (*Fol*4287) nach und nach eliminiert werden, bis nur noch Chromosomen des Stammen *Fo*47 übrig bleiben. In einigen wenigen Fällen allerdings, können ein oder zwei *Fol*4287-Chromosomen überleben und werden in das Hybridgenom integriert, hierunter das Pathogenitätschromosom.

Im letzten experimentellen Teil haben wir uns mit der Regulierung der Heterokaryonformation auseinander gesetzt. In **Kapitel Vier** untersuchen wir die Rolle von „suppressor of fusion“ (SUF), ein hypothetischer Transkriptionsfaktor der Ndt80 Familie, auf Fusion sowie Heterokaryonformation. Wir beschreiben eine neue Funktion für ein Ndt80-Homolog als einen nährstoffabhängigen Regulator von Hyphenfusion. Stämme mit einer Deletion im SUF-Gen zeigen einen Hyperfusionsphänotyp. Des Weiteren führte die Kultivierung von inkompatiblen SUF-Deletionsstämmen zu erhöhter Heterokaryonformation.

Mit diesen Erkenntnissen haben wir eine Grundlage geschaffen, die zu der Entschlüsselung der Mechanismen des horizontalen Chromosomentransfers beitragen. In **Kapitel Fünf** diskutiere ich die Ergebnisse in einem breiteren Kontext und komme zu folgender Schussfolgerung: Der horizontale Transfer des Pathogenitätschromosomen ist das Produkt einer asexuellen Rekombination gefolgt von einseitiger und gezielter Chromosomeneliminierung, vor der sich übertragbare Chromosomen schützen können.

ACKNOWLEDGEMENTS
I would like to thank Lotje van der Does for translation into Dutch and Julia Schnetzer for help with the German translation.

Acknowledgements

As so many before me, there are many people who supported me during my PhD intellectually, emotionally and practically. Words won't be enough to emphasize the gratitude I owe every single one of you. But still I will try my best…

First, I would like to thank my promoter **Ben** for his support during my work and answering all the stupid questions towards the end. Thanks for being open for my ideas and critical about my work. **Martijn**, I don't even know where to start. You are the best supervisor imaginable. I almost lost faith that there is a supervisor, not only capable to guide me through my project, but also has the emotional strength to guide me through life with all its ups and downs. Then I met you. I have so many things I have to be grateful for and I learned so much from you. It was a pleasure and an honor to work with you. The supervisor team, of course, is not complete without **Frank** and **Harrold**. Thank you for the critical input, discussion, and last but not least fun times …

Petra, I owe you so much more than your own paragraph. You are the soul and the heart of the team and the wheels that keep everything running. You are the fountain of practical knowledge, the source of tidiness, the awe-inspiring organizer, the mountain path that keeps us alive … Joking aside, thank you for everything, it would be too much to name. Although you might not always feel it, each one of us appreciates what you do for us and is grateful for all your help.

The dream team, **Sarah, Ido and Patrick**, I would like for being part of something wonderful. I loved my project and I am so happy to have worked with people as passionate about their work as I was. Of course, in this context, I also want to thank **Lotje**, who started the project and later joined us again and influenced my work with great ideas. You all made the new start in Amsterdam so much easier and more fun.
Next, I would like to thank **Sjoerd, Bas, and Jasper** for their help with the project and making me laugh so much. All of you will make your impression on the world. **Martin,** you were taken from us too soon. For you, I want to believe that there is a life beyond, where your soul can still make many people smile. Who knows, if unicorns really existed …

Michel, Christa, Rob, and Teun thank you for PSM inputs, discussions and overall interest in my project and my opinion. It was a great experience to see how the collaboration between Fyto and Plantsphys works. **Erik Manders** and **Ronald Breedijk**, thank you for a great collaboration and your support. **Michael, Lanelle** and the team I would like to thank for the great experience and the help I received at OSU and further input for my project.

Sumolena, Maaike and Peter, we made a great organizing committee and I am proud of what we managed. **Val** thanks for reminding me of how inspiring and refreshing French youth can be. **Like** and **Hanna,** thank you for all the baby-related tips. **Nico,** until next time we share a bench together. **Georgios, Mara, Fleur, Ewa, Biju, Lisong, Heni, Xiaotang, Lingxue, DJ, Francesca, Benjamin, Chris, Marieke, and Sayantani,** thanks for all your help, discussion, outings, and borrels. **Manon, Marijn, Maria, and Jim** good luck and success for the future. I wish you as much enjoyment as I experienced.

Magda (happy Monday) I envy you energy and am proud to have worked with you. **Carlos** and **Fionn,** I am forever grateful for your friendship and company. My liver does not necessarily agree. **Johannes,** die Welt ist auf jeden Fall reicher mit dir. **Ringo, Petra B, Michel dV, Arjen, Eleni, Silke, Ale, Carlito, Steven, Alex, Wendy, Fariza** and all the plantphys people I might have forgotten, thanks for a great time in Amterdam and at the UvA. I will definitely try to implement Friday evening borrels at my next station.

In over five years I met a lot of new people and re-united with old friends at the UvA. We laughed, ranted, despaired, and generally enjoyed life together. Thank you UvA and Amsterdam for a great work and life experience.

However, not only my friends and colleagues from Amsterdam helped me during my PhD. And I also would like to thank a few people from outside. **Max**, dank dir für die Gestaltung meines Covers. **Julia,** du weißt, dass ich ohne dich gar nicht erst soweit gekommen wäre. Auch wenn wir uns nicht mehr so oft sehen können, wie wir es uns wünschen, du bist ein Teil unseres Lebens und ich vermisse dich jeden Tag.

And finally the "La Familia". Natürlich will ich auch meiner Familie danken, ohne die ich sicherlich nicht hier wäre. Meiner **Mutter** habe ich soviel zu verdanken. 1. Sie hat mich in diese Welt gebracht und zu dem Menschen erzogen, der ich heute bin (bitte macht ihr deswegen keine Vorwürfe). 2. Sie hat alles für uns Kinder aufgegeben und uns immer zum Höchsten angespornt. 3. Letztendlich hat sie auch praktisch zu der Fertigstellung meiner Arbeit beigetragen, indem sie sich um unseren kleinen Sonnenschein gekümmert hat, damit ich die Zeit aufbringen konnte Wissenschaft zu betreiben. Meinen Brüdern **Arash** und **Anoush** möchte ich dafür danken, dass sie mir alles zutrauen (manchmal zu viel). Durch diese Einstellung unterstützt, habe ich auch manche lebensverändernde Entscheidungen treffen können, ohne mit der Wimper zu zucken. Auch für die Unterstützung meiner erweiterten Familie

möchte ich mich bedanken. Durch **Esther** habe ich eine Schwester gewonnen, die immer ein offenes Ohr hat und mit einem tollen Humor einen immer wieder zum Lachen bringen kann. Meinen Schwiegereltern **Edith** und **Franz** danke ich für ihre Unterstützung in allen Bereichen. **Edith,** ich vermisse dich jeden Tag.

At last, but definitely not least, I want to thank the love of my life, **Sven.** Wieder einmal reichen Worte nicht aus, um meine Liebe oder Dankbarkeit auszudrücken. Aber ich werde natürlich wie immer meinen Senf abgeben. Dass ich mal einen Menschen treffe, der so kompatibel ist mit mir, hätte ich mir nie erträumt. Nicht einmal der ¨Franz¨, der Froschkönig oder der Cartoonparkplatz konnten uns von unserem Ziel abbringen. Ich bin jeden einzelnen Tag dankbar, dass du mein Leben bereicherst. Unser Glück ist seit fast 2 Jahren komplett durch unseren kleinen Sonnenschein. **Helena,** hat Licht in unser Leben gebracht und uns die Kraft gegeben, mit harten Schicksalsschlägen zurechtzukommen. Ich bin so stolz und voller Liebe für euch.

I want to take the opportunity once again to thank you, esteemed reader, friends, family and the unicorny magic that made my stay in Amsterdam so enjoyable and fruitful. I love you all.

Publications

Shahi S, Fokkens L, Houterman PM, Rep M. **Suppressor of fusion, a *Fusarium oxysporum* homolog of Ndt80, is required for nutrient-dependent regulation of anastomosis**, Fungal Genetics and Biology, accepted for publication.

Shahi S, Beerens B, Bosch M, Linmans J, Rep M. **Nuclear dynamics and chromosome transfer in heterokaryotic colonies of *Fusarium oxysporum***, 2016 Fungal Genetics and Biology 91 20-31.

Vlaardingerbroek I, Beerens B, Shahi S, Rep M. **Fluorescence Assisted Selection of Transformants (FAST): Using flow cytometry to select fungal transformants**, 2015 Fungal Genetics and Biology 76 104-109, doi:10.1016/j.fgb.2015.02.003.

Shahi S, Beerens B, Manders EMM, Rep M. **Dynamics of the Establishment of Multinucleate Compartments in *Fusarium oxysporum***, 2015 Eukaryotic Cell, 14:1 78-85, doi:10.1128/EC.00200-14.

Bidzinski P, Noir S, Shahi S, Reinstädler A, Gratkowska DM, Panstruga R. **Physiological characterization and genetic modifiers of aberrant root thigmomorphogenesis in mutants of *Arabidopsis thaliana MILDEW LOCUS O* genes**, 2014 Plant Cell Environ, 37: 2738–2753. doi:10.1111/pce.12353.

Kunz HH, Scharnewski M, Berlepsch Sv, Shahi S, Fulda M, Flügge UI, Gierth M. **Nocturnal energy demand in plants**, 2010 Plant Signaling & Behavior, 5-7: 1-3.